US Army Corps of Engineers

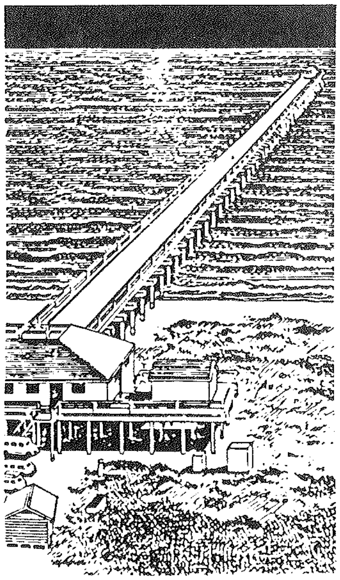

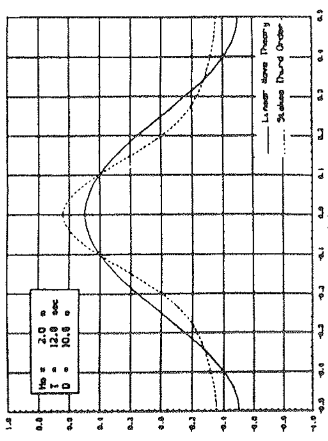

MISCELLANEOUS PAPER CERC-87-10

A NUMERICAL MODEL FOR SHOALING AND REFRACTION OF THIRD-ORDER STOKES WAVES OVER AN IRREGULAR BOTTOM

by

Mary A. Cialone, Nicholas C. Kraus

Coastal Engineering Research Center

DEPARTMENT OF THE ARMY
Waterways Experiment Station, Corps of Engineers
PO Box 631, Vicksburg, Mississippi 39180-0631

May 1987

Final Report

Prepared for DEPARTMENT OF THE ARMY
US Army Corps of Engineers
Washington, DC 20314-1000

Unclassified

SECURITY CLASSIFICATION OF THIS PAGE

REPORT DOCUMENTATION PAGE

Form Approved
OMB No. 0704-0188
Exp. Date: Jun 30, 1986

1a. REPORT SECURITY CLASSIFICATION Unclassified	1b. RESTRICTIVE MARKINGS
2a. SECURITY CLASSIFICATION AUTHORITY	3. DISTRIBUTION/AVAILABILITY OF REPORT Approved for public release; distribution unlimited.
2b. DECLASSIFICATION/DOWNGRADING SCHEDULE	
4. PERFORMING ORGANIZATION REPORT NUMBER(S) Miscellaneous Paper CERC-87-10	5. MONITORING ORGANIZATION REPORT NUMBER(S)
6a. NAME OF PERFORMING ORGANIZATION USAEWES, Coastal Engineering Research Center 6b. OFFICE SYMBOL (If applicable)	7a. NAME OF MONITORING ORGANIZATION
6c. ADDRESS (City, State, and ZIP Code) PO Box 631 Vicksburg, MS 39180-0631	7b. ADDRESS (City, State, and ZIP Code)
8a. NAME OF FUNDING/SPONSORING ORGANIZATION US Army Corps of Engineers 8b. OFFICE SYMBOL (If applicable)	9. PROCUREMENT INSTRUMENT IDENTIFICATION NUMBER
8c. ADDRESS (City, State, and ZIP Code) Washington, DC 20314-1000	10. SOURCE OF FUNDING NUMBERS PROGRAM ELEMENT NO. | PROJECT NO. | TASK NO. | WORK UNIT ACCESSION NO

11. TITLE (Include Security Classification)
A Numerical Model for Shoaling and Refraction of Third-Order Stokes Waves Over an Irregular Bottom

12. PERSONAL AUTHOR(S)
Cialone, Mary A., Kraus, Nicholas C.

13a. TYPE OF REPORT	13b. TIME COVERED	14. DATE OF REPORT (Year, Month, Day)	15. PAGE COUNT
Final Report	FROM Jan 85 TO Apr 86	May 1987	196

16. SUPPLEMENTARY NOTATION
Available from National Technical Information Service, 5285 Port Royal Road, Springfield VA 22161.

17. COSATI CODES			18. SUBJECT TERMS (Continue on reverse if necessary and identify by block number)
FIELD	GROUP	SUB-GROUP	Mathematical models (LC) Shoaling (WES) Water waves (LC)

19. ABSTRACT (Continue on reverse if necessary and identify by block number)

A numerical model for wave refraction and shoaling of third-order Stokes waves over an irregular bottom is presented. The model solves for wave height, angle, and number directly on a rectangular grid. Required input are the deepwater wave height, period, and direction and the bathymetry in the region of interest. The model employs a finite difference scheme. The irrotationality equation of the wave number vector is solved for the wave angle, and the conservation of energy flux equation is solved for the wave height. Iteration is required. A closed form expression, to third-order, for the time-averaged, vertically integrated energy flux is derived. Stokes' second definition of wave celerity is used in the derivation to reduce the number of intermediate calculations. Expressions for the wave energy and the group velocity are also derived. The model is written such that both first-order (linear) and third-order

(Continued

20. DISTRIBUTION/AVAILABILITY OF ABSTRACT ☒ UNCLASSIFIED/UNLIMITED ☐ SAME AS RPT. ☐ DTIC USERS	21. ABSTRACT SECURITY CLASSIFICATION Unclassified
22a. NAME OF RESPONSIBLE INDIVIDUAL	22b. TELEPHONE (Include Area Code) | 22c. OFFICE SYMBOL

DD FORM 1473, 84 MAR

83 APR edition may be used until exhausted.
All other editions are obsolete.

SECURITY CLASSIFICATION OF THIS PAGE
Unclassified

19. ABSTRACT (Continued).

stokes wave theory model computations may be conducted. The modeling process begins at higher intermediate depth, or deep water, and waves are propagated shoreward until an Ursell number of 25 or another, user-specified, value is reached. The model is applied for the following cases: (a) comparison of small amplitude and finite amplitude wave refraction and shoaling on a plane beach, (b) refraction and shoaling over an irregular bottom configuration, and (c) comparison of the model shoaling predictions to laboratory data of Iversen (1951).

The results show that finite amplitude wave shoaling curves consistently lie higher than small amplitude shoaling curves. Finite amplitude waves refract slightly more than small amplitude waves in deep water and refract less than small amplitude waves in shallow water. The model can be applied to transform waves over an irregular bottom as long as caustics do not occur.

PREFACE

The investigation described herein was authorized as a part of the Civil Works Research and Development Program by the Office, Chief of Engineers (OCE), US Army Corps of Engineers. Work was performed under the Surf Zone Sediment Transport Processes work unit which is part of the Shore Protection and Restoration Program at the Coastal Engineering Research Center (CERC) of the US Army Engineer Waterways Experiment Station (WES). Messrs. J. H. Lockhart, Jr., and John G. Housley were OCE Technical Monitors.

The study was conducted from 1 January 1985 through 30 April 1986 by Ms. Mary A. Cialone, Hydraulic Engineer, and Dr. Nicholas C. Kraus, Research Physical Scientist and Principal Investigator, Surf Zone Sediment Transport Processes work unit, Research Division (CR), CERC. This report has substantially the same content as the thesis submitted to Mississippi State University by Ms. Cialone in partial fulfillment of the requirements for an M.S. degree in Civil Engineering. Dr. Kraus was the thesis advisor. This study was performed under general supervision of Dr. James R. Houston, Chief, CERC; Mr. Charles C. Calhoun, Jr., Assistant Chief, CERC; and Dr. Charles L. Vincent, Program Manager, Shore Protection and Restoration Program, CERC; and under direct supervision of Mr. H. Lee Butler, Chief, CR, CERC.

COL Dwayne G. Lee, CE, was Commander and Director of WES during publication of this report. Dr. Robert W. Whalin was Technical Director.

TABLE OF CONTENTS

TABLE OF CONTENTS (Continued)

LIST OF TABLES

LIST OF FIGURES

LIST OF FIGURES (Continued)

I. INTRODUCTION

A finite amplitude wave refraction and shoaling numerical model based on Stokes third-order wave theory is developed in this report. Improved prediction methods for wave refraction and shoaling are needed to better estimate waves in the nearshore zone, which generate nearshore currents and sediment transport. The finite amplitude wave model developed in this report uses a more accurate description of water wave propagation than the commonly applied small amplitude wave theory. In finite amplitude wave theory, a more accurate representation of the wave motion is obtained by retaining terms neglected in small amplitude wave theory.

The model developed herein is intended to take monochromatic waves from deep or "deeper" water to intermediate depth water. It, or any other model based on Stokes wave theory, cannot be used to directly calculate breaking waves. This is a theoretical limitation well documented and examined in this study. However, the model can be used to provide the seaward boundary condition for a shallow water wave model based on cnoidal or small amplitude wave theory, for example.

A major part of this report is the derivation of the wave energy flux to third-order using the 3rd-order Stokes wave theory of Isobe and Kraus (1983a). Although others have developed expressions for the energy flux, the derivation of this fundamental quantity has never been clearly described. In addition, there are some problems with previous work. The expression for the energy flux given by Tsuchiya and Yasuda (1981) appears to be divergent in the deepwater limit and the expression for the flux given by Le Méhauté and Webb (1964) is somewhat inconvenient for applications. The derivation of the energy flux given in this study is unique in that Stoke's second definition of wave celerity (defined in Section II) is used to condense the integration for the energy flux.

The energy flux and irrotationality condition of the fluid are employed to calculate finite amplitude wave properties (height and direction) directly on a bathymetric grid. The calculation procedure is simpler to program than the traditional wave ray method. The program is verified by computing special limiting cases for which exact solutions are known, as well as by comparison to laboratory data. Example calculations for irregular bathymetry are also given.

II. HISTORICAL WORK ON STOKES WAVE THEORY

George Gabriel Stokes (Stokes 1847) is the originator of the wave theory bearing his name. Stokes derives a solution to the water wave problem for waves of permanent form and finite height by using a trigonometric series. In his theory, the unknown variables describing the flow are developed as power series in terms of a small physical quantity called the perturbation parameter. (Stokes selects the wave steepness, H/L , where H is the wave height and L is the wavelength, as the perturbation parameter, hence the theory is valid in relatively deep water.) Using a perturbation procedure, successive approximations of presumably higher accuracy can be developed. Linear or small amplitude wave theory is found to be a first approximation of the wave motion. Stokes found it difficult to obtain terms beyond the second approximation due to the nonlinearity of the free surface boundary conditions and because the free surface itself is an unknown function of the independent variables. Consequently, Stokes obtains the third approximation by another method: a double power series expansion. This method is based on the assumption that a series solution exists in terms of trigonometric and hyperbolic functions whose arguments are multiples of those Stokes had already obtained for the first and second-order approximations. Thus is formed a Stokes wave: a progressive wave with a surface profile represented by a series of cosine functions. Higher-order solutions are obtained more easily by extending Stoke's first method to include the perturbation expansion of the free surface, the wave celerity, and the velocity potential. This eliminates the need for an *a priori* assumption about the form of the free surface.

To simplify the solution process, Stokes wave theory (and all perturbation-type wave theories) are derived in a reference frame moving with the wave celerity, rendering the motion steady. Hence, the wave celerity must be specified to convert the solution to a fixed reference. In the moving reference frame a unique solution exists, but the wave celerity must be specified by some physical consideration apart from the perturbation procedure to convert to the fixed reference frame.

Stokes realized there were many ways to specify the wave celerity. After considering the physics of the wave problem, he proposed two definitions of wave celerity, which are generally called the "first definition" and "second definition" of Stokes. The first definition states that the average value of the horizontal water particle velocity over one wave period is zero in the fixed coordinate system, or mathematically:*

$$C = \frac{\int_0^T (C + u)\, dt}{\int_0^T dt} . \tag{2.1}$$

The second definition states that the average mass transport over one wave period through a vertical section is zero in the fixed coordinate system, or mathematically:

$$C = \frac{\int_0^T \int_{-D}^{N} (C + u)\, dz\, dt}{\int_0^T \int_{-D}^{N} dz\, dt} . \tag{2.2}$$

---

* Notation is defined in Fig 3.1 and Appendix F.

Other definitions of wave celerity have been proposed. The definition of wave celerity used by various authors of Stokes-type wave theories will be introduced with each theory. In general, it is found by calculation that the numerical value of the celerity does not vary greatly between definitions. However, there is a theoretical or philosophical distinction.

Skjelbreia and Hendrickson (1960) use five terms in a Stokes-type trigonometric series and the first definition of wave celerity to obtain a fifth-order wave theory. They assume a perturbation trigonometric series form for the velocity potential and water surface elevation, and a perturbation series form for the wave celerity and Bernoulli constant. By substituting the series into the two free surface boundary conditions, they evaluate the twenty unknown series constants using an iterative method. The procedure involves grouping terms of equal order of the perturbation parameter and sub-grouping terms of equal power of the cosine function. This results in twenty equations which are solved for the twenty unknown series constants. Lastly, Skjelbreia and Hendrickson solve for the wave number and perturbation parameter. The results of their theory and the values of the series coefficients are presented in tabular form. (It should be noted that Nishimura, Isobe, and Horikawa (1977) found a sign error in the expression for the fourth-order wave celerity of Skjelbreia and Hendrickson.)

Skjelbreia and Hendrickson compare their results to those of small amplitude wave theory and the third-order approximation of Skjelbreia (1958). A secondary hump in the third-order wave profile with an Ursell number (defined in Equation 3.21) of 43.2 was found. It is now known that such a distortion results from the application of Stokes theory beyond its range of validity. This will be discussed in Section III C.

De (1955), Chappelear (1961), and Fenton (1985) also present fifth-order Stokes wave theories. Fenton uses an extrapolation method to numerically check various fifth-order wave theories. From this process, Fenton concluded that his and Chappelear's theories are numerically correct to fifth-order, but Skjelbreia and Hendrickson's theory has an error in the dynamic free surface boundary condition. In order to find this error, Fenton rederives his solution using Skjelbreia and Hendrickson's expansion parameter. Thus, Fenton numerically found the sign error in the fourth-order wave celerity term, previously discovered by Nishimura, Isobe, and Horikawa (1977). Any applications of Skjelbreia and Hendrickson's theory which have not incorporated the proper sign in the wave celerity expression are therefore incorrect at fifth-order. Since Fenton found Chappelear's theory to be numerically correct at fifth-order, he concluded that discrepancies between Chappelear and De's theories meant De's theory is also incorrect at fifth-order.

Dailey (1978) summarizes and applies the fifth-order wave theory of Chappelear (1961) to calculate water particle velocities and accelerations. (This fifth-order application is a good source for engineering use). Dailey evaluates the wave number, wave steepness and relative water depth by using an iterative technique to solve three nonlinear equations.

Le Méhauté and Webb (1964) use the principle of conservation of transmitted energy (energy flux) to calculate wave shoaling. They extract a third-order wave theory from the fifth-order analytical solution of Skjelbreia and Hendrickson to use for their calculations of energy flux, average energy, and group velocity to a third order of approximation. A comparison of theoretical and experimental results showed that higher-order theoretical approximations better described the experimental data than linear wave theory. They recommend using Stokes theory for values of the Ursell number (see Section III C) less than ten.

Koh and Le Méhauté (1966 a,b) use the principle of conservation of energy flux and the fifth-order solution of Skjelbreia and Hendrickson to calculate wave shoaling. They found that the fifth-order theory predicts a shoaling coefficient larger than linear wave theory, but slightly smaller than third-order theory. Koh and Le Méhauté recommend using third-order theory because its range of applicability is the one most often encountered ($.10 < D/L < .25$, where D is the water depth and L is the wavelength).

Tsuchiya and Yamaguchi (1972) recalculate the Stokes wave theory of Skjelbreia and Hendrickson to a fourth order of approximation using Stoke's second definition of wave celerity. Using the experimental results of Iwagaki and Yamaguchi (1968), they found the theoretical wave celerity for fourth-order Stokes waves using the second definition of wave celerity gave better agreement with experimental laboratory data than the theoretical wave celerity using the first definition. Tsuchiya and Yamaguchi conducted an experiment to calculate the horizontal water particle velocity at the wave crest and trough. It appears that the theory using the second definition of wave celerity yields slightly better results than the theory using the first definition. By comparing the theoretical and experimental wave profiles, Tsuchiya and Yamaguchi show that both theories agree with the experimental data quite well in Figure 2.1. It should be noted that the Ursell number is 19 in Figure 2.1 and 133 in Figure 2.2. Secondary humps in Figure 2.2 are due to the application of Stokes wave theory beyond its range of validity. This will be discussed in Section III C.

Tsuchiya and Yasuda (1981) develope a Stokes wave theory to third order without direct specification of a definition of wave celerity. Instead, Tsuchiya and Yasuda make an assumption about the periodicity of the velocity potential. Expressions for the kinetic energy and energy flux are derived. Although not stated by the original authors, a problem appears to exist in their solution. In the deepwater limit, their determined energy flux diverges exponentially. This will be discussed in Section III E.

Bretschneider (1960) presents a finite amplitude wave theory which is complete to any order for which it is calculated. He uses a summation harmonic series, with each term in an unexpanded form. Expansion of the hyperbolic and trigonometric terms in the series results in an approximation to the exact theory which is identical to Stokes wave theory to the same order. Bretschneider notes that there is some loss in accuracy in the expanded form. This may be because the unknown free surface is approximated by a finite number of terms. In his paper, the coefficients for the unexpanded and expanded forms are given for orders one through five. This theory does not appear to have had wide acceptance in the coastal engineering field.

Schwartz (1974) extends Stoke's perturbation theory to order seventy using a computer to determine the series coefficients. Rather than

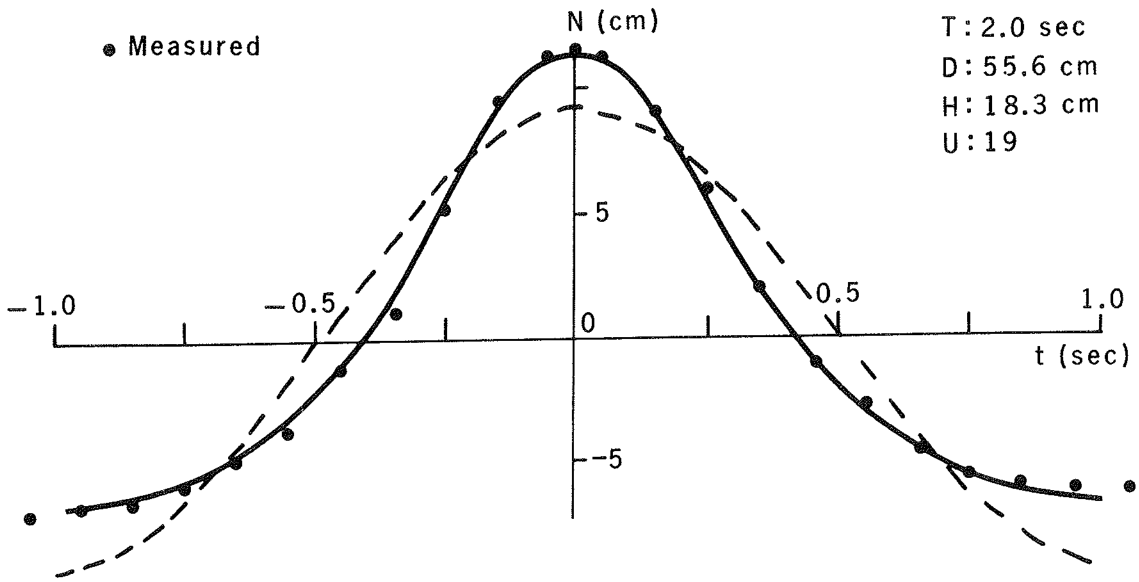

Figure 2.1. Theoretical versus experimental wave profiles (after Tsuchiya and Yamaguchi 1972)

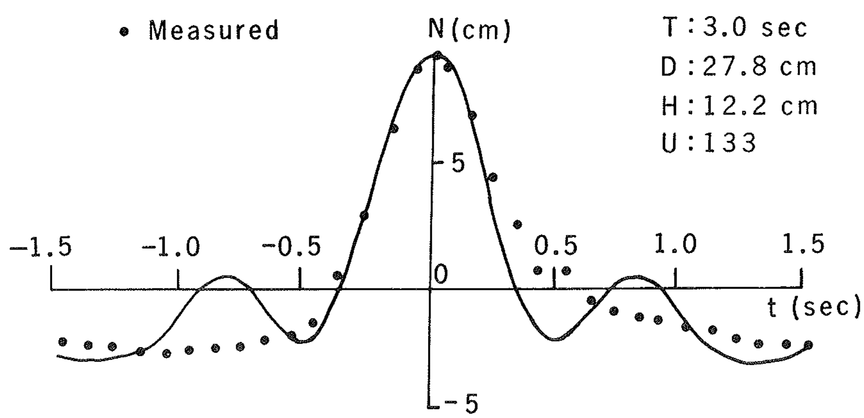

Figure 2.2. Theoretical versus experimental wave profiles (after Tsuchiya and Yamaguchi 1972)

solve the problem in the physical plane, he maps one fluid cycle (wavelength) into an annulus in the complex plane to simplify the calculations, and uses Pade approximations of polynomials to aid in the series summations. In order to accurately predict the highest wave (Michell 1893, Havelock 1919), Schwartz reformulates the problem with wave height as the independent parameter. A single-valued function of the transformation coefficient is thus obtained. For the transformed case, solutions to order H^{48} are computed in finite water depths and solutions to order H^{117} are computed for infinite depth water.

Nishimura, Isobe, and Horikawa (1977) also derive very high-order solution of Stokes waves using a computer to determine the series coefficients.

Finally, Isobe and Kraus (1983a) present a pedagogical derivation of a third-order Stokes wave theory, applying Stoke's second definition of wave celerity. The wave celerity resulting from the first definition is also given. The systematic methodology used by Isobe and Kraus in their solution process makes their derivation clean and useable, unlike many other solutions which are not fully developed or use a difficult notation. Therefore, it is Isobe and Kraus' derivation that is used as a basis for the calculations of the wave energy, energy flux, and group velocity for this thesis. A summary of the third-order derivation by Isobe and Kraus is given in Section III B.

III. STOKES WAVE THEORY

A. Overview of Finite Amplitude Wave Theory

In order to understand finite amplitude wave theory, one must have a clear understanding of small amplitude wave theory and the water wave boundary value problem.

Small amplitude (or linear) wave theory is the first approximation to a more rigorous theoretical description of wave behavior. In fact, small amplitude wave theory results as the leading order solution of Stoke's formal perturbation theory. In this developement, the wave height is assumed to be infinitessimal. One might think of linear wave theory as the base from which to build a Stokes wave theory or as a finite amplitude wave theory in which the wave height is infinitely small.

The objective of any wave theory is to formulate and solve a boundary value problem describing the behavior of water wave motion. The formulation of a boundary value problem involves expressing the physical situation in mathematical terms to obtain a unique solution. The solution to a surface wave, boundary value problem generally involves the determination of three basic unknowns: the free surface elevation, N, the velocity potential, Φ, and the pressure, P. The formulation of the surface water wave boundary value problem will be briefly described.

1. A region of interest is established (Figure 3.1). The solution to a given boundary value problem depends on the wave height, H, the wavelength, L, and the water depth, D, as shown in Figure 3.1. Three characteristic, dimensionless ratios can be obtained from these three quantities: H/L, H/D, and L/D. Waves become more nonlinear

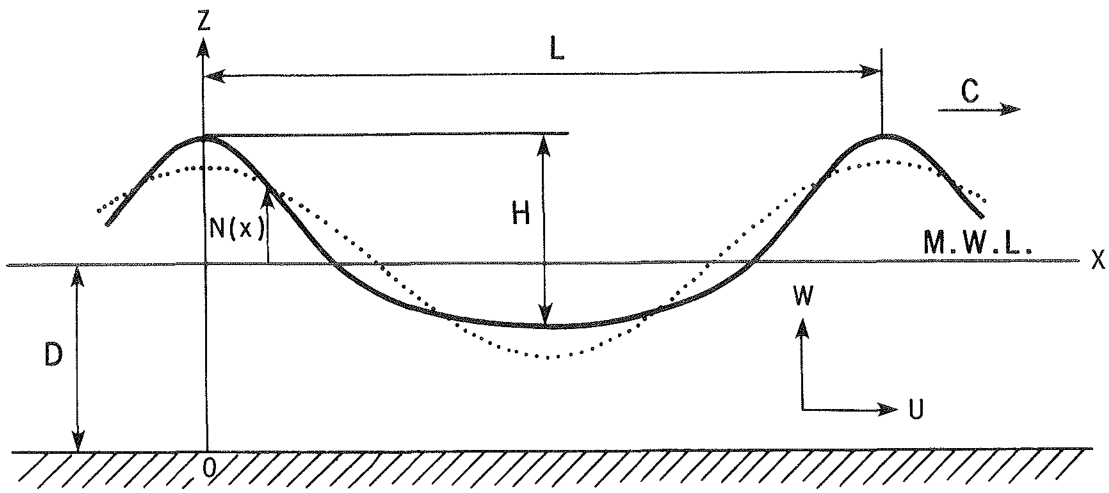

Figure 3.1. Definition sketch (after Isobe and Kraus 1983a)

(or finite) as these ratios increase. A more detailed description will be presented in Section III C.

2. Next, one determines a differential equation that must be satisfied within the region of interest. For irrotational flow in an incompressible fluid, a velocity potential exists which satisfies the two-dimensional continuity equation (the Laplace equation):

$$\nabla^2 \Phi = 0 \ . \tag{3.1}$$

This is the linear, partial differential equation which governs the region of interest.

3. In order to solve the governing equation, one must specify the boundary conditions of the problem. That is, there could be an infinite number of solutions to the differential equation; the boundary

conditions determine the solution which is relevant to the physical situation. The kinematic boundary conditions mathematically state that there is no flow across an interface, in order for the interface to exist. The kinematic bottom boundary condition for a horizontal bottom is simply

$$w = 0 \qquad \text{at } z = -D \,, \tag{3.2}$$

or in words, flow at a horizontal bottom is tangential to the bottom. The kinematic free surface boundary condition is

$$w = \frac{\partial N}{\partial t} + u \frac{\partial N}{\partial x} \qquad \text{at } z = N \,, \tag{3.3}$$

or in words, a particle on the free surface remains on the free surface. The dynamic free surface boundary condition describes the pressure distribution on the free surface. A free surface cannot support a pressure variation as can a fixed or solid surface; it deforms to maintain uniform pressure. The dynamic free surface boundary condition is described by the Bernoulli equation:

$$\frac{\partial \Phi}{\partial t} + \frac{1}{2}\left(u^2 + w^2\right) + gN = \frac{P_B}{\rho} \qquad \text{at } z = N, \tag{3.4}$$

where P_B/ρ is defined as the Bernoulli constant. The pressure at the free surface was taken to be zero at the free surface, by convention.

The lateral boundary conditions for the region of interest are prescribed by:

$$\overline{N} = 0 \tag{3.5a}$$

and

$$N(0) - N\left(\frac{L}{2}\right) = H \; . \tag{3.5b}$$

The Bernoulli equation

$$\frac{\partial \Phi}{\partial t} + \frac{1}{2}(u^2 + w^2) + gz + \frac{P}{\rho} = \frac{P_B}{\rho} \tag{3.6}$$

is also needed in the solution process if the pressure is required.

4. The water wave problem represented by Equations 3.1 through 3.6 is solved for the velocity potential (which yields the water particle velocities), free surface elevation, and the pressure. Methods of solution include linearization, power series, and numerical methods. Small amplitude wave theory falls under the first category of solution method. The wave height is assumed to be much smaller then the wavelength. A further assumption of small amplitude wave theory is that all motions are small. Terms involving squares of the velocity components then become negligible. (After the linearized solution is obtained, these assumptions can be checked.) Thus, small amplitude wave theory simplifies the solution to the water wave problem by: (1) linearizing the free surface boundary conditions, and (2) prescribing the free surface boundary conditions at $z = 0$.

In finite amplitude wave theory, the free surface boundary conditions are nonlinear and prescribed at $z = N$, where N is the unknown free surface elevation. Power series solutions in terms of a small perturbation parameter can be found in these cases. Stokes wave theory and cnoidal wave theory both use power series solutions.

In Stokes wave theory, the wave steepness is regarded as a small parameter and the solution is developed for finite values of the relative water depth. The small parameter is called the perturbation parameter and the other parameter is called the auxiliary parameter by Isobe and Kraus (1983a). Stokes theory is valid in relatively deep water where the wave steepness is not large and the relative water depth is fairly large. The validity of Stokes theory, to any order, breaks down in shallow water ($D/L<0.1$), where the wave steepness becomes increasingly large and the relative water depth approaches zero.

In cnoidal wave theory (Korteweq and DeVries 1895, Keulagan and Patterson 1940, Isobe and Kraus 1983b), the relative wave height is taken as the perturbation parameter and the modulus of the elliptic integral is commonly taken as the auxiliary parameter. Hence, cnoidal theory is valid in relatively shallow water ($.02<D/L<.10$) (Keulagan and Patterson 1940). Unlike Stokes wave theory, for which the first-order solution is equivalent to small amplitude wave theory, the first-order solution of cnoidal wave theory is nonlinear.

The third method of solving the wave problem is a numerical solution (e.g., Dean 1965). In a numerical solution, the differentials are replaced by finite differences. Such solutions are not convenient in engineering applications because they require tables. Numerical methods are also computer intensive, and not easily adaptable to microcomputers. Unlike analytical solutions, in which the equations for the various physical quantities can be explicitly studied and insights obtained, numerical methods lack this capability because the coefficients are determined numerically. However, numerical methods of solution can provide solutions of very high accuracy.

B. A Third-Order Stokes Wave Theory

A complete derivation of a Stokes third-order wave theory is given by Isobe and Kraus (1983a). Their solution is used as the basis for the finite amplitude wave refraction and shoaling model developed in this report; therefore, a summary of the derivation of their solution method is in order.

Governing Equations

The conservation of mass equation for two-dimensional, irrotational motion in an inviscid, incompressible fluid reduces to the Laplace equation:

$$\Psi_{xx} + \Psi_{zz} = 0 \tag{3.7}$$

or

$$\nabla^2\Psi = 0 \ , \tag{3.8}$$

where Ψ is the stream function. The subscripts denote partial differentiation with respect to that variable. Surface water wave motion is described by this partial differential equation. Figure 3.1 displays the region of interest. In this figure, H denotes the wave height, L is the wavelength, D is the water depth, N is the water surface elevation, C is the wave celerity, and x and z are the horizontal and vertical coordinates, respectively. Equation 3.8 is the governing equation for this region. The boundary conditions are:

$$\Psi = 0 \qquad \text{at } z = -D \ , \tag{3.9}$$

$$\Psi = Q \qquad \text{at } z = N \ , \tag{3.10}$$

and

$$\frac{1}{2}\left(u^2 + w^2\right) + gN = \frac{P_B}{\rho} \qquad \text{at } z = N \ , \tag{3.11}$$

where Q is the flow rate across a vertical section, g is the gravitational acceleration, ρ is the fluid density, and P_B/ρ is the Bernoulli constant. The steady-state Bernoulli equation,

$$\frac{1}{2}\left(u^2 + w^2\right) + gz + \frac{P}{\rho} = \frac{P_B}{\rho} \ , \tag{3.12}$$

is also needed in the solution process if the pressure is required. Steady-state motion is achieved by allowing the coordinate system to move with the wave celerity, C. Two additional equations used for obtaining a solution,

$$\overline{N} = 0 \tag{3.13}$$

and

$$N(0) - N\left(\frac{L}{2}\right) = H \ , \tag{3.14}$$

follow from the definition of water depth, D, and wave height, H, respectively. (It should be noted that in order to simplify the solution process, all the parameters are nondimensionalized as follows:

η = free surface elevation = kN

d = still water depth = kD

q = flow rate = kQ/C_{IK}

p = pressure = kP/C_{IK}

ψ = the stream function = $k\Psi/C_{IK}$

$C_{IK} = \sqrt{\frac{g}{k} \tanh kD}$.)

Solution Process

Equations 3.8 through 3.14 are used to solve for the stream function, water surface elevation, and the pressure. A general analytical solution cannot be obtained because of the nonlinearity of the free surface boundary conditions, but a power series solution can be found (Stokes wave theory and cnoidal wave theory).

In a perturbation method, it is assumed that the solution can be represented by a power series expansion in terms of a small parameter known as the perturbation parameter. In the Isobe-Kraus derivation, the perturbation parameter, ε , is proportional to the wave steepness and is given by:

$$\varepsilon = \frac{kH}{2} . \tag{3.15}$$

The auxiliary parameter, δ , is proportional to the relative water depth and is given by:

$$\delta = kD . \tag{3.16}$$

Isobe and Kraus apply standard perturbation methods to the unknown variables, much as Stokes had done. That is, all variables to be solved for (ψ, η, p, q) are expanded in a power series of the perturbation parameter. For example:

$$\psi = \psi_0 + \varepsilon\psi_1 + \varepsilon^2\psi_2 + \varepsilon^3\psi_3 + \ldots . \tag{3.17}$$

The series expansion of ψ is then substituted into the governing equation and bottom boundary condition and terms of equal order of the perturbation parameter are gathered. According to the theory of power series, the coefficients of each order of epsilon on the left and right-hand sides must be equal. To third order, this results in eight equations from Equations 3.1 and 3.2. The free surface boundary conditions need a closer examination because they are nonlinear in ψ and η . A Taylor series expansion of η about the mean water level is used to approximate η at the free surface. The expansion is substituted into the free surface boundary conditions and again, equal orders of epsilon are gathered. This results in eight additional equations from the two unexpanded free surface boundary conditions. Expansion of Equations 3.13 and 3.14 result in eight more equations.

The problem now consists of determining the nondimensional series coefficients at each order of i (ψ_i , η_i , p_i , q_i ,...). This is done in a systematic manner, beginning with the first-order equations. The zeroth-order equations are those equations that are a function of ε to the power zero, therefore they are treated in a simpler manner. First, two observations are made which simplify the solution: (1) It is clear that the zeroth-order contribution to the stream function describes uniform flow and is therefore only a function of the elevation z, or:

$$\psi_0 = b_{00}\, z \ , \tag{3.18}$$

where b_{00} is an arbitrary constant to be determined. (2) The zeroth-order surface elevation is the mean water level:

$$\eta_0 = d \ , \tag{3.19}$$

which must be true in the absence of wave motion. The quantities q_0 and p_0 are also a function of the constant b_{00} . It becomes apparent in the course of the derivation that the solution to the zeroth order is not fully determined until the the series constant b_{00} is determined. This is accomplished at the first order of solution. This process is repeated at every order of the solution procedure. Therefore, a solution to a given order is not complete until part of the solution to the next higher order is determined.

The systematic procedure used to solve for the higher order equations consists of the following steps:

(1) Separation of variables is applied to the nth-order stream function.

(2) The derivatives of the nth-order stream function are substituted into the nth-order Laplace equation.

(3) The solution for the nth-order stream function is deduced from the differential equation.

(4) The solution for η_n , q_n , and p_n follow by simple substitutions and only one constant, b_{on} , remains unknown. This must be determined at the next order of solution.

The highest order of solution desired in this case is third order and, in principle, the solution process must continue to fourth order to determine the third-order unknown constant, b_{03} . However, Isobe and Kraus argued that there is a pattern in the constants $b_{00} \neq 0$, $b_{01} = 0$, $b_{02} \neq 0$, and concluded that b_{03} must equal zero. This completes the solution for ψ , η , p , and q in the moving coordinate system to a third order of approximation.

C. Range of Validity

The problem of selecting the most suitable finite amplitude wave theory for a given application will be discussed. It is a difficult problem because different theories may better reproduce particular characteristics of interest (C , u , w , N) for a given set of wave conditions.

Small amplitude wave theory is commonly assumed to be uniformly valid over the entire range of relative water depths, whereas the range of validity of finite amplitude wave theories is more restrictive. (In fact, small amplitude wave theory is not valid in many cases; however, since it is always "well behaved," it is often applied.) In the derivation of small amplitude wave theory, the wave height is regarded as an extremely small quantity, whereas in finite amplitude wave theory the wave height is allowed to take on realistic values. Thus, the wave steepness (H/L) and relative wave height (H/D) parameters become significant in finite amplitude wave theory. (Two parameters are needed to describe waves of permanent form.) The standard approach is to regard one parameter as small and develop a theory for finite values of the other parameter. Isobe, Nishimura, and Horikawa (1982) demonstrated that a so-called double-series perturbation approach was inferior to the single-series approach. The single-series procedure results in two main categories of perturbation-type, finite amplitude wave theories: Stokes wave theory and cnoidal wave theory. For Stokes theory, the wave steepness, H/L , is assumed to be small and the theory is developed for finite values of the relative water depth, D/L . For cnoidal wave theory, the relative wave height H/D is regarded as a small quantity and the theory is developed, in effect, for finite values of the shallow water Ursell parameter U_s , where

$$U_s = \frac{gHT^2}{D^2} . \tag{3.20}$$

The range of validity of both Stokes and cnoidal theories have been quantitatively examined by several authors (Laitone 1962; Dean 1970; Le Méhauté 1976; Nishimura, Isobe, and Horikawa 1977). Le Méhauté summarizes the results on the range of validity of perturbation wave theories in graphical form (Figure 3.2).

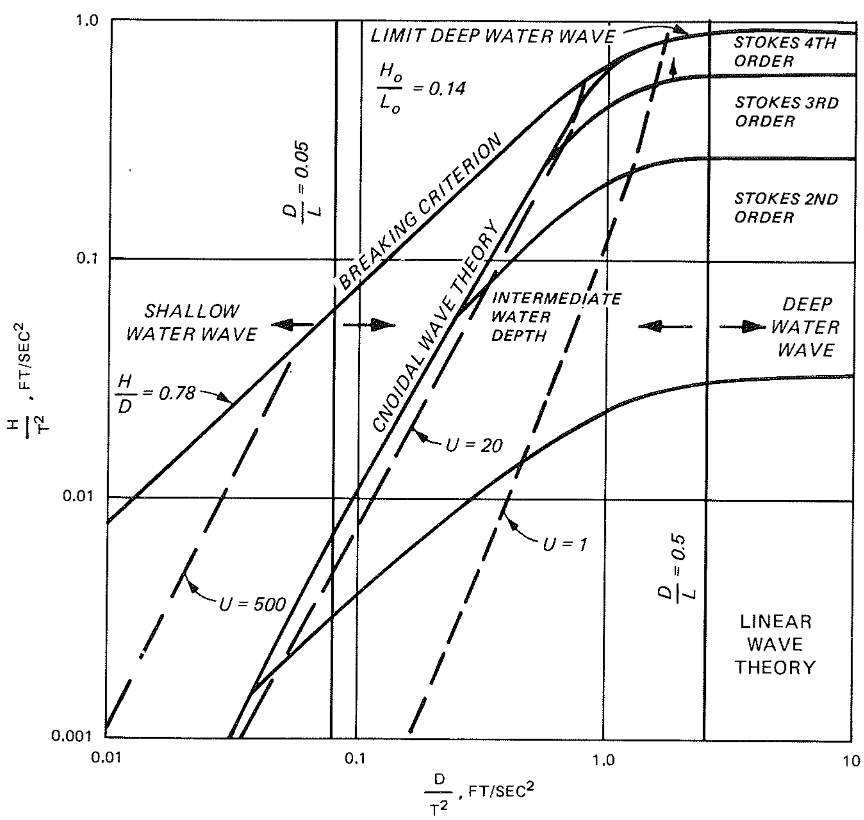

Figure 3.2. Limits of validity of various wave theories (after Le Méhauté 1976)

Keulegan (as presented by Rouse 1950) classifies Stokes, cnoidal, and solitary wave theories according to: (1) the relative importance of the wave steepness and relative wave height and (2) the value the relative water depth. Keulegan does not establish exact ranges of validity, but states that Stokes-type wave theories are generally applicable in the region where $D/L > 0.10$. Cnoidal theories are applied in the region $0.10 > D/L > 0.02$, overlapping the Stokes theory region near a relative water depth value of 0.10. Solitary wave theory is applied in very shallow water ($D/L < 0.02$). Figure 3.3 displays Keulegan's classification of finite amplitude waves.

Laitone (1962) evaluates the ranges of validity of third-order Stokes theory and cnoidal theories by comparing wave celerities. He found that Stokes theory is applicable for $D/L > 0.125$ and cnoidal theories are applicable for $D/L < 0.20$. These results are limited because only a reasonable value of the wave celerity is considered. The accuracy of other parameters (u, w, N) may be poor.

Dean (1970) evaluates the numerical fits of forty wave conditions to the two free surface boundary conditions to find the relative validity of several water wave theories. The Simpson's rule numerical approximations to the root-mean-square errors are defined by Dean for the kinematic and dynamic free surface boundary conditions. This is used to measure the boundary condition errors for the various wave theories for different wave conditions. Figures 3.4a and 3.4b show the results of Dean's investigation. Dean emphasizes that the method used to assess the various theories does not necessarily imply the best overall fit,

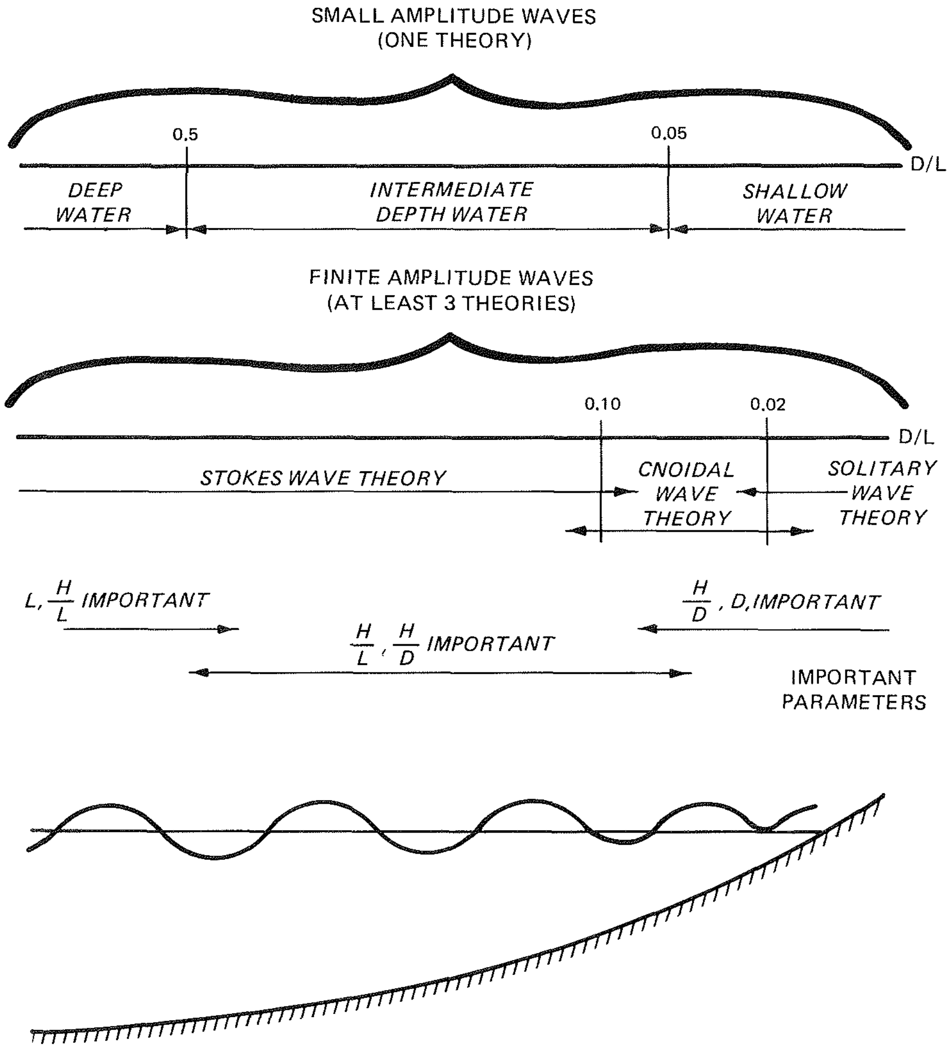

Figure 3.3. Classification of finite amplitude waves
(after Keulegan, as presented by Rouse, 1950)

but rather the best fit to the free surface boundary conditions.

Nishimura, Isobe, and Horikawa (1977) investigate the convergence domains of very high-order Stokes and cnoidal solutions using a Dombs-Sykes (1957) type of plot. Figure 3.5 shows the convergence domains estimated by Nishimura, Isobe, and Horikawa. In the figure, A1 is the coefficient of the first component in their solution for the surface profile. The authors point out that the convergence domains depend on the definition of the perturbation and auxiliary parameters, ε and δ, respectively. Isobe and Kraus' (1983a,b) derivations of a third-order Stokes theory and a second-order cnoidal theory are governed by these convergence ranges.

In summary, perturbation theories (such as Stokes and cnoidal theory) are valid over certain ranges. A perturbation theory is described as being "outside its range of validity" if the contributions from higher-order terms in a perturbation series become comparable or larger than lower-order terms. This will be discussed in the following paragraph.

Generally, Stokes theory is valid in relatively deep water and cnoidal theory is valid in relatively shallow water, but the range of validity of Stokes and cnoidal theories overlap in relatively shallow water. In the overlap region the Ursell parameter, defined as

$$U = \frac{HL^2}{D^3} , \tag{3.21}$$

can be used to decide which theory is applicable, since it incorporates both the relative wave height and wave steepness. (Actually, the Ursell

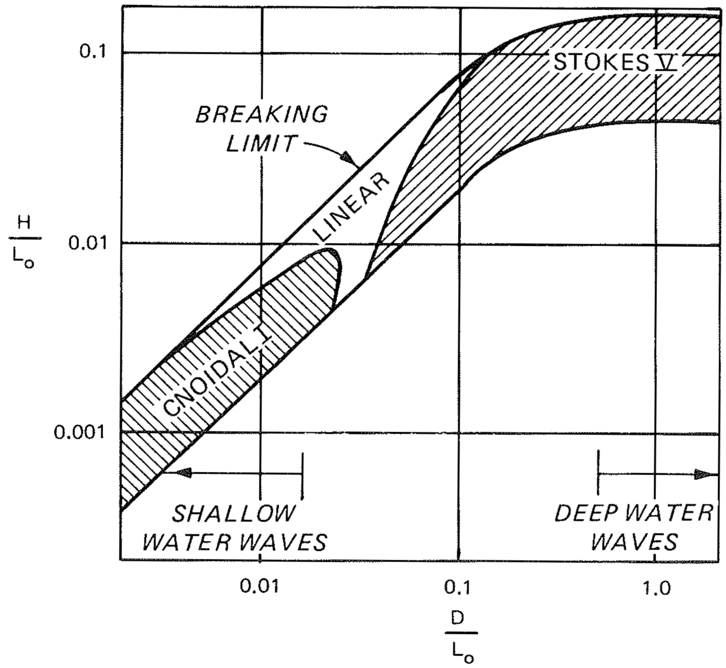

Figure 3.4a. Periodic wave theories providing best fit to dynamic free surface boundary condition (analytical theories only) (after Dean and Dalrymple 1984)

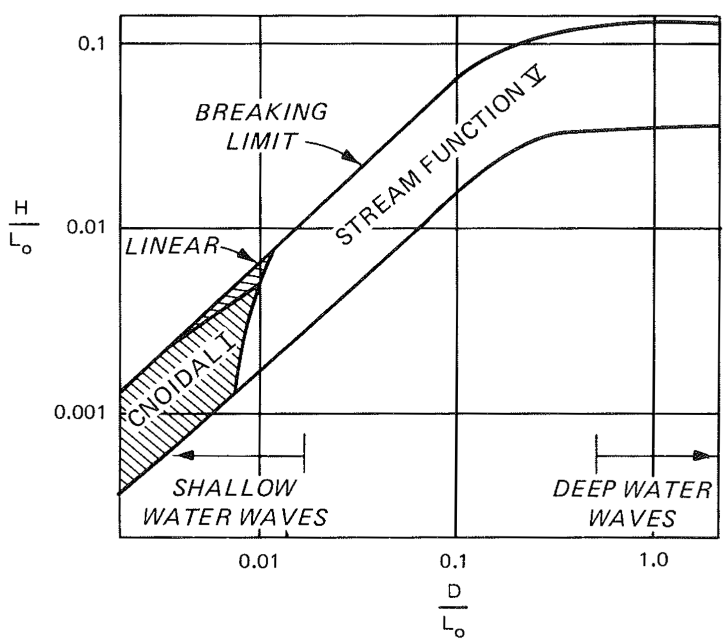

Figure 3.4b. Periodic wave theories providing best fit to dynamic free surface boundary condition (analytical and stream function theories) (after Dean and Dalrymple 1984)

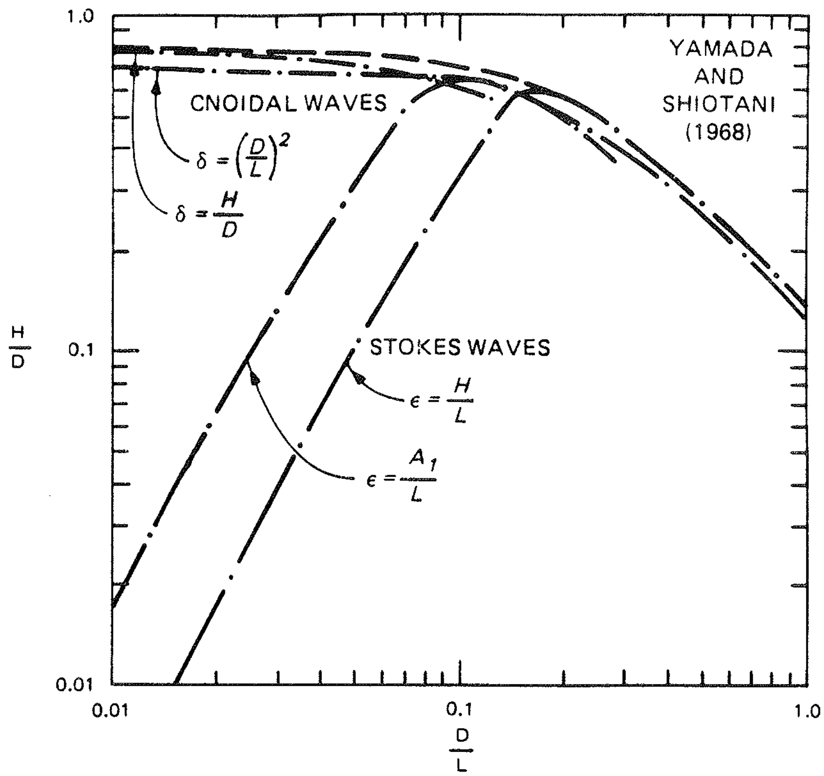

Figure 3.5. Convergence domain of the Stokes Wave
(after Nishimura, Isobe, and Horikawa 1977)

parameter reduces to U_s of Equation 3.18 in the overlap region, where the depth is relatively shallow.) Various recommendations have been made for the critical value of the Ursell parameter separating the ranges of validity of Stokes and cnoidal wave theory. The various recommendations for the critical Ursell number are covered in a discussion recently given by Kraus, Cialone, and Hardy (1987). Stokes theory should be used if the Ursell number is less than the critical value and cnoidal theory should be used if the Ursell number is greater than the critical value. The critical value of the Ursell parameter is somewhat dependent on the details of the theory (e.g., definition of wave celerity and selection of expansion parameters), and on the criterion used to judge validity (e.g., Dean's (1965, 1970) boundary condition fit, comparison to a particular measured quantity (u , w , N) as Laitone (1962) did, or existence of secondary peaks in the wave profile). Table 3.1 displays critical values of the Ursell parameter explicitly stated or inferred from context from several sources. Chu (1975), who was one of the first to attempt to model the refraction and shoaling of finite amplitude waves, switches between third-order Stokes theory and first-order cnoidal theory at an Ursell number of:

$$U = 7.5 + \frac{25H}{D} \ . \tag{3.22}$$

Table 3.1

Critical Values of the Ursell Parameter

Source	Critical U
Le Méhauté and Webb (1964)	10
Skovgaard and Petersen (1977)	15
Dean (1970)	20
Isobe, Nishimura, and Horikawa (1982)	25
Isobe and Kraus (1983 a,b)	25
Le Méhauté (1976)	26
Shore Protection Manual (1984)	26
Horikawa (1978)	30
Laitone (1962)	48

Some examples of problems associated with range of validity were noted earlier in the literature (Skjelbreia and Hendrickson 1960, and Tsuchiya and Yamaguchi 1972). Following Isobe and Kraus (1983a), a critical Ursell number of 25 is deemed suitable (Table 3.1) and Stokes theory should be used if the Ursell number is less than or equal to this value. Skjelbreia and Hendrickson applied Stokes theory well beyond this limit ($U = 43.2$). Tsuchiya and Yamaguchi's application yields an Ursell number of 133, clearly outside the range of validity of Stokes wave theory. In such cases, secondary humps in the wave profile are observed and erroneous numerical values are obtained.

D. Derivation of Energy Flux, Energy, and Group Velocity

From the conservation of wave energy, the onshore energy flux per unit alongshore length is constant. Energy flux, F, is defined as the rate at which energy is transferred from a generating source (e.g., a rock thrown into a pond) to any given location. It is the time rate of doing work. Mathematically,

$$F = \int_{-D}^{N} f_i \, u \, dz \, , \tag{3.23}$$

where

F = energy flux,

f_i = external forces on the system,

u = horizontal water particle velocity,

dz = incremental unit of depth,

$-D$ = elevation of the bottom, and

N = free surface elevation.

The mean energy flux, $\overline{F}$, is given by:

$$\overline{F} = \frac{1}{T} \int_{t}^{t+T} \int_{-D}^{N} f_i \, u \, dz \, dt \, , \tag{3.24}$$

where

T = wave period

dt = incremental unit of time.

Denoting the time average over one wave period with an overbar, Equation 3.24 is equivalently,

$$\overline{F} = \overline{\int_{-D}^{N} f_i \, u \, dz} \, . \qquad (3.25)$$

What forces, f_i , *transfer energy from one fluid section to another?* The dynamic pressure f_1 (including the potential energy) and the inertia force per unit volume, f_2 , transfer wave energy:

$$f_1 = P + \rho g(z - \overline{N}) \qquad (3.26)$$

$$f_2 = \frac{\rho}{2} (u^2 + w^2) \qquad (3.27)$$

Inserting (3.26) and (3.27) into (3.25) yields:

$$\overline{F} = \overline{\int_{-D}^{N} \left[P + \rho g(z - \overline{N}) + \frac{\rho}{2} (u^2 + w^2)\right] u \, dz} \, . \qquad (3.28)$$

This is equivalent to Phillip's (1977) Equation 3.6.17 and Horiguchi's (1982) Equation 1. Expanding and rearranging,

$$\overline{F} = \rho \overline{\int_{-D}^{N} \left[\frac{P}{\rho} + gz + \frac{1}{2} (u^2 + w^2) - g\overline{N}\right] u \, dz} \, . \qquad (3.29)$$

From the Bernoulli equation, Equation 3.29 can be written in the following form:

$$\overline{F} = \rho \overline{\int_{-D}^{N} \left[-\Phi_t - g\overline{N}\right] u \, dz} \, , \qquad (3.30)$$

where Φ_t denotes the partial differentiation of the velocity potential with respect to time. Noting that

$$u = \Phi_x(x - Ct, z) \tag{3.31}$$

(where Φ_x is the partial differentiation of the velocity potential with respect to the direction of wave propagation, x) and

$$\Phi_t = \frac{\partial}{\partial t}\int \phi_x \, dx \ , \tag{3.32}$$

it is concluded that

$$\Phi_t = -Cu + \text{constant} \ . \tag{3.33}$$

Substituting (3.33) into (3.30) and separating (3.30) into two integrals yields:

$$\overline{F} = \rho C \overline{\int_{-D}^{N} u^2 \, dz} \quad -\rho(g\overline{N} + \text{constant}) \overline{\int_{-D}^{N} u \, dz} \ . \tag{3.34}$$

If Stoke's second definition of wave celerity (Equation 2.2) is used, then

$$\overline{\int_{-D}^{N} u \, dz = 0} \ . \tag{3.35}$$

Therefore,

$$\overline{F} = \rho\, C \int_{-D}^{N} \overline{u^2\, dz} \ . \tag{3.36}$$

Thus, the second definition of wave celerity is used to condense the integration for the mean energy flux to one integral and $\overline{F}$ is uniquely determined by evaluating this integral. The derivation of the mean energy flux is not a trivial matter and is given in Appendix A. This fundamental quantity is used for calculating wave shoaling and its determination is a central part of this report.

To a third-order of approximation, the mean energy flux is obtained by evaluating (3.36) with

$$u = u_0 + u_1 \cosh k(z + D) \cos\theta + u_2 \cosh 2k(z + D) \cos 2\theta$$
$$+ u_3 \cosh 3k(z + D) \cos 3\theta \tag{3.37}$$

from the Isobe-Kraus derivation of a third-order Stokes wave theory. The final result from Appendix A is:

$$\overline{F} = \frac{\gamma H^2 n C_{IK}}{8} + \frac{\gamma k^2 H^4 C_{IK}}{16} B \tag{3.38}$$

where:

$$B = -\frac{c(1 + n)}{4kD} + \frac{n}{64}(-27c^6 + 15c^4 - 61c^2 + 57)$$
$$+ \frac{1}{64}(9c^6 + 3c^4 - 13c^2 + 33) + \frac{3 \cosh 2kD(c^2 - 1)}{4(\cosh 2kD - 1)}$$
$$+ \frac{9kD(c^4 - 2c^2 + 1)}{64c \sinh^4 kD}$$

γ = the specific weight of water

H = wave height

$$n = \frac{1}{2}\left(1 + \frac{2kD}{\sinh 2kD}\right)$$

$$C_{IK} = \sqrt{\frac{g}{k} \tanh kD}$$

k = the finite amplitude wave number

c = coth kD.

The average kinetic and potential energy are determined from the following integrals:

$$\overline{KE} = \frac{\rho}{2} \overline{\int_{-D}^{N} (u^2 + w^2)\, dz} \qquad (3.39)$$

$$\overline{PE} = \rho g \overline{\int_{-D}^{N} z\, dz} \; . \qquad (3.40)$$

The evaluation of these integrals yields the average energy per unit surface area of a wave, $\bar{E}$ or:

$$\bar{E} = \overline{KE} + \overline{PE} \; . \qquad (3.41)$$

The final result of the derivation of average energy is:

$$\overline{E} = \frac{\gamma H^2}{8} + \frac{\gamma k^2 H^4}{128}\left[-\frac{c}{kD} + \frac{1}{8}(-9c^6 - 6c^4 - 17c^2 + 24)\right.$$

$$\left. + \frac{3(c^2 - 1)\cosh 2kD}{(\cosh 2kD - 1)}\right] . \qquad (3.42)$$

The actual derivation is given in Appendix B.

The group velocity is defined as the rate at which energy is transferred, or:

$$\overline{F} = \overline{E} C_g \qquad (3.43)$$

therefore,

$$C_g = \frac{\overline{F}}{\overline{E}} . \qquad (3.44)$$

The derivation of C_g for third-order Stokes waves is given in Appendix C.

E. Energy Flux Comparison

As previously stated, energy flux is the fundamental quantity required to calculate wave shoaling and its determination is a central part of this report. Although a limited number of expressions for the energy flux of third-order and fifth-order Stokes waves can be found in the literature, they appear to contain either errors or inconvenient mathematical formulations. Therefore, the energy flux to third order was rederived from the basic equations (Appendix A). Also, the procedure used to calculate the energy flux is unique because Stoke's second definition of wave celerity is used to simplify the integration for $\overline{F}$. A completely independent evaluation of the flux, serves to verify the limited previous work and substantiate the final result, which is of great importance.

Energy flux expressions have been given in three Stokes wave theory developments: Le Méhauté and Webb (1964), Koh and Le Méhauté (1966), and Tsuchiya and Yasuda (1981). Herein, these available expressions for the energy flux are compared at the deepwater limit, where all Stokes theories should approach small amplitude wave theory. (The deepwater limit condition is $kD \rightarrow \infty$.) The expressions do not completely reduce to small amplitude wave theory due to the finite-amplitude effect, as will be shown in this section.

Tsuchiya and Yasuda's theory is derived without direct specification of a definition of wave celerity. Instead, they make an assumption about the periodicity of the velocity potential. Their expression for the energy flux (Tsuchiya and Yasuda 1981, pg. 32, Equation 94) is given as:

$$W = \frac{1}{2}\rho g a^2 C \left[\frac{1}{2}\left(1 + \frac{2kD}{\sinh 2kD}\right) + (ka)^2 \left(\frac{\cosh^2 2kD + 3 \cosh 2kD + 2}{16 \sinh^4 kD} \right.\right.$$

$$+ \frac{3}{4} \sinh^2 kD + \frac{9(2kD + \sinh 2kD)}{64 \sinh^7 kD \cosh kD} + \frac{3(\cosh kD + \cosh 3kD)}{8 \sinh^4 kD \cosh kD}$$

$$\left.\left. + \frac{kD \tanh kD + \sinh^2 kD}{2 \sinh^4 kD} \right) \right] \tag{3.45}$$

where:

W = the mean energy flux = $\overline{F}$

a = the first-order wave amplitude.

This quantity tends to infinity in the deepwater limit due to the second correction term, namely:

$$\frac{3}{4} \sinh^2 kD \ .$$

It is concluded that the expression for energy flux presented by Tsuchiya and Yasuda is divergent and of questionable use in deeper water (assuming there was no typographical error in their expression, Equation 3.45).

Le Méhauté and Webb (1964) extract a third-order wave theory from the fifth-order analytical solution of Skjelbreia and Hendrickson (1960), which uses Stoke's first definition of wave celerity. In their derivation for the mean energy flux, Le Méhauté and Webb simplify the integration by using the Bernoulli equation, as was done in this report (Section III D). Since Skjelbreia and Hendrickson's theory was derived for the first definition of wave celerity, Le Méhauté and Webb could not employ the further simplification based on the second definition of wave celerity, as was done here (Section III D). The average energy flux calculated by Le Méhauté and Webb is given (Le Méhauté and Webb 1964, pg. 29, Equation 19) by

$$F_{avg} = \frac{\pi \rho C_3^2 \lambda^2}{8k^2 T} \frac{1}{s^2} \left\{ 4(sc + kD) + \lambda^2 \left[\frac{(sc + kD)}{4s^6}(-20c^6 + 16c^4 + 4c^2 + 9) + \frac{sc}{2s^4}(16c^4 + 2c^2 + 9) \right] \right\} \tag{3.46}$$

where:

F_{avg} = the mean energy flux = $\overline{F}$

$$C_3 = \sqrt{\frac{g}{k} \tanh kD \left[1 + \lambda^2 \left(\frac{8c^4 - 8c^2 + 9}{8s^4} \right) \right]}$$

λ = the perturbation parameter = $\frac{\pi H}{L} - \lambda^3 \left(\frac{3(8c^6 + 1)}{64s^6} \right)$

$s = \sinh kD$

$c = \cosh kD$.

The notation employed by Le Méhauté and Webb is somewhat cumbersome due to the complexity of λ . For any Stokes wave theory, the leading order term for the mean energy flux should be equivalent to $\overline{F}$ from small amplitude wave theory or,

$$\overline{F} = \frac{\gamma H^2 n C}{8} . \tag{3.47}$$

This is difficult to determine in a straightforward manner from the expression for the mean energy flux given in Equation 3.46 because of the interdependency of the variables.

Koh and Le Méhauté (1966) also use the fifth-order analytical solution of Skjelbreia and Hendrickson (1960) to calculate the energy flux and ultimately, wave shoaling (to fifth-order). To third-order, their results and assumptions are identical to those of Le Méhauté and Webb. However, it should be noted that there is an apparent typographical error in the expression for the third-order energy flux, F_2 (Koh and Le Mehaute, Equation 4, pg. 2007). It is believed that the last term in F_2 should be divided by two, not four.

A comparison of the expressions for $\overline{F}$ given by Le Méhauté and Webb, Koh and Le Méhauté, Tsuchiya and Yasuda, and the present authors is accomplished at the deepwater limit ($kD \to \infty$). The resulting deepwater expressions for $\overline{F}$ should be identical to third-order, but may differ at higher orders due to different assumptions in the derivation such as the definition of wave celerity and the choice of the perturbation parameter. As was mentioned previously, the expression for $\overline{F}$ given by Tsuchiya and Yasuda is divergent in the deepwater limit. The deepwater limit for $\overline{F}$ given by Le Mehaute and Webb, Koh and Le Méhauté, and that derived here are found to be identical to the third order of approximation. The mean energy flux tends to

$$\overline{F}_d = \frac{\gamma H_o^2 C_o}{16}\left(1 + 2\varepsilon_o^2\right) \tag{3.48}$$

in deepwater, where the subscript d denotes deepwater and C_o is the deepwater wave celerity, L_o/T . Equation 3.48 can be restated in terms of fundamental quantities as:

$$\overline{F}_d = \frac{\gamma H_o^2 L_o}{16T}\left[1 + 2\left(\frac{\pi H_o}{L_o}\right)^2\right] \qquad (3.49)$$

The first term in Equation 3.49 corresponds to the energy flux from small amplitude wave theory and the second term is a correction for the finite amplitude effect. It is important to note that the finite amplitude effect is present even at the deepwater limit! Table 3.2 displays some numerical examples of the percent increase in $\overline{F}_d$ due to the finite amplitude effect. The more significant effect obviously occurs with steeper waves, since the perturbation parameter, ε , is proportional to H/L . Therefore, finite amplitude model results will differ from small amplitude model results throughout the solution domain, with the more dramatic differences occurring in shallower water (where the wave height is larger and the wavelength is smaller) and for steeper waves.

Based on agreement at the deepwater limit, it is believed that Le Méhauté and Webb (1964), Koh and Le Méhauté (1966), and the present authors have derived expressions for $\overline{F}$ which are correct to a third order of approximation. However, the procedure presented here has the advantages that: (1) it is based on a well-documented derivation of a third-order Stokes theory and (2) the second definition of wave celerity is used to simplify the integration for the mean energy flux, thereby reducing the number of calculation steps and the possibility for error. The latter advantage would become particularly important if the integration procedure were carried to higher order.

Table 3.2

The Finite Amplitude Effect on $\overline{F}_d$

H_o (m)	T (sec)	L_o (m)	$\frac{H_o}{L_o}$	$2\varepsilon_o^2$	Per-cent*
1.0	6.0	56.2	0.02	0.0063	0.63
2.0	6.0	56.2	0.04	0.0250	2.50
3.0	6.0	56.2	0.05	0.0563	5.63
1.0	8.0	99.9	0.01	0.0020	0.20
2.0	8.0	99.9	0.02	0.0079	0.79
3.0	8.0	99.9	0.03	0.0178	1.78
1.0	10.0	156.1	0.01	0.0008	0.08
2.0	10.0	156.1	0.01	0 0032	0.32
3.0	10.0	156.1	0.02	0.0073	0.73

* Percent change in $\overline{F}_d$

IV. THEORY OF SURFACE WATER WAVE TRANSFORMATION

A. Refraction

As a wave propagates into shallow water over a sloping sea bottom, its height, length, celerity, and direction change with depth. Accurate prediction of these nearshore wave parameters is required in almost all coastal engineering projects.

Refraction is the process by which the direction of a wave changes as it moves into shallow water at an angle to the bottom contours. The portion of the wave in shallower water moves slower than the portion of the wave in deeper water. Therefore, the wave pivots, or bends, to align itself with the contour (Figure 4.1). Refraction diagrams can be constructed to show how waves change direction from deepwater to any arbitrary water depth (Shore Protection Manual, 1984, pg. A-46). Wave rays, showing the direction of wave advance, and/or wave crests are drawn on the refraction diagram. The refraction coefficient, K_r , defined as the square root of the ratio of the spacing between adjacent wave rays in deep water and in an arbitrary depth of water, is used to measure the convergence or divergence of the rays.

In the early years of coastal engineering, refraction diagrams were constructed by hand with the aid of a template (Wiegel 1964). All such work was based on linear wave theory. Graphical methods (such as the polygon method and the circular arc method) are somewhat subjective and are also time-consuming, but can provide a quick overview in cases of refraction over simple topography. Abernathy and Gilbert (1975) cite a significant deficiency with the construction of conventional refraction diagrams. They found that the number and selection of wave

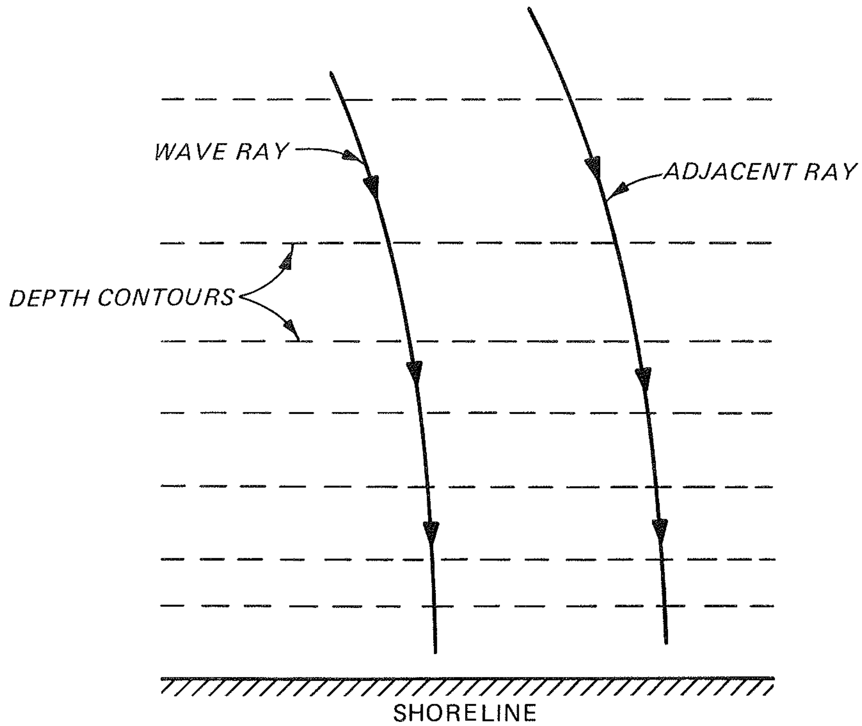

Figure 4.1. Wave refraction

rays refracting from the offshore boundary can result in large variations in the refraction coefficient. Such variation is often unacceptable to the needs of a coastal engineer due to the latent ambiguity.

Since the early 1960's, refraction diagrams have been constructed by using computer programs (Wilson, 1966; Dobson, 1967; and others). These programs incorporate the ray equation derived by Munk and Arthur (1951) into their solution process. Munk and Arthur's pioneering work, which provides an analytical means for determining the path of a wave ray and the wave ray separation distance, will be briefly outlined.

Ray theory and the ray equation developed by Munk and Arthur (1951) are based on the optical analogy to water wave refraction. Beginning with Fermat's principle, which states that a wave ray is the path of minimum travel time, Munk and Arthur derive the ray equation.

Thus, the ray equation determines the path of wave rays and is given by,

$$\frac{d\alpha}{ds} = -\frac{1}{C}\frac{dC}{dn}, \tag{4.1}$$

where:

α = the angle between the wave ray and the x axis (Figure 4.2)

s = the arc length along the ray

C = wave celerity

n = the arc length along the wave front.

Equation 4.1 links the curvature of the wave ray, $\frac{d\alpha}{ds}$, with the local wave celerity and the gradient of the celerity along the direction of

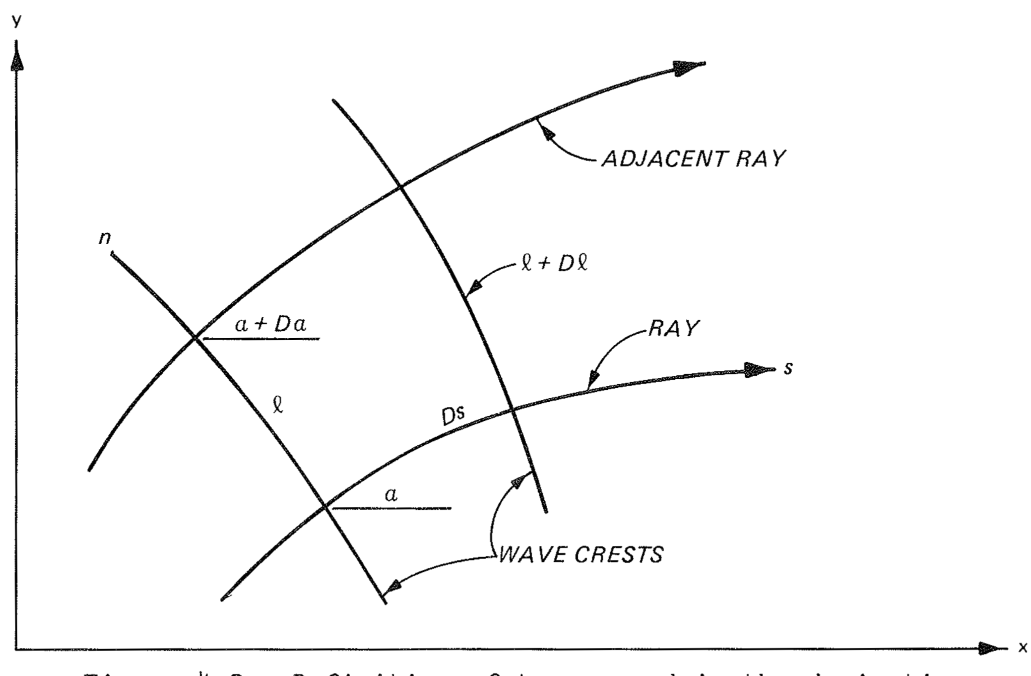

Figure 4.2. Definition of terms used in the derivation of the ray equation and the equation of ray separation (after Munk and Arthur 1951)

the wave front. Physically, this means that the wave ray bends toward the direction of lower celerity.

The equation of ray separation expresses the convergence or divergence along a ray,

$$\frac{1}{\beta}\frac{d\beta}{ds} = \frac{d\alpha}{dn} , \tag{4.2}$$

where β = the ray separation factor. Equations 4.1 and 4.2 are manipulated to give

$$\frac{d^2\beta}{ds^2} + p(s)\frac{d\beta}{ds} + q(s)\beta = 0 , \tag{4.3}$$

where

$$p(s) = -\frac{1}{C}\left(\cos\alpha\frac{\partial C}{\partial x} + \sin\alpha\frac{\partial C}{\partial y}\right)$$

and

$$q(s) = \frac{1}{C}\left(\sin^2\alpha\frac{\partial^2 C}{\partial x^2} - 2\sin\alpha\cos\alpha\frac{\partial^2 C}{\partial x\partial y} + \cos^2\alpha\frac{\partial^2 C}{\partial y^2}\right).$$

This is the equation of wave intensity. Basically, Equation 4.3 is used with

$$\frac{dx}{dt} = C\cos\alpha , \tag{4.4}$$

$$\frac{dy}{dt} = C\sin\alpha , \tag{4.5}$$

and

$$\frac{ds}{dt} = C \tag{4.6}$$

to provide an analytical means of determining locations along a wave ray and the spacing between the rays, or more simply, wave refraction. (The wave celerity, C, is determined from the dispersion relation.) Numerous numerical programs for linear wave refraction are based on this theory (e.g., Wilson 1966, Dobson 1967). Other authors (Chu 1975, Headland and Chu 1984) present programs for calculating finite amplitude waves by means of the wave ray method.

In this report, a different approach is used to determine the refraction of water waves over an arbitrary bottom. The basic procedure was originally implemented by Noda et al. (1974) for small amplitude waves.

The wave phase Ω is a scalar quantity ($\Omega = kx \cos \alpha + ky \sin \alpha - \sigma t$) which is constant along a wave crest. From vector analysis, a vector normal to this quantity is given by

$$\text{normal} = \nabla \Omega \ . \tag{4.7}$$

If we define the wave number vector, $\vec{k}$, as

$$\vec{k} = \nabla \Omega \ , \tag{4.8}$$

then this represents the wave number perpendicular to the wave crest, or equivalently, in the direction of wave advance. Again, from vector analysis, the curl of the gradient of a scalar quantity is identically zero or,

$$\nabla \times \vec{k} = 0 \ . \tag{4.9}$$

Substituting the components of $\vec{k}$ into Equation 4.9 yields,

$$\frac{\partial}{\partial x}(k \sin \alpha) - \frac{\partial}{\partial y}(k \cos \alpha) = 0 . \tag{4.10}$$

Expanding Equation 4.10 results in the following,

$$k \cos \alpha \frac{\partial \alpha}{\partial x} + k \sin \alpha \frac{\partial \alpha}{\partial y} = \cos \alpha \frac{\partial k}{\partial y} - \sin \alpha \frac{\partial k}{\partial x} . \tag{4.11}$$

In the method of Noda et al. (1974) and in this report, Equation 4.11 is used to solve for the wave direction, α , using a numerical (finite difference) technique. Thus the irrotationality condition on $\vec{k}$ (Equation 4.9) is used to determine wave refraction. The solution for α is accomplished at discrete points (e. g., on a grid system); therefore, Equation 4.11 is put into finite difference form. This will be shown in Section V.

Use of the irrotationality condition on the wave number vector provides a cleaner method for calculating wave refraction than the ray method, and it is also less computer intensive. Ray theory involves numerous interpolations because it is required to "shoot" wave rays in from the offshore boundary to an arbitrary point, which is not necessarily a grid point. Two advantages which are lost by not using ray theory are: (1) the intuitively appealing continuous wave ray produced by ray theory and (2) the ability to artificially eliminate or avoid caustics. (A caustic is a point at which two wave rays cross. Mathematically, a caustic causes a divergence which may not physically exist.) If a caustic develops, a model using ray theory can "shoot" a different ray in from the offshore boundary, whereas a model using the irrotationality of the wave number vector will stop operating because of the divergence. In practical situations, if a caustic occurs, the topography could be smoothed or another procedure taken to remove the divergence. These procedures are not investigated in this report.

Weighing the advantages against the disadvantages, for most applications it appears to be more practical to use the irrotationality condition of $\vec{k}$ to determine wave refraction over an arbitrary bottom. Values of wave-related quantities obtained directly on a grid can then be used as input to other numerical models, such as sediment transport and nearshore circulation models.

B. Shoaling

The transformation of a wave as it travels from one depth to another, but usually from deep to shallow water, is called wave shoaling. As was mentioned in Section IV A, a wave changes in height, length, celerity, and direction as it propagates into shallow water. The change in wave height is mathematically described by the conservation of wave energy. Neglecting the frictional effect of the bottom slope, as well as other possible energy gains and losses, this conservation law requires that the transmitted energy, or energy flux, be constant

$$\nabla \cdot F = 0 \; . \tag{4.12}$$

For ease of explanation, linear wave shoaling will first be presented and the more rigorous finite amplitude wave shoaling will be explained in Section V D. For the purpose of explanation, assume straight and parallel bottom contours and waves that are incident normal to the contours; the first-order solution to Equation 4.12 reduces to

$$\left(\frac{\gamma H^2 nC}{8}\right)_1 = \left(\frac{\gamma H^2 nC}{8}\right)_o \; . \tag{4.13}$$

Solving for H_1/H_o ,

$$\frac{H_1}{H_o} = \sqrt{\frac{C_o}{2nC_1}} \tag{4.14}$$

or

$$\frac{H_1}{H_o} = \sqrt{\frac{C_{go}}{C_{g1}}} \ . \tag{4.15}$$

The square root of the ratio of group speeds is defined as the shoaling coefficient, K_s (linear wave theory).

Figure 4.3 displays the shoaling coefficient as a function of dimensionless depth. From deep water, K_s first decreases to a minimum value of 0.913, then increases rapidly as the depth diminishes. A mathematical explanation for the variation (decrease, then increase) in K_s is given. In deepwater, n changes more rapidly than the ratio of wave celerities and K_s decreases. Next, the ratio of wave

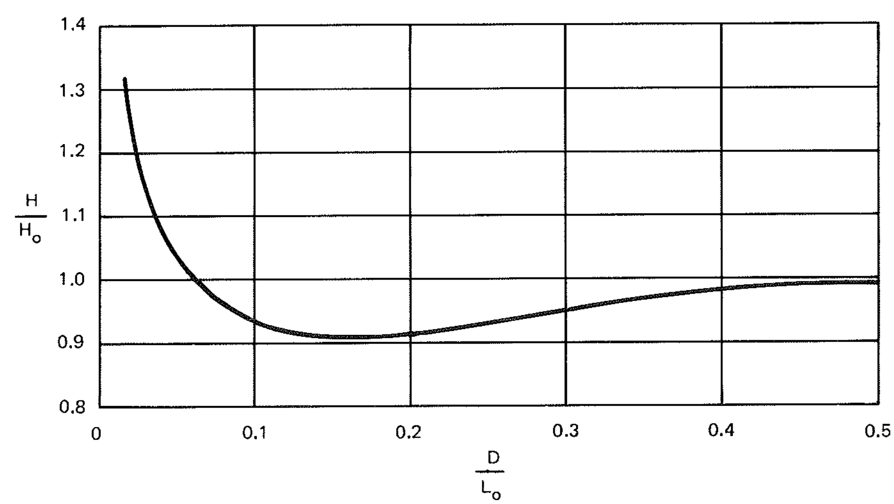

Figure 4.3. Wave shoaling

celerities begins to dominate and K_s increases. Although K_s decreases then increases, the shoaling coefficient is generally regarded as greater than unity and one associates wave shoaling with waves "peaking up" as the water depth gradually decreases. The physical reason for the increase in wave height (or K_s) is that the wave slows down while still conserving energy flux. Therefore, the wave height must increase.

In conclusion, the conservation of wave energy must balance the change in wave height with the change in celerity, as a wave propagates in shoaling water. In shallow water, the wave celerity decreases and the group velocity approaches the wave celerity. The energy is then transmitted with the wave celerity and the wave height must therefore increase in order to conserve energy flux. This is the process of wave shoaling.

V . THE NUMERICAL MODEL

A. General

A numerical wave transformation model for third-order Stokes waves is developed in this report. The solution for the wave number, k , wave angle, α , and wave height, H , is accomplished on a finite difference grid using iterative techniques. The dispersion relation is solved for the wave number using a Newton-Raphson numerical method. The wave direction is obtained from the irrotationality condition of the wave number vector and the wave height is obtained from the equation of conservation of wave energy.

Figure 5.1 is a flow chart of the model with brief descriptions to the right of each subroutine. The three main subroutines, DISPERS, DELK, and DELF will be described in Sections V B, V C, and V D, respectively. As shown in Figure 5.1, an iterative scheme is used with subroutines DISPERS, DELK, and DELF to solve for k , α , and H , respectively. This is due to the interdependency of the third-order dispersion relation, the irrotationality of the wave number vector, and the equation of conservation of wave energy. The third-order dispersion relation (subroutine DISPERS) is solved for k , but depends on H ; the irrotationality of the wave number vector (subroutine DELK) is solved for α , but depends on k ; and the equation of conservation of wave energy (subroutine DELF) is solved for H, but depends on k and α . Therefore, after any one iteration through the three main subroutines, the new (or updated) values of k , α , and H are used for the next iteration through the three main subroutines. This procedure is

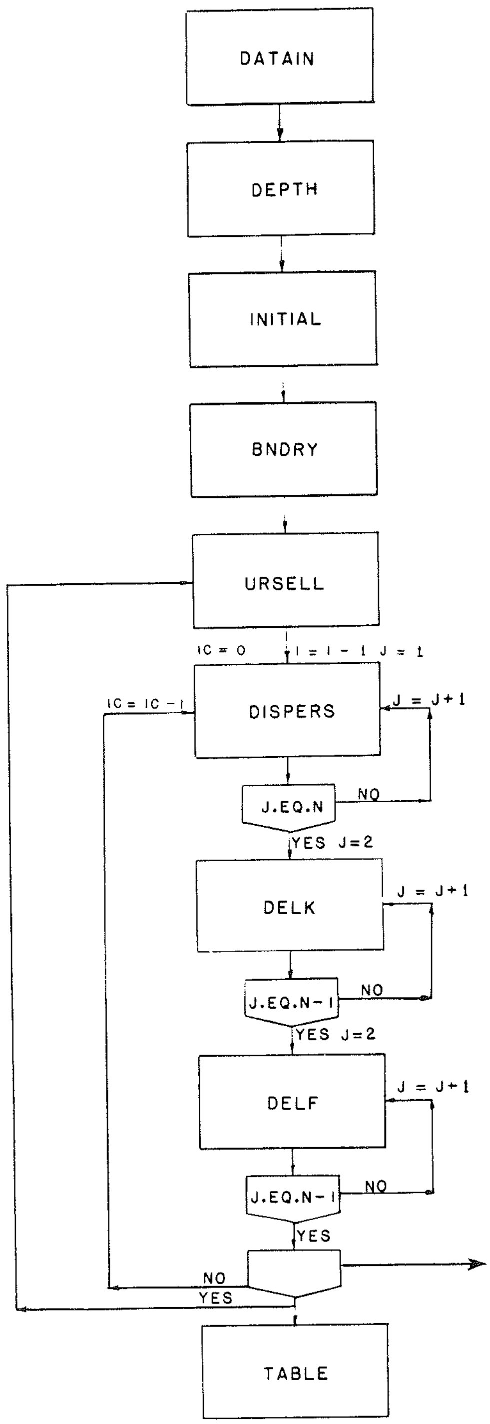

Read in the grid characteristics

Read in or calculate the depth in each cell

Calculate constants used in the model

Calculate H, k, and α on the boundary

Calculate the Ursell number at each grid point along the entire row

Solve the dispersion relation for $k_{J,I-1}$, and $C_{J,I-1}$

Solve the irrotationality condition equation for $\alpha_{J,I-1}$

Solve the energy flux equation for $H_{J,I-1}$

$H_{new} - H_{old} < Tol$

Produce a tabular listing of the model results

Figure 5.1. Flow chart

repeated until a specified tolerance is reached for each k , α ,and H value along a given row.

Subroutines BNDRY and URSELL will be explained in this section. The remaining subroutines are elementary and require no further explanation. A complete program listing is given in Appendix E.

Figure 5.2 shows an example of a finite difference grid and the general grid characteristics used in the model. The x-axis is in the on-offshore direction and the y-axis is in the longshore direction. There are M gridpoints in the x-direction, each separated by a distance of DX meters (or feet). There are N grid points in the y-direction, each separated by a distance of DY meters (or feet). The grid points are specified by (J , I) coordinates on the grid, where J is the counter in the y-direction ranging from 1 to N and I is the counter in the x-direction ranging from 1 to M .

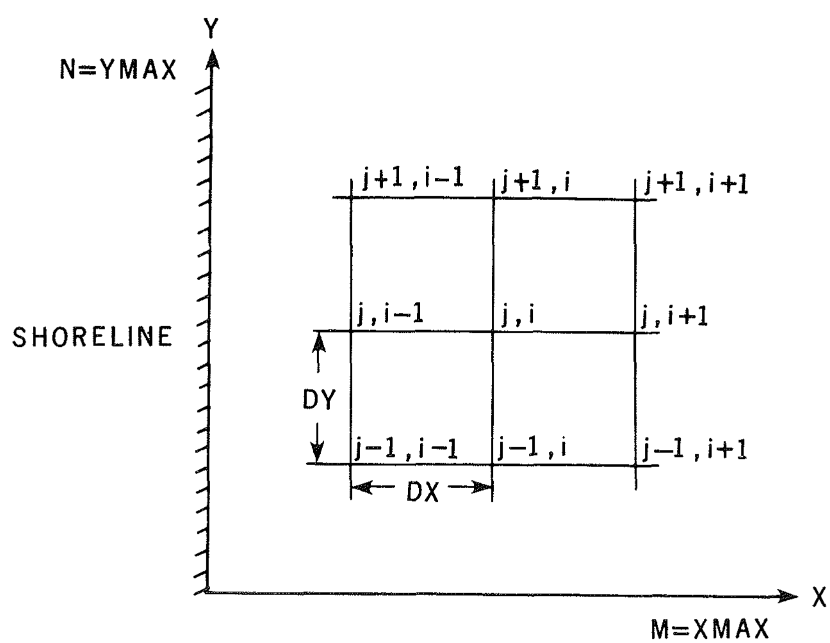

Figure 5.2. Definition sketch, finite difference grid

The solution process begins at the offshore boundary of the grid, I=M , (see subroutine BNDRY), then continues marching shoreward row by row. The solution for H , k , and α is completed at a given (I-1) row for all J values before a solution at the next shoreward row can be found. The solution at row (I-1) is completed by iterating (see Figure 5.1) until the solution converges. This occurs when a specified tolerance is reached. After completing the solution at row (I-1), this row becomes row "I" and the next shoreward (unknown) row becomes row "(I-1)" , where the solution for H , k , and α is obtained next. This "marching" procedure is repeated at each successive row. The solution procedure terminates if the limit to the range of validity of Stokes waves is reached (see subroutine URSELL).

1. Subroutine BNDRY

The solution at the offshore boundary is found by assuming the offshore contours are straight and parallel. Then, the dispersion relation is solved for k_{bc} , Snell's law is used to find α_{bc} , and the equation for conservation of wave energy provides H_{bc} , where the subscript bc means "at the offshore boundary." The dispersion relation applied at the offshore boundary is the same as the dispersion relation used in subroutine DISPERS. The conservation of wave energy equation applied at the offshore boundary is a similar, but a simplified version of the equation used in subroutine DELF. (There is no y-dependency because of the assumption of a plane beach.) Snell's law relates the change in wave direction to the change in wave celerity or,

$$\frac{\sin \alpha_{bc}}{C_{bc}} = \frac{\sin \alpha_o}{C_o} . \qquad (5.1)$$

Inserting $C = \sigma/k$, Equation 5.1 is equivalently,

$$k_{bc} \sin \alpha_{bc} = k_o \sin \alpha_o . \qquad (5.2)$$

Equation 5.2 is solved for α_{bc} . Using an iterative technique, the solution for k_{bc} , α_{bc} , and H_{bc} is obtained after a specified tolerance is reached.

The solution at the lateral boundaries is found by setting the boundary values equal to the values at adjacent grid points. That is,

$$\alpha\ (J=1,I) = \alpha\ (J=2,I) \qquad (5.3)$$

and

$$\alpha\ (J=N,I) = \alpha\ (J=N-1,I) . \qquad (5.4)$$

This boundary condition implies that the change in the variable (in this case α) in the y-direction is zero. Therefore, this boundary condition is most valid if the contours are nearly straight and parallel to the y-axis.

2. Subroutine URSELL

Stokes wave theory should be applied when the Ursell number (defined in Section III C) is less than a critical value. Following Isobe and Kraus (1983a), a critical Ursell number of 25 is deemed suitable

(Table 3.1) and Stokes theory is applied if $U < 25$. Therefore, after the solution is obtained at a given row (I-1), the value of the Ursell number is calculated at each grid point. This is to insure that the model is not applied beyond its range of validity. If an Ursell number of 25 is reached at any one grid point, the run is terminated, thereby avoiding the production of erroneous results. The application of a cnoidal wave model (Hardy and Kraus 1987) for the remaining (M-I) rows, or to the breaking point, would be appropriate.

B. Subroutine DISPERS

From Isobe and Kraus' (1983a) third-order derivation of a Stokes wave theory, the dispersion relation is

$$\frac{\sigma^2 D}{g} = kD \tanh kD \left[1 + \varepsilon^2 \left(\frac{9c^4 - 10c^2 + 9}{16} - \frac{c}{2kD} \right) \right]^2 . \qquad (5.5)$$

This equation is solved for the wave number, k , using the Newton-Raphson method. For the solution procedure, it is convenient to define

$$S = \frac{\sigma^2 D}{g} ,$$

$$x = kD ,$$

and

$$FAC = \left[1 + \varepsilon^2 \left(\frac{9c^4 - 10c^2 + 9}{16} - \frac{c}{2kD} \right) \right]^2 ;$$

therefore, the form of Equation 5.5 simplifies to

$$S = (x \tanh x) \cdot FAC . \qquad (5.6)$$

Bringing S to the right-hand side and defining $f(x)$,

$$f(x) = (x \tanh x) \cdot FAC - S \qquad (5.7)$$

or

$$f(x) = x \cdot FAC - S \coth x . \qquad (5.8)$$

The value of the independent variable, x, for which the function $f(x)$ is zero is obtained by the Newton-Raphson method.

In the Newton-Raphson method (see Figure 5.3), a first guess of $x = x_1$ is made and the value of $f(x_1)$ is calculated. The tangent to the $f(x)$ curve at $f(x_1)$ is extrapolated to intersect the x-axis (where $f(x)=0$). This becomes the second guess for x, or x_2. Again, $f(x_2)$ and the tangent at $f(x_2)$ are calculated and the procedure is repeated until the solution converges. This occurs when the difference between two consecutive approximations for x becomes so small that the desired accuracy is reached. Mathematically,

$$\tan(\mathrm{ANG}) = f'(x_1) = \frac{f(x_1) - f(x_2)}{x_1 - x_2} \tag{5.9}$$

or

$$f'(x_1) = \frac{f(x_1)}{x_1 - x_2} \tag{5.10}$$

since $f(x_2)$ is zero. Solving for x_2,

$$x_2 = x_1 - \frac{f(x_1)}{f'(x_1)} \tag{5.11}$$

or in general,

$$x^{(n+1)} = x^{(n)} - \frac{f\left(x^{(n)}\right)}{f'\left(x^{(n)}\right)}, \tag{5.12}$$

where the superscripts denote the guess (or iteration) number.

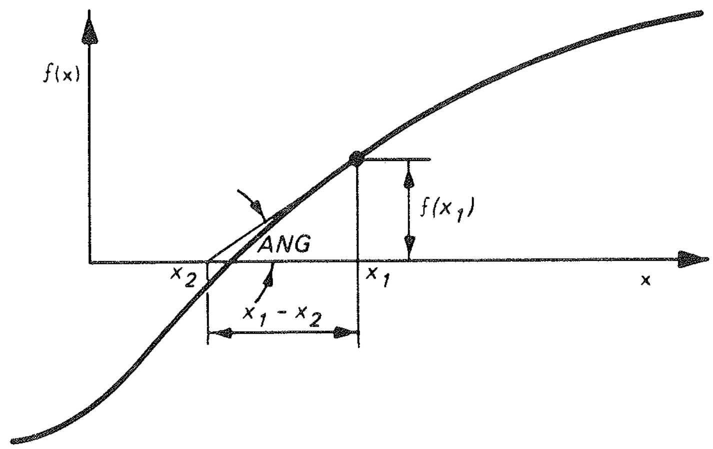

Figure 5.3. Newton-Raphson method

For the dispersion relation, $f(x)$ is given in Equation 5.8, but its derivative with respect to x must also be calculated.

$$f'(x) = FAC + S \operatorname{csch}^2 x \tag{5.13}$$

or

$$f'(x) = FAC + S(\coth^2 x - 1) \ . \tag{5.14}$$

Inserting Equations 5.8 and 5.14 into 5.12 yields

$$x^{(n+1)} = x^{(n)} - \frac{[x^{(n)}FAC - S \coth x^{(n)}]}{[FAC + S(\coth^2 x^{(n)} - 1)]} \ . \tag{5.15}$$

The solution for $x = kD$ is obtained by iterating until a specified tolerance is reached (for example, 0.0001). Dividing by the depth D, the solution for the wave number is completed.

C. Subroutine DELK

The irrotationality condition on the wave number vector,

$$\nabla \times \vec{k} = 0 \tag{5.16}$$

is solved to obtain the wave angle, α . Inserting the components of $\vec{k}$ into Equation 5.16 and expanding,

$$k \cos \alpha \frac{\partial \alpha}{\partial x} + \sin \alpha \frac{\partial k}{\partial x} + k \sin \alpha \frac{\partial \alpha}{\partial y} - \cos \alpha \frac{\partial k}{\partial y} = 0 \ . \tag{5.17}$$

Solving for $\frac{\partial \alpha}{\partial x}$,

$$\frac{\partial \alpha}{\partial x} = \frac{1}{k} \frac{\partial k}{\partial y} - \tan \alpha \left(\frac{1}{k} \frac{\partial k}{\partial x} + \frac{\partial \alpha}{\partial y} \right) \tag{5.18}$$

or in finite difference form

$$\frac{\alpha_{J,I} - \alpha_{J,I-1}}{\Delta x} = \frac{1}{\bar{k}} \frac{k_{J+1,I} - k_{J-1,I}}{2\Delta y} - \tan \bar{\alpha}_{J,I} \left(\frac{1}{\bar{k}} \frac{k_{J,I} - k_{J,I-1}}{\Delta x} + \frac{\alpha_{J+1,I} - \alpha_{J-1,I}}{2\Delta y} \right) \tag{5.19}$$

where the overbar denotes the average of the (J,I) value and the (J,I-1) value. Solving for $\alpha_{J,I-1}$ yields

$$\alpha_{J,I-1} = \alpha_{J,I} - \Delta x \left[\frac{1}{\bar{k}} \frac{k_{J+1,I} - k_{J-1,I}}{2\Delta y}\right.$$

$$\left. - \tan \bar{\alpha}_{J,I}\left(\frac{1}{\bar{k}} \frac{k_{J,I} - k_{J,I-1}}{\Delta x} + \frac{\alpha_{J+1,I} - \alpha_{J-1,I}}{2\Delta y}\right)\right] . \qquad (5.20)$$

The solution for $\alpha_{J,I-1}$ is obtained by iteration, since $\bar{\alpha}$ includes $\alpha_{J,I-1}$.

D. Subroutine DELF

The equation for the conservation of wave energy requires that the energy flux be constant or,

$$\nabla \cdot F = 0 \ . \tag{5.21}$$

This equation is solved to obtain the wave height, H . The third-order energy flux, derived in Appendix A, is therefore used in the solution for H . Inserting the components of the energy flux into Equation 5.21,

$$\frac{\partial}{\partial x}(\bar{F} \cos \alpha) + \frac{\partial}{\partial y}(\bar{F} \sin \alpha) = 0 \tag{5.22}$$

or in finite difference form,

$$\frac{\bar{F}_{J,I} \cos \alpha_{J,I} - \bar{F}_{J,I-1} \cos \alpha_{J,I-1}}{\Delta x}$$

$$+ \frac{\bar{F}_{J+1,I} \sin \alpha_{J+1,I} - \bar{F}_{J-1,I} \sin \alpha_{J-1,I} + \bar{F}_{J+1,I-1} \sin \alpha_{J+1,I-1} - \bar{F}_{J-1,I-1} \sin \alpha_{J-1,I-1}}{4\Delta y} = 0 \ . \tag{5.23}$$

The first term represents a forward difference in the x-direction and the second term represents a central difference in the y-direction. The second term also weights the known row (I) and the unknown row (I-1) equally such that the differencing in the y-direction is truely midway between rows (I) and (I-1). Defining

$$\mathrm{TERM2} = \frac{\bar{F}_{J+1,I} \sin \alpha_{J+1,I} - \bar{F}_{J-1,I} \sin \alpha_{J-1,I} + \bar{F}_{J+1,I-1} \sin \alpha_{J+1,I-1} - \bar{F}_{J-1,I-1} \sin \alpha_{J-1,I-1}}{4\Delta y}$$

$DX = \Delta x$

$FCOS = \bar{F}_{JI} \cos \alpha_{JI}$

and

$COS = \cos \alpha_{J,I-1}$

Equation 5.23 simplifies to

$$\bar{F}_{J,I-1} = \frac{FCOS + DX \cdot TERM2}{COS} . \tag{5.24}$$

Recall from Section III D, Equation 3.38,

$$\bar{F} = \frac{\gamma H^2 n C_{IK}}{8} + \frac{\gamma k^2 H^4 C_{IK} B}{16} \tag{5.25}$$

where

$$B = \frac{-c(1 + n)}{4kD} + \frac{n}{64}(-27c^6 + 15c^4 - 61c^2 + 57)$$

$$+ \frac{1}{64}(9c^6 + 3c^4 - 13c^2 + 33) + \frac{3 \cosh 2kD(c^2 - 1)}{4(\cosh 2kD - 1)}$$

$$+ \frac{9kD(c^4 - 2c^2 + 1)}{64c \sinh^4 kD} .$$

Inserting Equation 5.25 into Equation 5.24,

$$\frac{\gamma H^2 n C_{IK}}{8} + \frac{\gamma k^2 H^4 C_{IK} B}{16} = \frac{FCOS + DX \cdot TERM2}{COS} . \tag{5.26}$$

The first term in Equation 5.25 and 5.26 is the leading order term in the third-order energy flux and is equivalent to F from small amplitude wave theory. According to perturbation theory, the first term in a perturbation series (Equation 5.25) is significantly greater in magnitude than each successive term. Therefore, here we solve for the wave height from the first term in Equation 5.26 or,

$$H = \sqrt{\left[\frac{8}{\gamma n C_{IK}} \; \frac{FCOS + DX \cdot TERM2}{COS} - \frac{\gamma k^2 H^4 C_{IK} B}{16}\right]} \; . \qquad (5.27)$$

The solution for H is solved by iteration since the higher-order term in the conservation of wave energy equation

$$\frac{\gamma k^2 H^4 C_{IK} B}{16}$$

also contains H. As was mentioned in Section V A, the solution for k, α, and H on a given row (I-1) is obtained by iteration because of the interdependency of the three wave equations solved in subroutines DISPERS, DELK, and DELF.

VI. RESULTS

A. Test Cases: Small Amplitude Versus Finite Amplitude Wave Theory

1. Plane Beach

Introduction

It is well known that the calculation of wave shoaling based on small amplitude wave theory underpredicts the wave height, and small amplitude wave theory has also been found to overpredict wave refraction (Chu 1975). (Another interesting aspect of refraction was discovered in the course of this research and is presented later in this section.) The form of the small amplitude wave profile can also differ significantly from that of the finite amplitude wave profile. The magnitude of the error in quantities predicted by small amplitude wave theory (e.g., water particle velocity, wave height, wavelength, and surface profile) depends on the characteristics of the wave: the deepwater wave height, wave period (or length), and the water depth at which the wave is examined. Actual wave characteristics, such as the water particle velocity and the wave profile, deviate more significantly from the respective quantities predicted by small amplitude wave theory as: (1) the wave height increases and (2) the wavelength and water depth decrease. These factors are examined by using the numerical model developed for this thesis and as described in Section V. The model is capable of simulating small amplitude and finite amplitude (third-order Stokes) waves. Since first-order Stokes waves are equivalent to small amplitude waves, higher-order terms are set equal to zero in the model if small amplitude wave theory is selected.

For comparing small amplitude and finite amplitude waves, a plane beach with a 1:50 slope was selected. This slope is representative of the east coast of the United States. The various wave conditions for the comparison runs are given in Table 6.1. The small amplitude model runs are accomplished with only the first set of wave conditions (H = 1.0 m), since the value of the wave height does not affect the solution (except for the breaker location). The finite amplitude model results are a function of wave height, therefore the model is run for all the wave conditions shown in Table 6.1. These deepwater wave conditions are used to start the model solution process at the offshore boundary. The solution process consists of an iterative, marching scheme in the shoreward direction, which continues until the model can no longer be applied. For small amplitude wave model runs, this occurs if the breaking condition (H/D = 0.78) is reached. For finite amplitude wave model runs, this occurs if the range of validity of third-order Stokes waves is reached. This occurs at an Ursell number of 25. Application of a finite amplitude wave model outside its range of validity, as was done by Oh and Grosch (1985), is expected to produce erroneous results.

Figures 6.1 through 6.19 are a graphical interpretation of the calculated results. This explicit method of displaying results clearly shows the differences between predictions from small amplitude and finite amplitude wave theories, as will be discussed in the following paragraphs.

Wave Shoaling

Figures 6.1 through 6.5 display the effects of wave shoaling for various wave heights and periods. Wave height, nondimensionalized by

Table 6.1

Wave Conditions for Model Tests

H_o (m)	T (sec)	α_o (deg)
1.0	4, 6, 8, 10, 12	0, 30, 60
2.0	4, 6, 8, 10, 12	0, 30, 60
3.0	4, 6, 8, 10, 12	0, 30, 60

the deepwater wave height, is plotted against the water depth. Although the model applications begin at a depth of 50.0 m, the plots only show the results from a depth of 20.0 m to the depth where the model reaches its limit of applicability. The difference between small amplitude and finite amplitude wave model results are greatest in this shallow water region. Results from larger deepwater waves differ most significantly from small amplitude waves results. This is to be expected since small amplitude wave theory assumes the wave height is infinitely small. (Because of this assumption, the small amplitude model results need only be computed for a single wave height.) Also, larger waves have a larger perturbation parameter, H/L, (for a given wave period) and are therefore more "finite." By the same reasoning, a short period wave has a shorter wavelength and therefore a larger perturbation parameter. Short period waves are therefore more "finite" for a given wave height, and differ most significantly from small amplitude waves. This is verified in Figures 6.1 through 6.5.

It should be noted that longer period waves "feel the bottom" sooner, therefore they begin to shoal in deeper water. It can be inferred from this fact that a long period, finite amplitude wave will

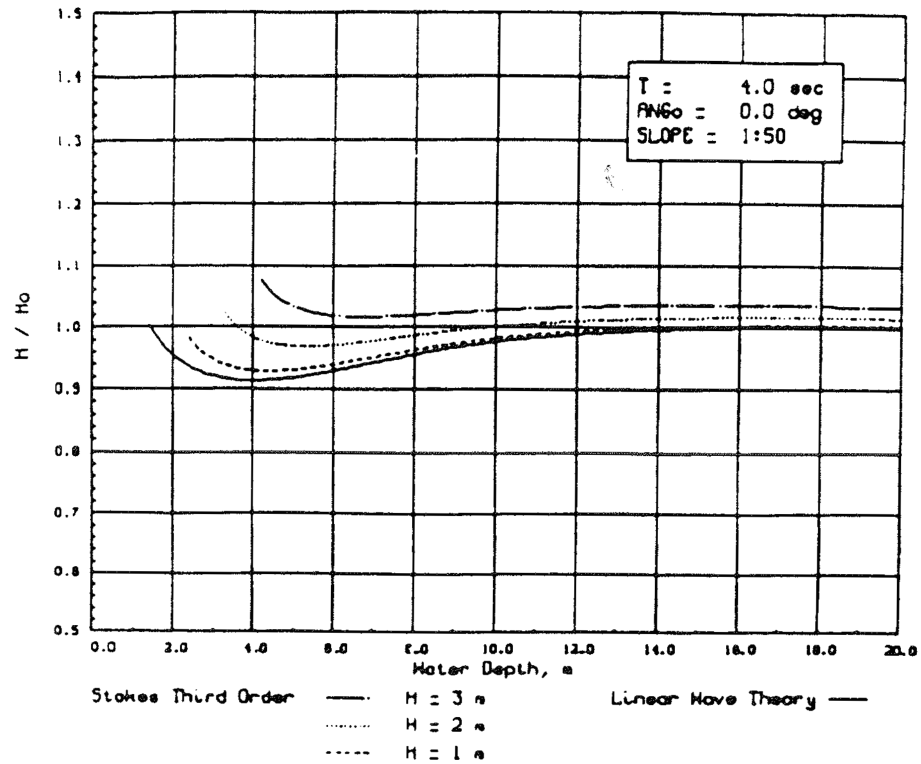

Figure 6.1. Wave shoaling over a plane beach

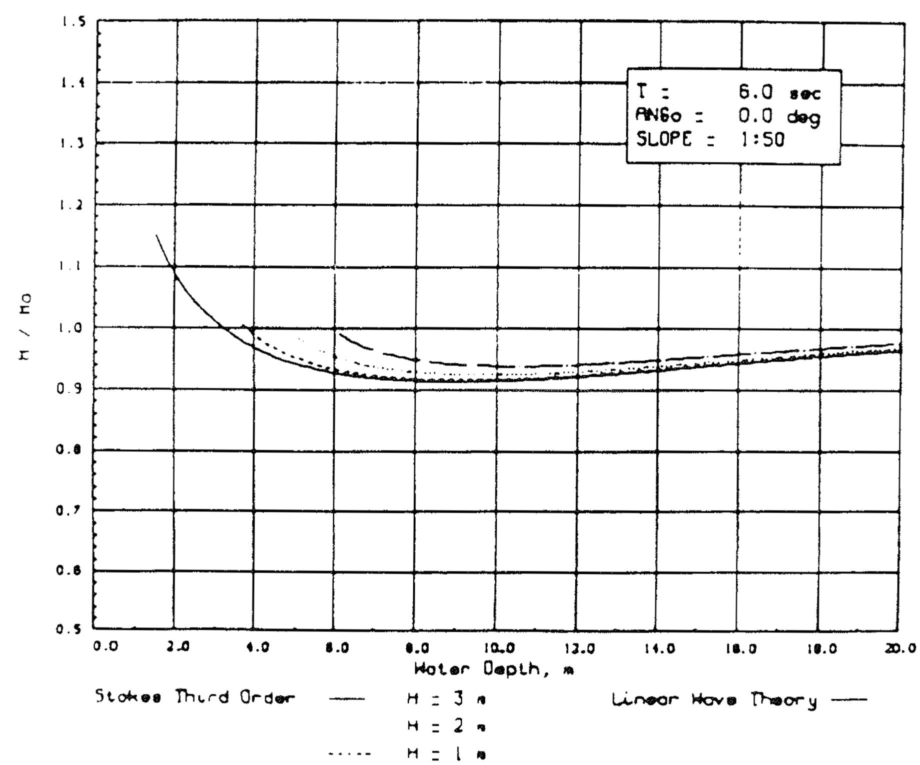

Figure 6.2. Wave shoaling over a plane beach

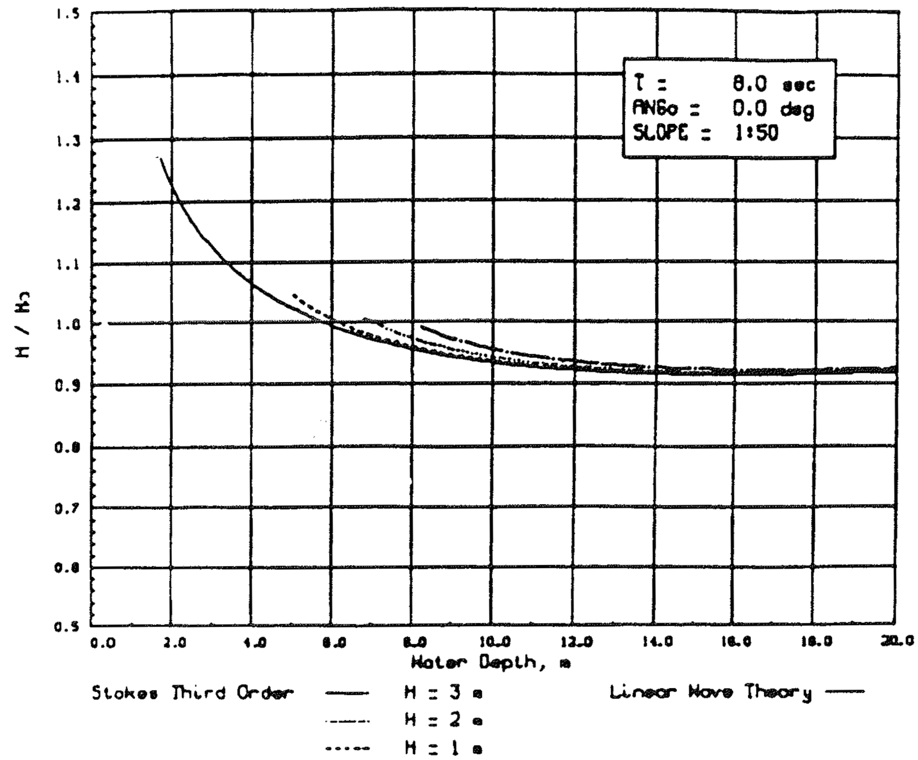

Figure 6.3. Wave shoaling over a plane beach

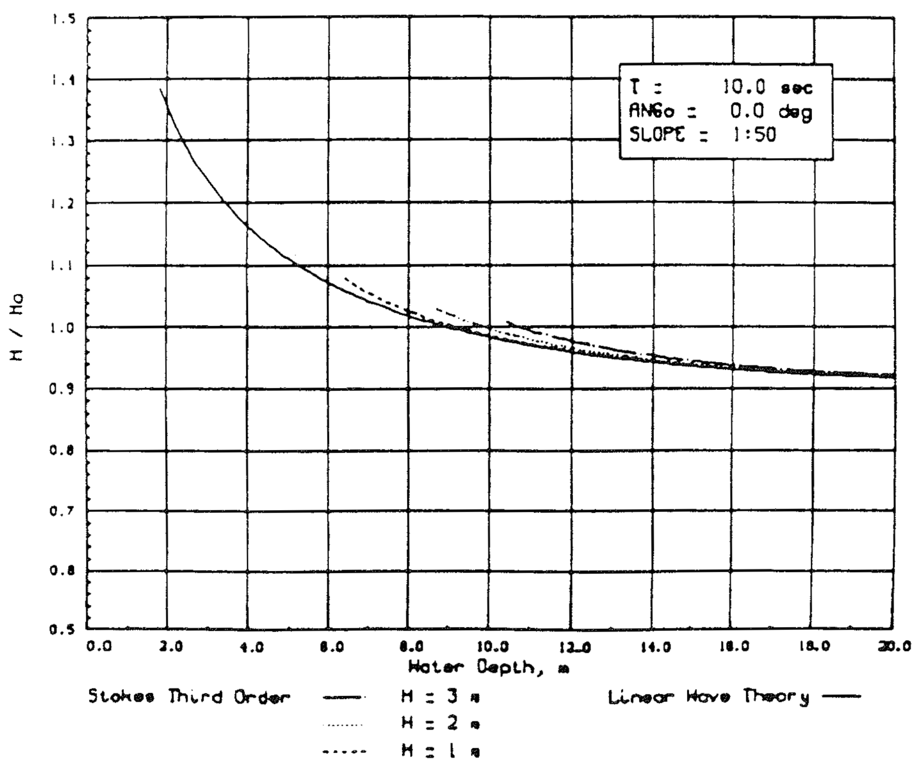

Figure 6.4. Wave shoaling over a plane beach

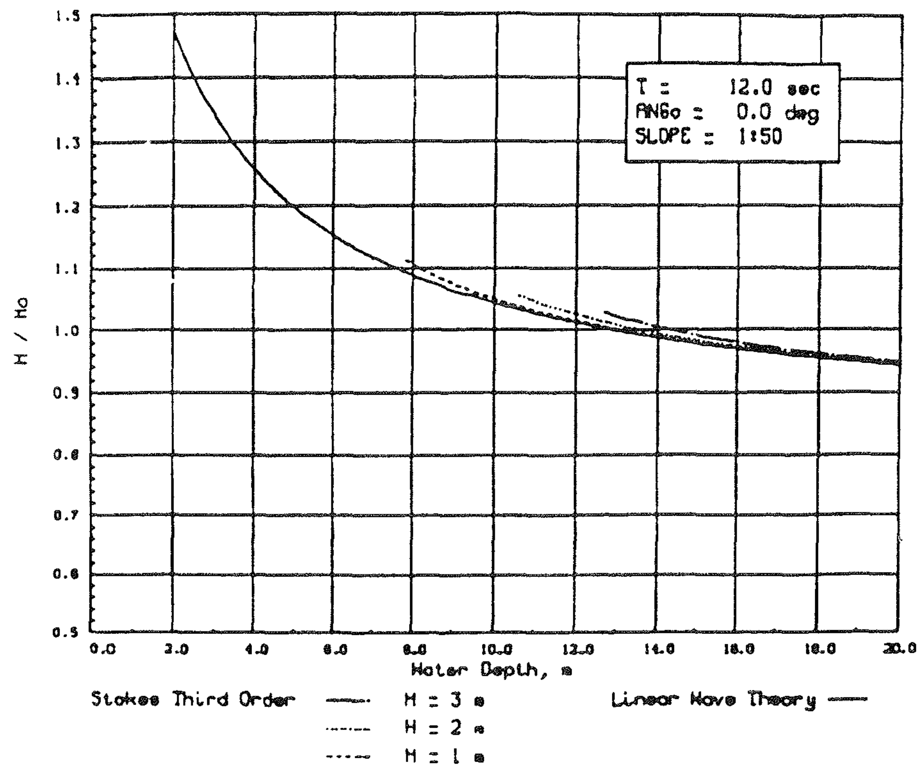

Figure 6.5. Wave shoaling over a plane beach

tend to "peak up" and break in deeper water (larger breaking wave height) than the corresponding small amplitude wave of the same deep-water characteristics. This has significant impact on the prediction of sediment transport since, e.g., the standard predictive expression for the longshore sediment transport is proportional to the wave height squared ("CERC" formula, Shore Protection Manual, 1984, Chapter 4). (Since the model developed in this thesis is based on Stokes theory, it is not valid in shallow water (near the breaker point) where longshore sediment transport is most significant; therefore, this aspect will not be examined in detail.)

Wave Profile

Figures 6.6 through 6.14 depict the change in the wave profile as a wave travels from deep water to the depth at which the wave reaches the limit to the range of validity of Stokes wave theory. The figures are generated using the wave profile equation derived by Isobe and Kraus in their derivation of a third-order Stokes wave theory (Isobe and Kraus 1983a, Equation 143),

$$N = \frac{1}{k} (N_1 \cos \theta + N_2 \cos 2\theta + N_3 \cos 3\theta) \ , \qquad (6.1)$$

and using the wave height and wavelength produced by the model for a given wave condition. In each figure, the wave profile nondimensionalized by its corresponding wave height (y-axis), is plotted for one wavelength (x-axis). The result predicted by small amplitude wave theory is represented by the solid line and that of finite amplitude wave theory is represented by the dashed line. Regardless of the water depth, linear waves maintain a sinusoidal shape. In contrast, finite amplitude waves become more peaked in shoaling water. The wave crest becomes higher and narrower and the trough becomes flatter and elongated. This asymmetry is of great importance in calculating the sediment transport threshold and direction, although it appears to be little discussed in the literature.

Figures 6.6 through 6.9 follow the change in wave profile as a 2.0-m, 6.0-sec wave travels from a water depth of 15.0 m to 5.0 m. From Figure 6.6 (D = 15.0 m) to Figure 6.7 (D = 10.0 m), the Ursell number remains small, the wave height decreases slightly, and the finite amplitude wave profile deviates somewhat from the small amplitude wave profile. From Figure 6.2, one can see that between these depths the shoaling coefficient gradually decreases, verifying the decrease in wave

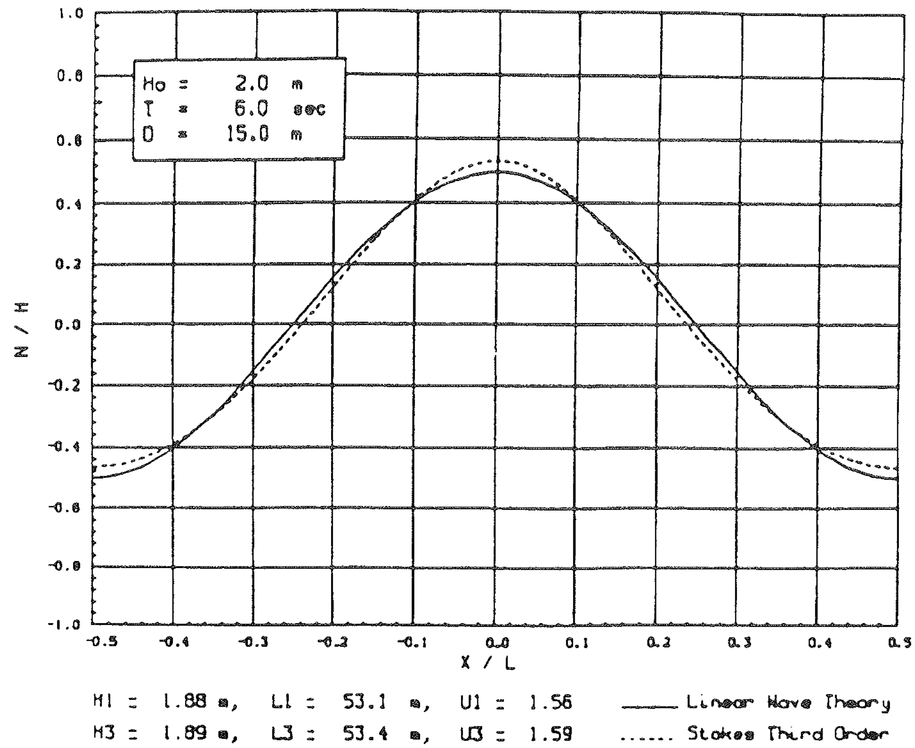

Figure 6.6. Wave profile comparison

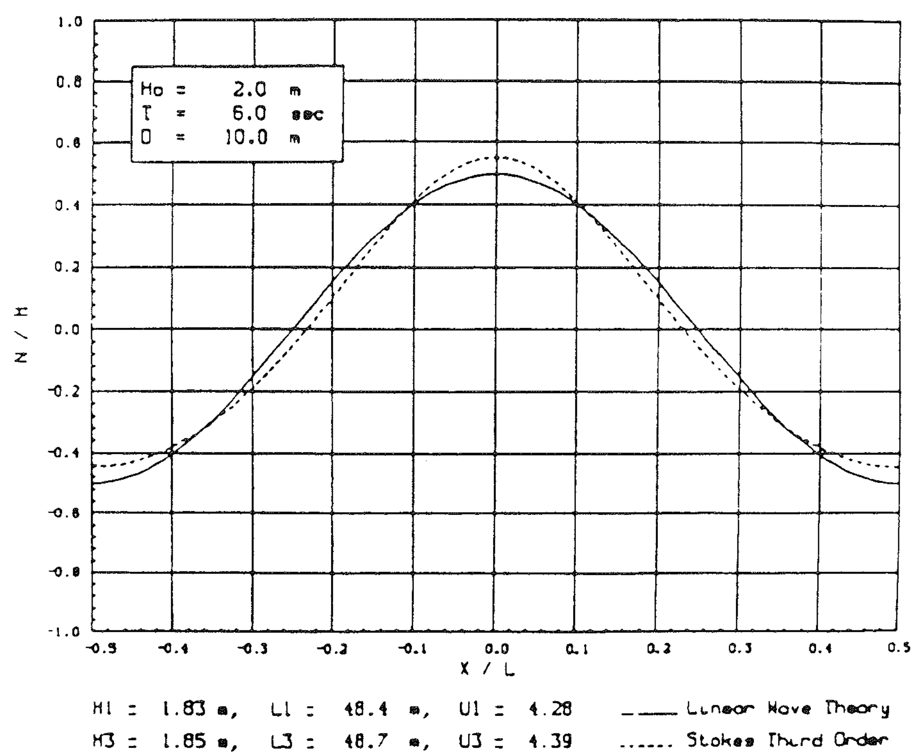

Figure 6.7. Wave profile comparison

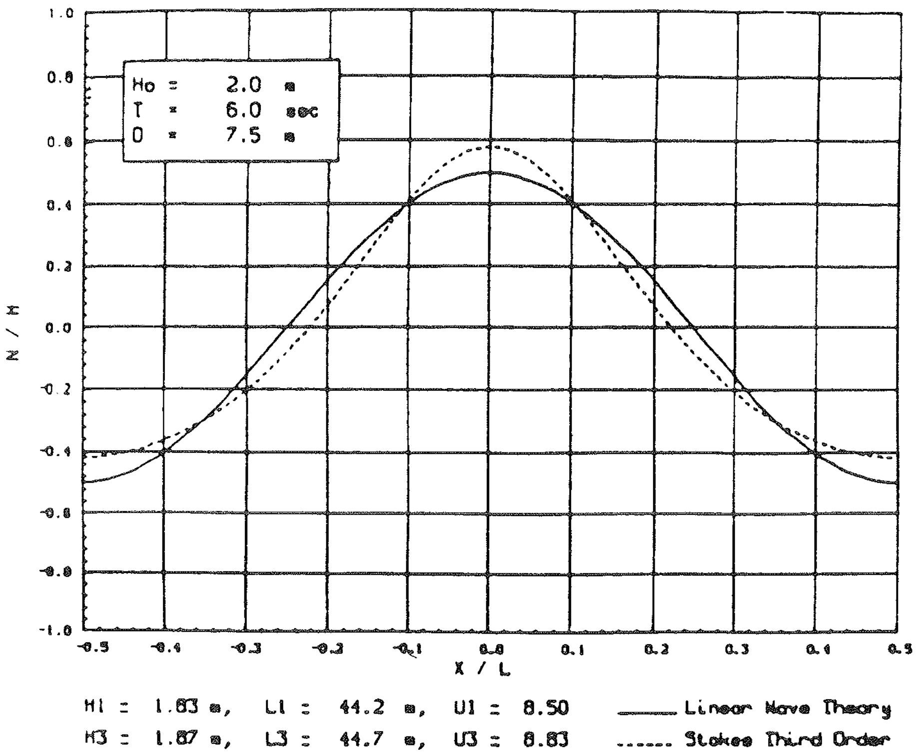

Figure 6.8. Wave profile comparison

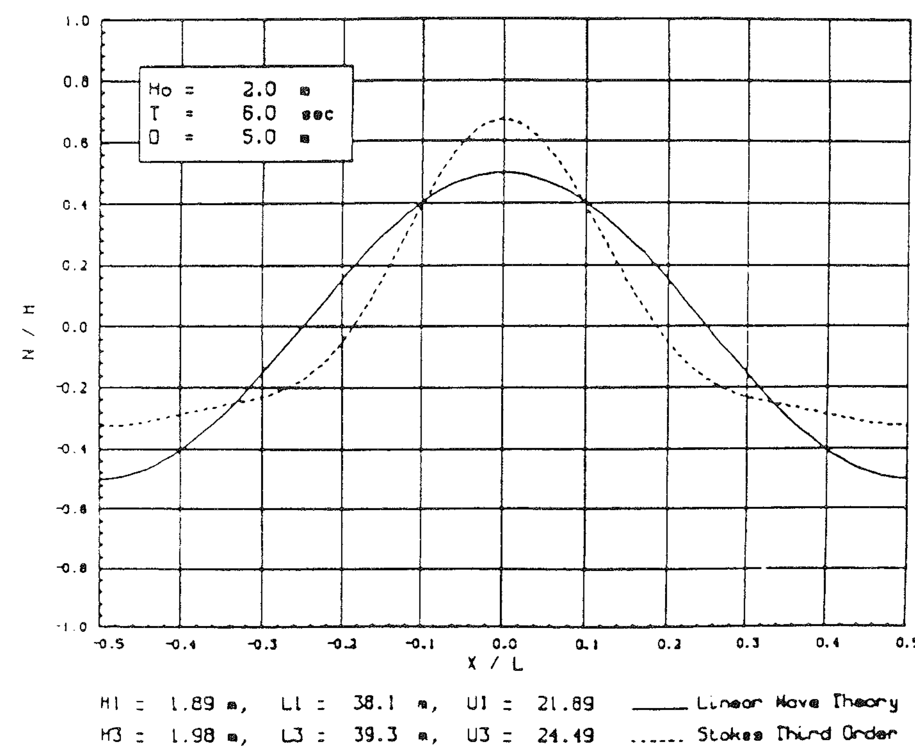

Figure 6.9. Wave profile comparison

height between Figures 6.6 and 6.7. Between Figures 6.7 and 6.8, the Ursell number becomes still larger, the wave height increases slightly, and the difference between the small amplitude and finite amplitude wave profiles becomes more pronounced. In Figure 6.9, the finite amplitude wave approaches the limit of the range of validity of Stokes waves ($U3 = 24.49$). The finite amplitude wave height is 9 cm larger than the small amplitude wave height, as calculated by shoaling theory, and the finite amplitude wave crest is approximately 36 cm higher than the small amplitude wave crest. This clearly shows that the finite amplitude wave will reach the limiting steepness, $H/L = 0.14$ (Michell 1893), sooner and will therefore break in deeper water than the small amplitude wave. Again, it is emphasized that this model is not valid at the breaker line and calculations are terminated before the limiting Ursell number ($U = 25$) is reached.

Figures 6.10 through 6.14 compare wave profiles in 5.0 m of water for various wave heights (1, 2, 3 m) and wave periods (4, 6, 8, 10, 12 sec). The longer period waves reach the limit of the range of validity of Stokes waves in water deeper than 5.0 m; therefore, they are examined at their limiting depth. This is indicative of the fact that longer period waves shoal in deeper water than shorter period waves, thereby reaching the limit of Stokes waves "sooner." From the figures it is clear that a long period wave has a profile which differs more significantly from a small amplitude wave profile than would a short period wave, in a given water depth. In conclusion, (1) profiles of larger waves differ more strongly from small amplitude wave profiles and (2) longer period waves show a more marked change in the wave profile

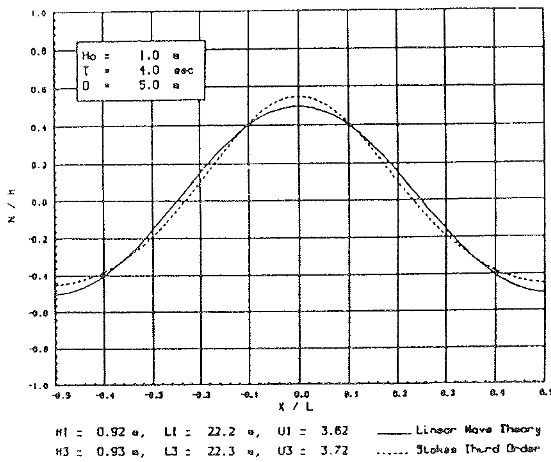

a.

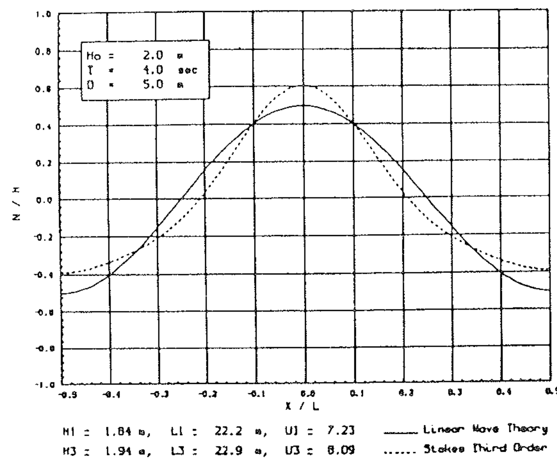

b.

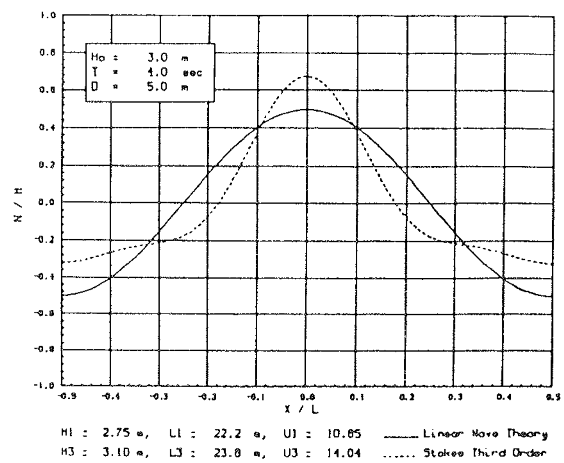

c.

Figure 6.10. Wave profile comparison

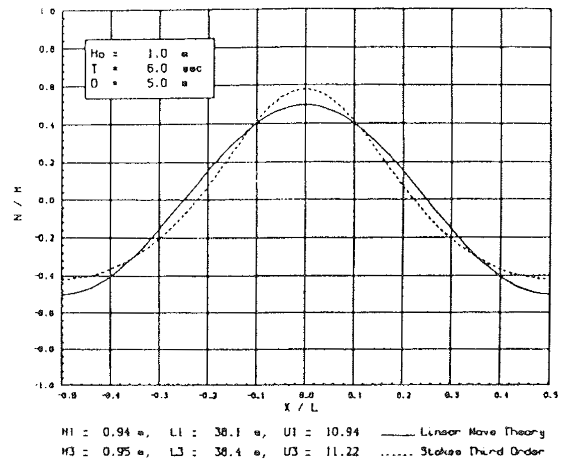

a.

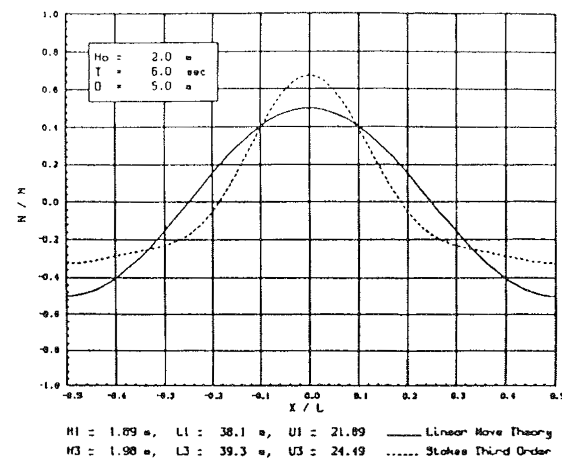

b.

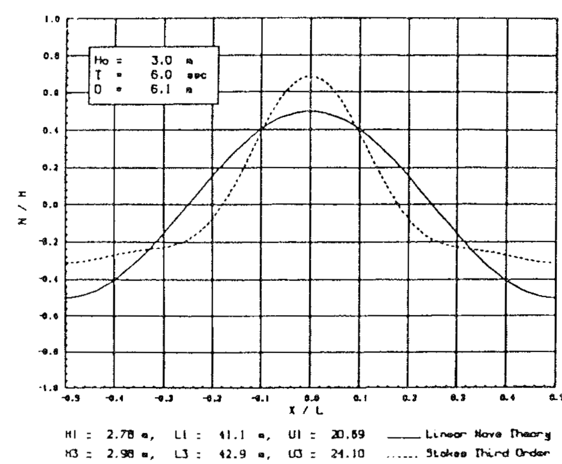

c.

Figure 6.11. Wave profile comparison

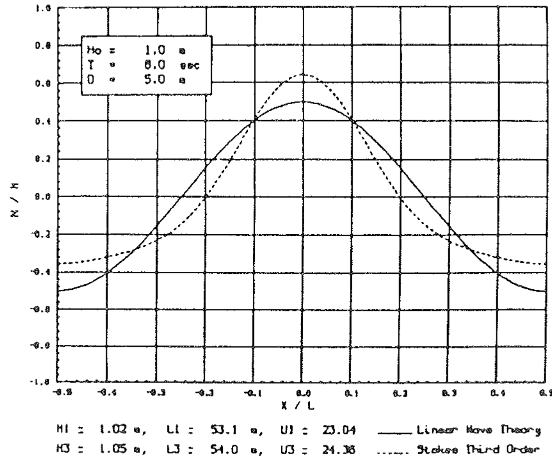

a.

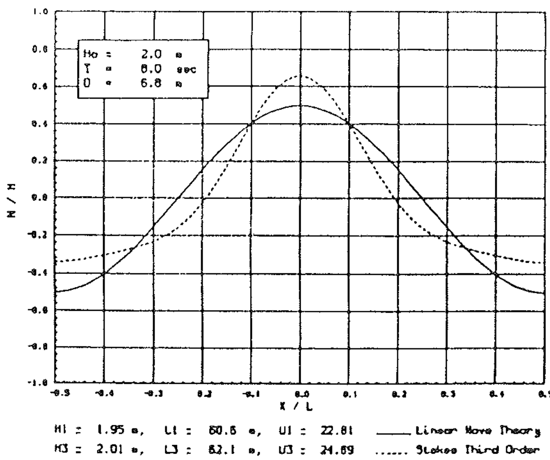

b.

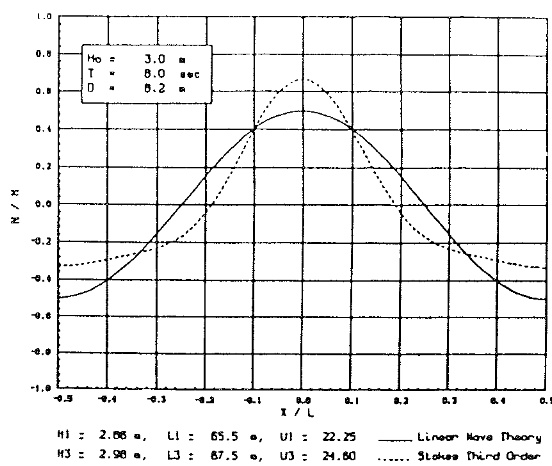

c.

Figure 6.12. Wave profile comparison

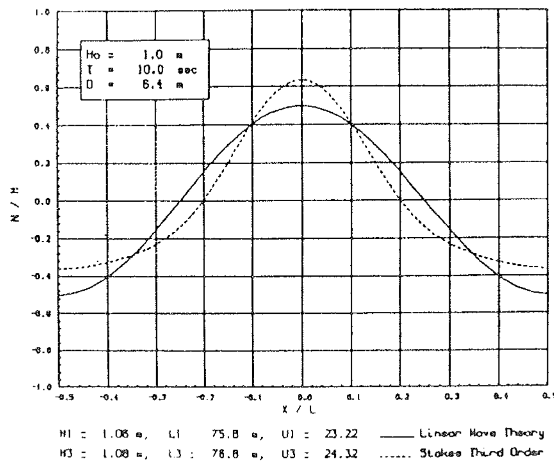

a.

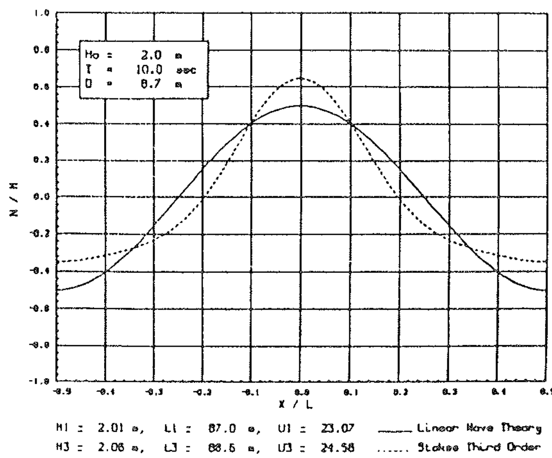

b.

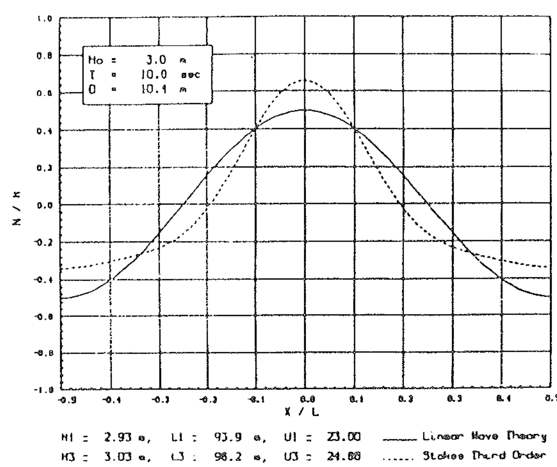

c.

Figure 6.13. Wave profile Comparison

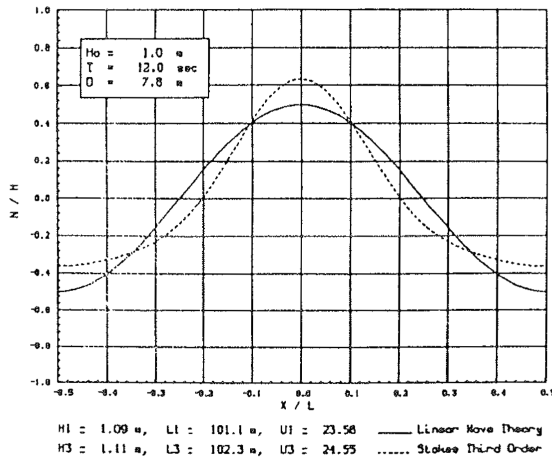

a.

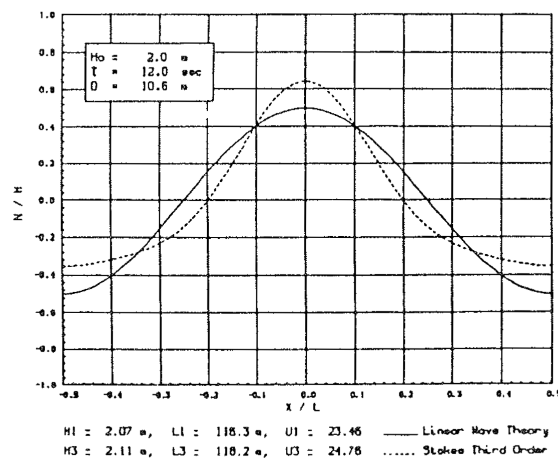

b.

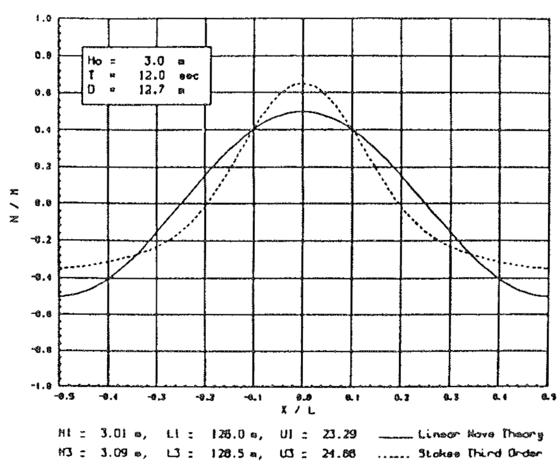

c.

Figure 6.14. Wave profile comparison

from the small amplitude wave profile than would a short period wave.

On examination of Figure 6.10c, the finite amplitude wave profile shows signs of the formation of secondary humps (at $x/L = \pm 0.35$). Although the Ursell number ($U = 14.04$) is not near the limit to the range of validity of Stokes waves, the wave steepness, H/L, (which is proportional to the perturbation parameter) is large ($H/L = 0.13$) in relation to the relative water depth, $D/L = 0.21$, (which is proportional to the auxiliary parameter). This violates the assumption in the derivation of Stokes wave theory, that the perturbation parameter is small (whereas the auxiliary parameter can take on finite values). In addition, Michell's criterion for the limiting steepness ($H/L = 0.14$) is nearly reached. This reiterates the importance of the wave steepness in Stokes wave theory and the need for checking the wave steepness criterion in the wave model.

<u>Wave Refraction</u>

Figures 6.15 through 6.19 display the change in wave angle as a wave travels from deepwater to a depth at which the limiting condition for Stokes waves applies. In each figure, the results of linear wave refraction are represented by a solid line and those of finite amplitude wave refraction are represented by dashed lines. The linear waves are permitted by the model to transform until the breaking criterion, $H/D = 0.78$, is reached, therefore the solid lines extend further shoreward than the dashed lines.

An interesting phenomenon found in the course of this research is that finite amplitude waves do not refract less than small amplitude waves throughout the full solution domain. This aspect appears

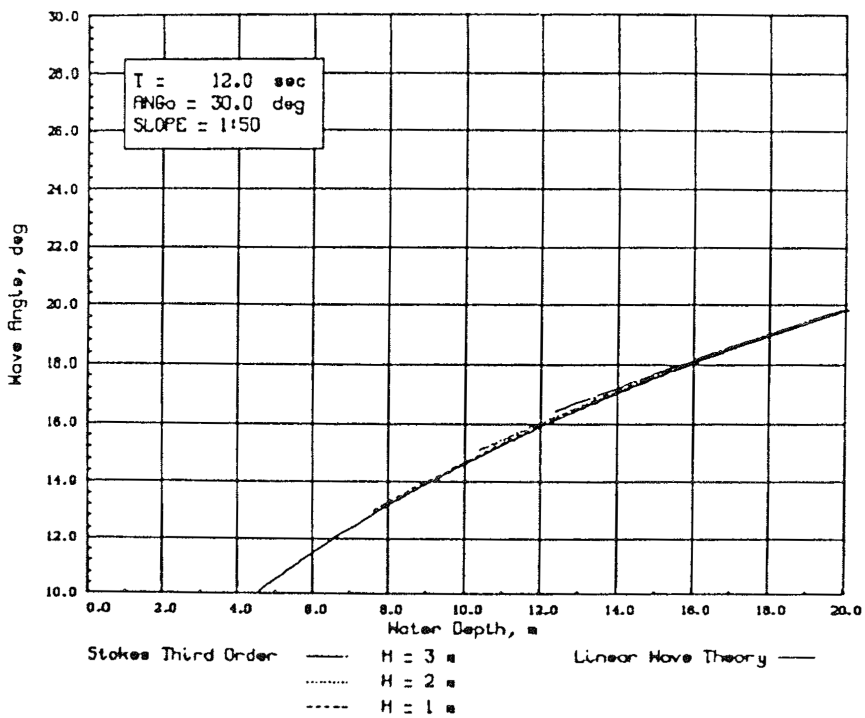

a.

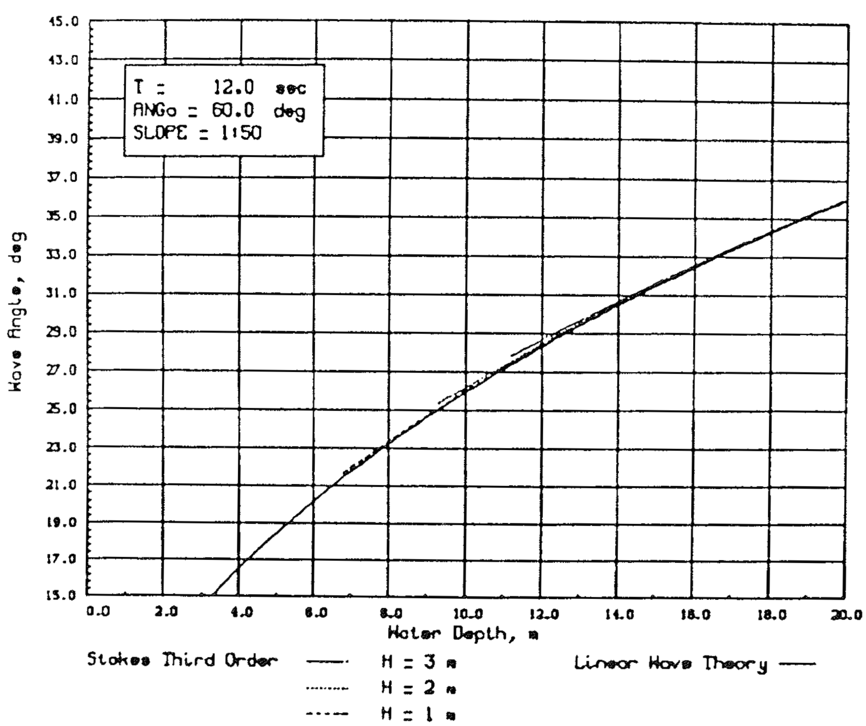

b.

Figure 6.15. Wave refraction over a plane beach

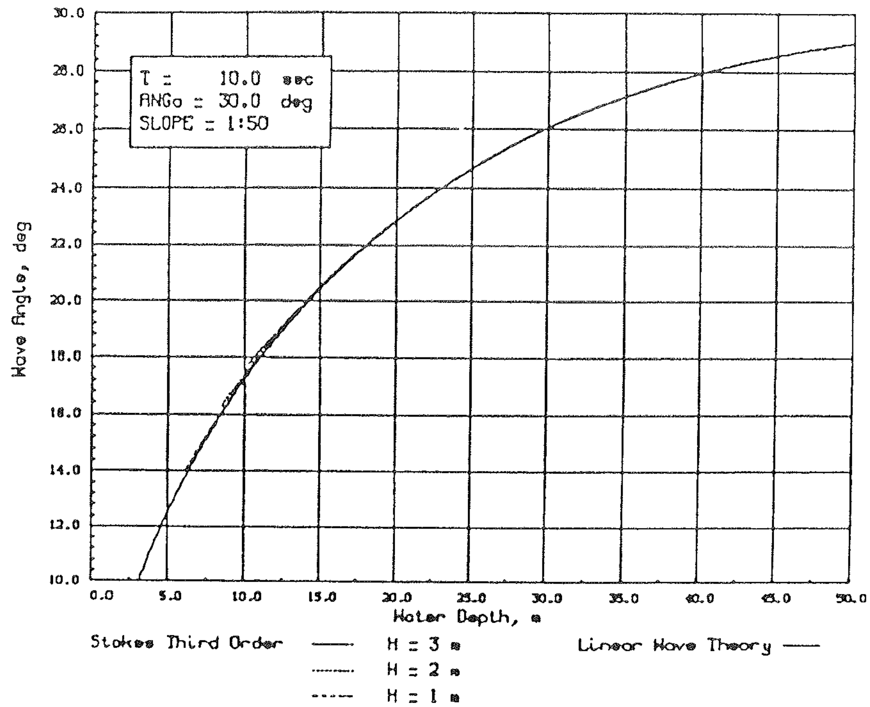

a.

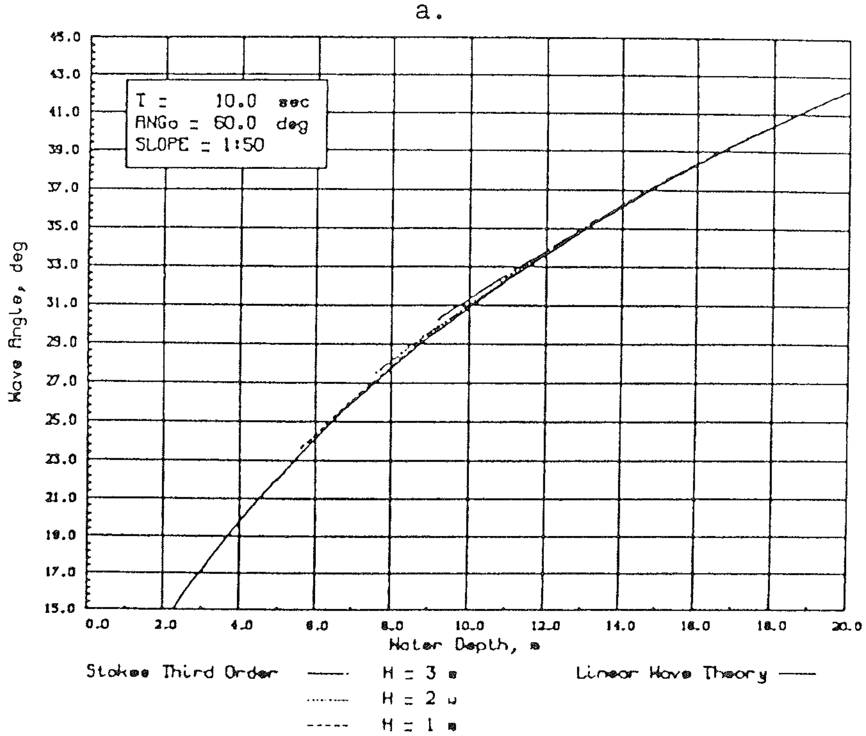

b.

Figure 6.16. Wave refraction over a plane beach

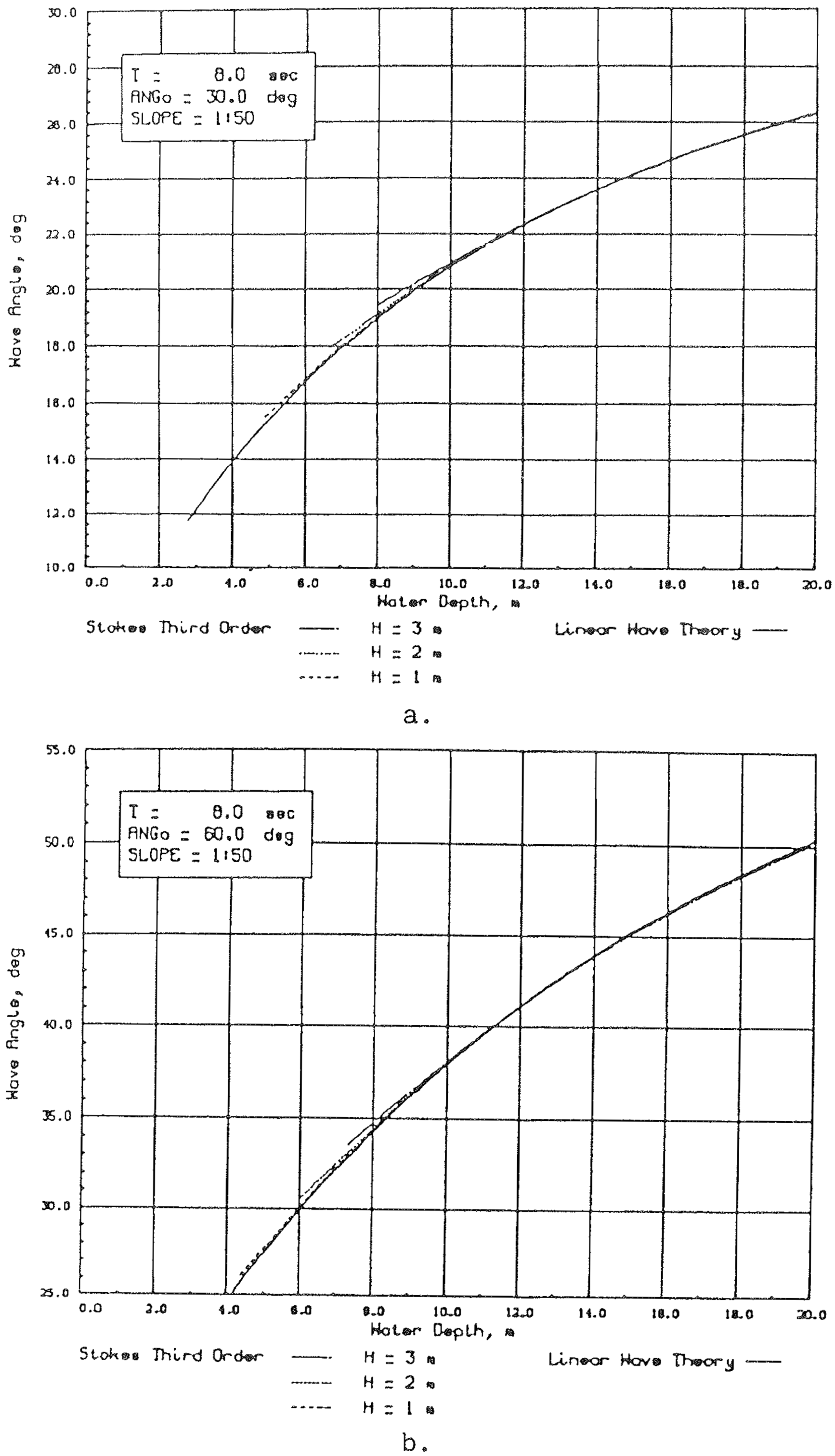

Figure 6.17. Wave refraction over a plane beach

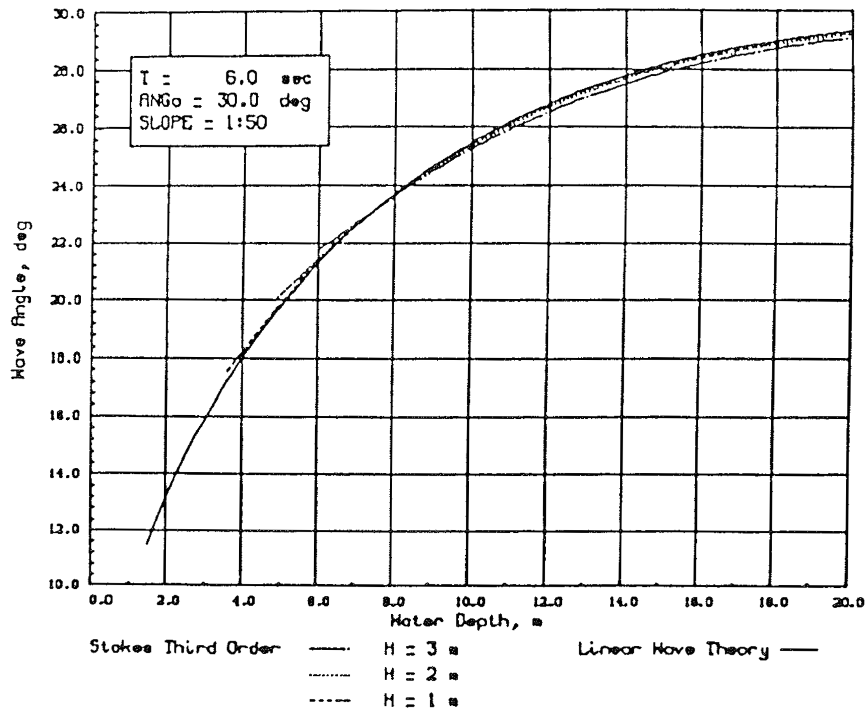

a.

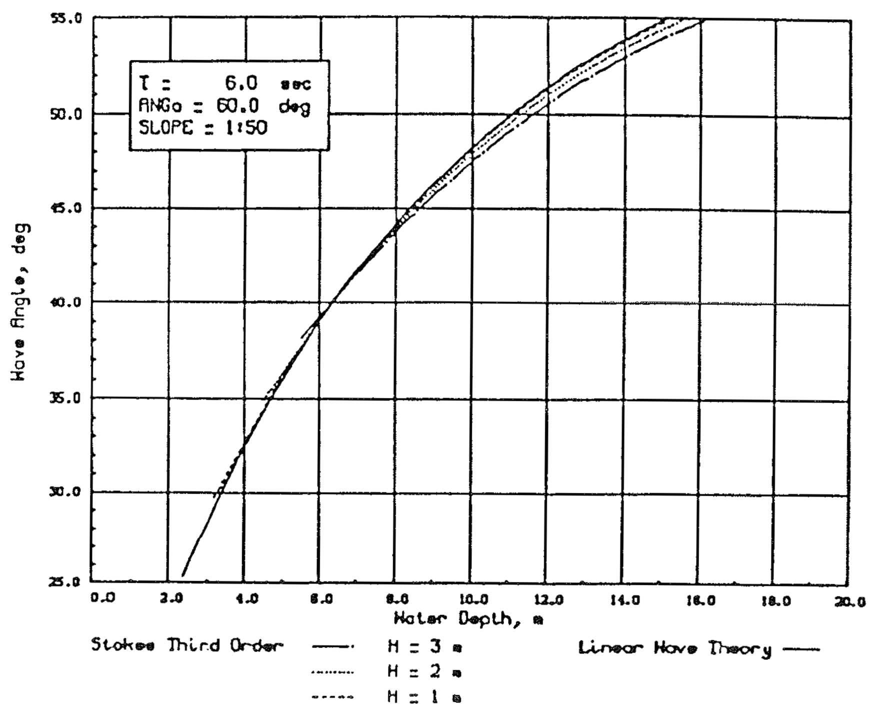

b.

Figure 6.18. Wave profile comparison

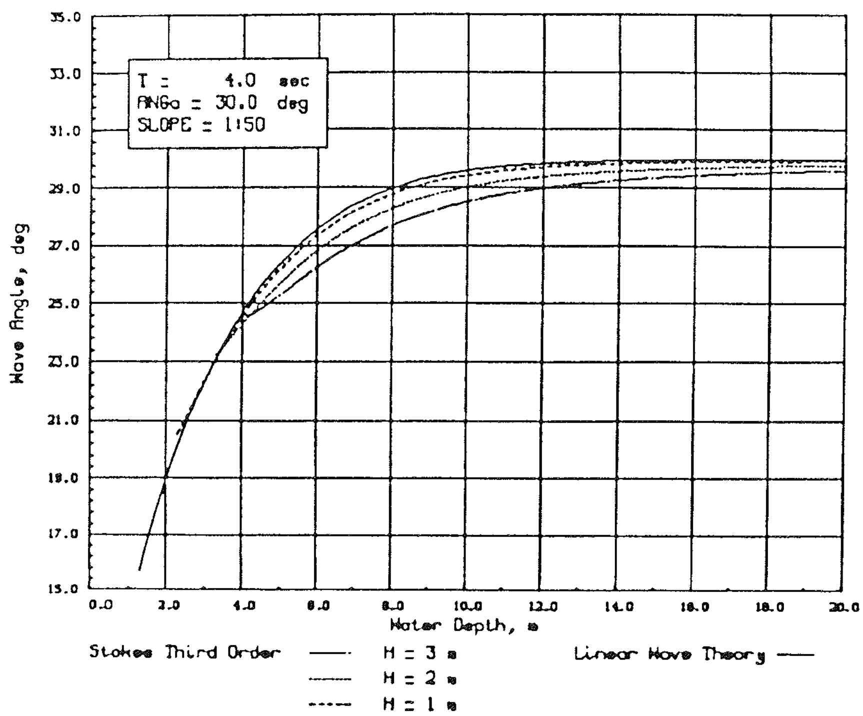

a.

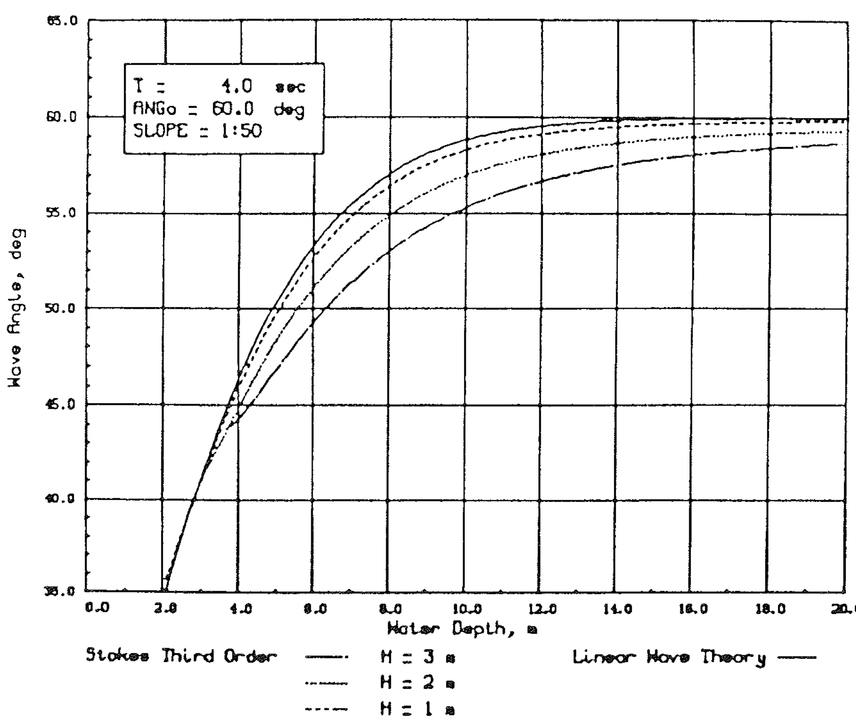

b.

Figure 6.19. Wave profile comparison

not to have been previously noted. Oh and Grosch (1985), in their investigation of third-order Stokes wave refraction, apparently missed this effect because of their incorrect calculation of wave shoaling. Here, it is found that in deeper water, finite amplitude waves refract more than small amplitude waves and in shallower water they refract less. This can be explicitly demonstrated by examining Snell's law (Equation 5.2) for small amplitude and finite amplitude wave refraction over a plane beach.

$$k^{(1)} \sin \alpha^{(1)} = k_o^{(1)} \sin \alpha_o \tag{6.2}$$

or

$$\sin \alpha^{(1)} = \frac{L^{(1)}}{L_o^{(1)}} \sin \alpha_o \ , \tag{6.3}$$

where

L_o = deepwater wavelength

and

α_o = deepwater wave angle.

The superscripts denote the order of the solution. Similarly for third-order Stokes waves,

$$\sin \alpha^{(3)} = \frac{L^{(3)}}{L_o^{(3)}} \sin \alpha_o \ . \tag{6.4}$$

Dividing 6.4 by 6.3 yields,

$$\frac{\sin \alpha^{(3)}}{\sin \alpha^{(1)}} = \frac{L^{(3)}}{L^{(1)}} \frac{L_o^{(1)}}{L_o^{(3)}} \quad . \tag{6.5}$$

By examining the third-order dispersion relation given by Isobe and Kraus (1983) (Equation 5.5) at the deepwater limit, it is found that

$$L_o^{(3)} = L_o^{(1)} \left(1 + \varepsilon_o^2\right). \tag{6.6}$$

It is interesting to note that Equation 6.6 is compatible with an equation for the wave celerity obtained by Stokes (1847) in his original work (if it is evaluated at the deepwater limit). Therefore the ratio of the deepwater wavelengths, $L_o^{(1)}/L_o^{(3)}$, is a constant less than unity, with the actual value depending upon the deepwater perturbation parameter, $\varepsilon_o = H_o/L_o^{(1)}$. The ratio of the wave angles then becomes a function of the ratio of the wavelengths. The linear wavelength is a function of the water depth and the deepwater wavelength or

$$L^{(1)} = f(D, T) \ . \tag{6.7}$$

The finite amplitude wavelength has the additional dependency on wave height, or

$$L^{(3)} = f(D, T, H) \ . \tag{6.8}$$

It is found that the H dependency of $L^{(3)}$ causes the overall ratio,

$$\frac{L^{(3)}}{L^{(1)}} \frac{L_o^{(1)}}{L_o^{(3)}} \tag{6.9}$$

to have a similar shape or depth dependency as the shoaling coefficient, K_s (Figure 4.3). That is, the overall ratio first decreases than increases, becoming greater than unity in shallower water. Therefore, it is concluded that the wave angle calculated by finite amplitude theory is less than the corresponding wave angle calculated by small amplitude theory in deeper water (more refraction), and greater than the small amplitude wave angle in shallower water (less refraction).

Table 6.2 displays numerical values of the ratio given in Equation 6.9, and the corresponding small amplitude and finite amplitude wave angles and H/H_o values as a function of depth for a 2.0-m, 6.0-sec wave, with $\alpha_o = 30$ deg . From the table it is observed that the ratio is less than unity at a depth of 30.0 m, then decreases to a minimum value of 0.993 between the 10.0 and 15.0 m depths. Finally, the ratio begins to increase at a depth of 9.0 m and quickly surpasses unity (D = 6.5 m). A comparison of the first-order and third-order wave angles shows that the "finite amplitude wave angles" are smaller (more refraction) than the "small amplitude wave angles" in deeper water. The wave angles differ by, at most, 0.15 deg in deeper water. This occurs when the ratio is at a minimum (0.993). If the ratio becomes greater than unity, the finite amplitude wave angles become larger (less refraction) than the small amplitude wave angles. The small amplitude waves refract more quickly than the finite amplitude waves in shallow water. The angles differ by 0.41 deg at the 5.0 m depth. A comparison of the shoaling of the first-order and third-order waves shows that finite amplitude waves are consistently larger than small amplitude waves, with the greatest difference occurring in shallow water. It should be noted

Table 6.2

Numerical Example for Wave Refraction

D (m)	$\frac{L^{(3)}}{L^{(1)}} \frac{L_o^{(1)}}{L_o^{(3)}}$	$\alpha^{(1)}$ (deg)	$\alpha^{(3)}$ (deg)	$\frac{H^{(1)}}{H_o}$	$\frac{H^{(3)}}{H_o}$
5.0	1.018	19.81	20.22	0.905	0.947
5.1	1.015	19.97	20.34	0.904	0.943
5.2	1.014	20.13	20.47	0.902	0.939
5.3	1.012	20.29	20.59	0.901	0.936
5.4	1.011	20.44	20.72	0.900	0.933
5.5	1.009	20.60	20.84	0.899	0.930
6.0	1.004	21.32	21.46	0.894	0.920
6.5	1.001	21.99	22.06	0.892	0.912
7.0	0.998	22.61	22.61	0.890	0.908
7.5	0.997	23.19	23.17	0.889	0.905
8.0	0.996	23.72	23.67	0.889	0.903
8.5	0.995	24.22	24.15	0.890	0.903
9.0	0.994	24.68	24.59	0.891	0.903
10.0	0.993	25.51	25.39	0.896	0.906
11.0	0.993	26.22	26.09	0.901	0.910
12.0	0.993	26.83	26.69	0.908	0.916
13.0	0.993	27.35	27.21	0.915	0.923
14.0	0.993	27.80	27.65	0.922	0.929
15.0	0.993	28.17	28.03	0.930	0.936
20.0	0.994	29.32	29.21	0.962	0.967
25.0	0.995	29.76	29.68	0.983	0.987
30.0	0.996	29.92	29.87	0.993	0.996

NOTE: H_o = 2.0 m , T = 6.0 sec , and α_o = 30.0 deg that the first-order shoaling coefficient, $H^{(1)}/H_o$, includes the effect of refraction, therefore the tabulated values are somewhat less than a strict, linear shoaling curve.

Comments

For the purpose of calculating the longshore sediment transport rate in the surf zone, the breaking wave angle, α_b , is needed. Although a Stokes wave model is not valid at the breaker line, the following can be surmised. From the general trend in the wave angle discussed in the previous paragraph, it can be inferred that a small amplitude wave will have a smaller value of the wave angle than the corresponding finite amplitude wave at breaking. Therefore, small amplitude wave theory overpredicts refraction at the breaker line and would presumably underpredict the longshore sediment transport rate. The undeprediction of the wave height by small amplitude wave theory compounds the problem of the low sediment transport rate predicted by small amplitude wave refraction.

In conclusion, as compared to third-order Stokes wave theory, small amplitude wave theory underpredicts the wave height throughout the solution domain, underpredicts wave refraction in deeper water, and overpredicts wave refraction in shallower water. It is reasonable to believe that these trends should continue to the breaker line. A finite amplitude wave model applicable at the breaker line would then predict a greater longshore sediment transport rate than would a small amplitude wave model. In addition, the wave profile and orbital velocities (Isobe and Kraus 1983a) are found to be quite different between finite amplitude and small amplitude waves.

2. Irregular Bottom Topography

The numerical model of finite amplitude refraction and shoaling is capable of predicting refraction and shoaling over an irregular bottom of reasonably smooth gradients. In this section, refraction and shoaling over a valley and a shoal will be examined. Figures 6.20 and 6.21 display the bottom configurations for the shoal and the valley, respectively.

Figure 6.22 shows the wave height and water depth in the longshore direction at various depths for the shoal. As the wave advances, it converges on the shoal and a caustic forms behind, or shoreward of, the shoal. That is, the waves bend inward and eventually cross each other. This typifies one limitation of the method used to calculate refraction in the model. The formation of a caustic can be artificially avoided to some extent if the ray method is used. If a caustic develops, a model using ray theory can "shoot" a different ray in from the offshore boundary. Alternatively, the method used in this thesis can be modified to include a smoothing scheme to eliminate some caustics. But, there is no theoretical justification for employing a smoothing scheme. The model as developed in this project uses no smoothing scheme; therefore the rigorous, theoretical solution of refraction is demonstrated here. Caustics, or wave ray crossings, can only be eliminated by employing a theory which allows energy movement across wave rays (or along a wave crest). This is the phenomenon known as wave diffraction. Incorporation of diffraction in the model is beyond the scope of the present work. For the extension to a combined refraction-diffraction approach, the interested reader is referred to Berkhoff 1972, Radder 1979, Lui 1984, and Ebersole 1985.

Figure 6.23 shows the wave height and water depth in the longshore direction at various depths for the valley. In this case, the wave energy disperses as the wave advances and the wave height decreases over the valley.

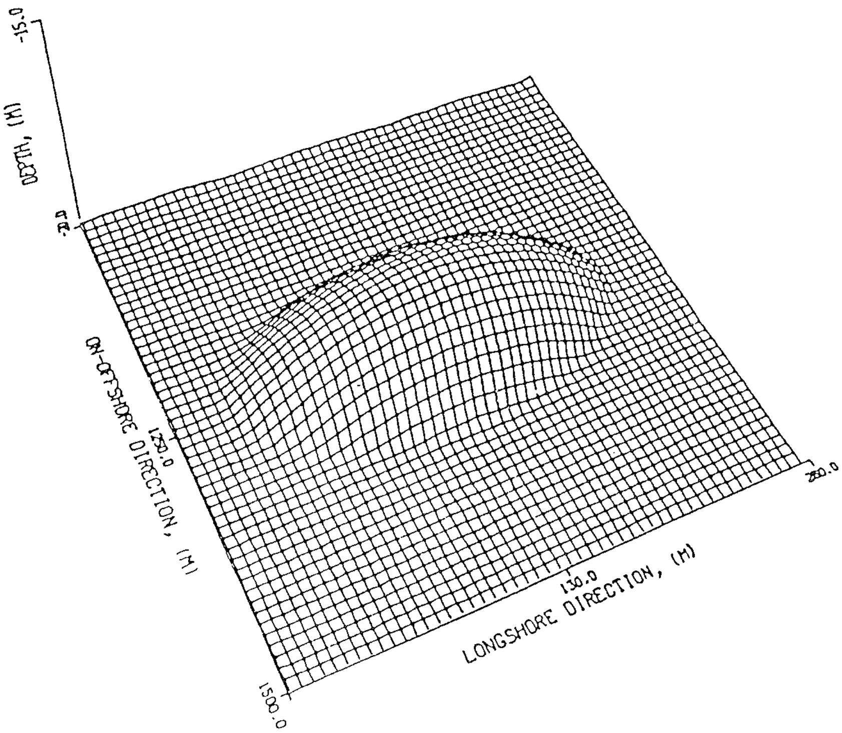

Figure 6.20. Bathymetric feature: shoal
(Note: this is a portion of the grid)

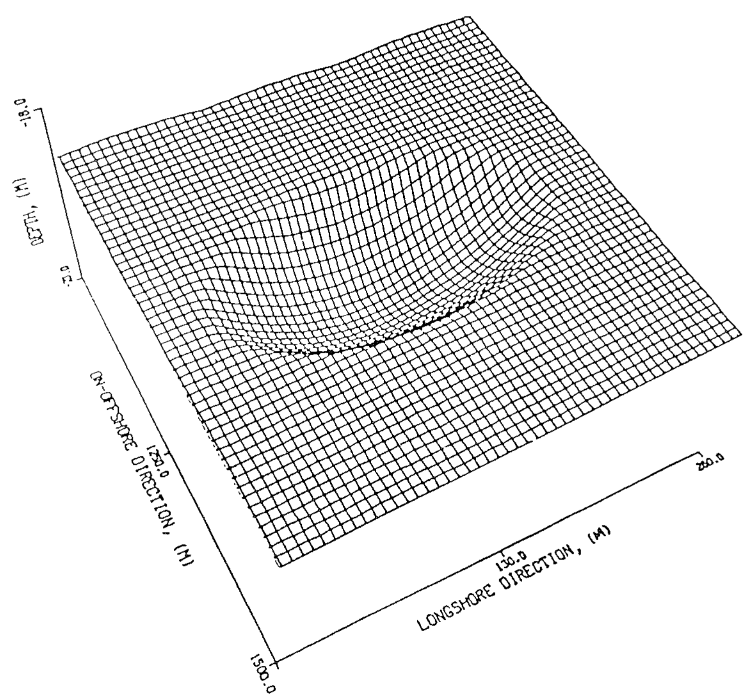

Figure 6.21. Bathymetric feature: valley
(Note: this is a portion of the grid)

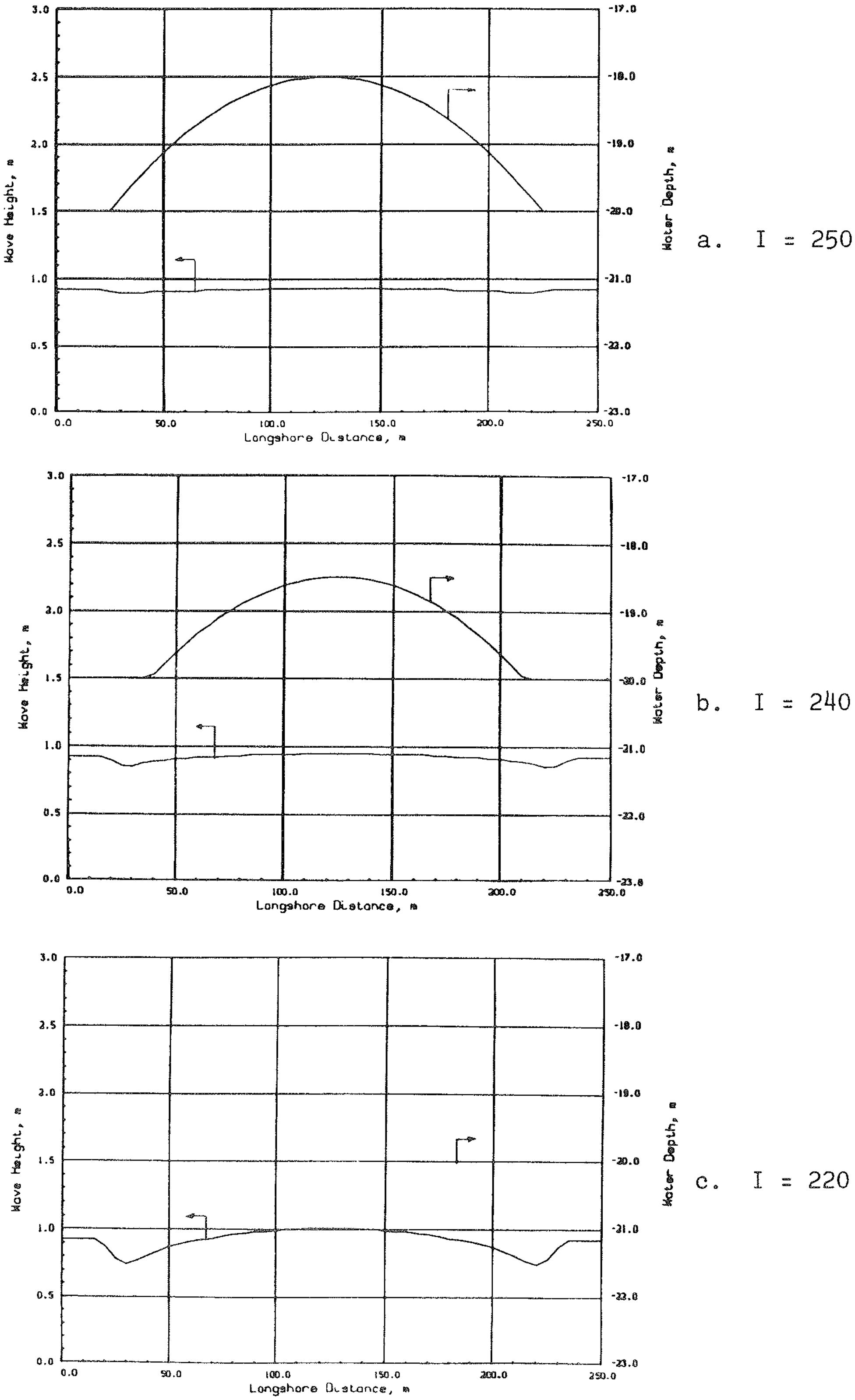

Figure 6.22. Wave height and water depth in the longshore direction: shoal

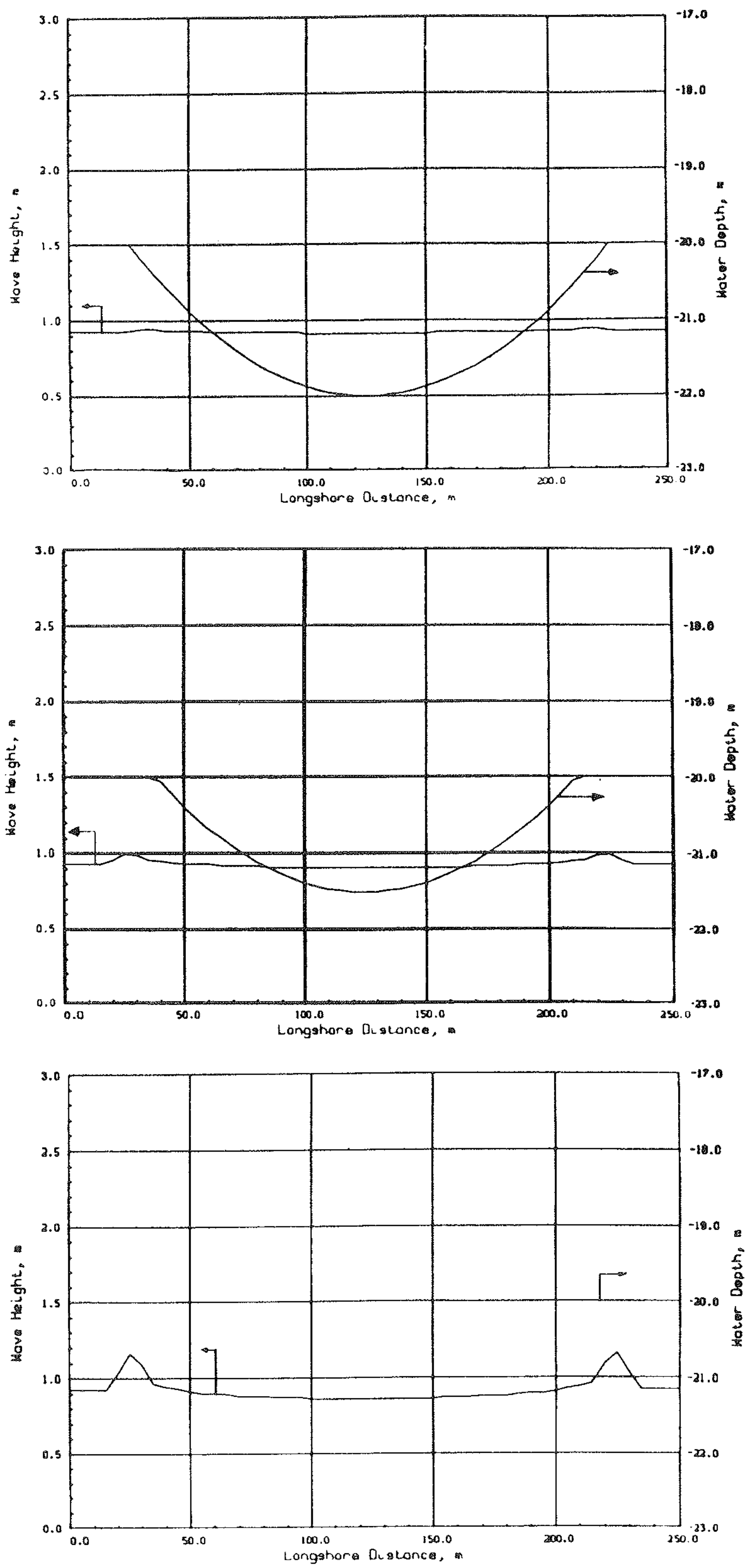

a. I = 250

b. I = 240

c. I = 220

Figure 6.23. Wave height and water depth in the longshore direction: valley

B. Comparison of Model Results with Laboratory Data on Wave Shoaling

Wave height predictions from the model developed for this thesis were compared to the laboratory data of Iversen (1951). Iversen conducted tests in a 1 ft. by 3 ft. by 54 ft. flume to study wave shoaling and wave breaking. As part of the wave transformation experiment, the wave height was measured using vertical point gages at 29 locations along the length of the flume for 11 wave conditions (Figure 6.24). Point gage readings of the crest and trough elevation provided the wave height at each location.

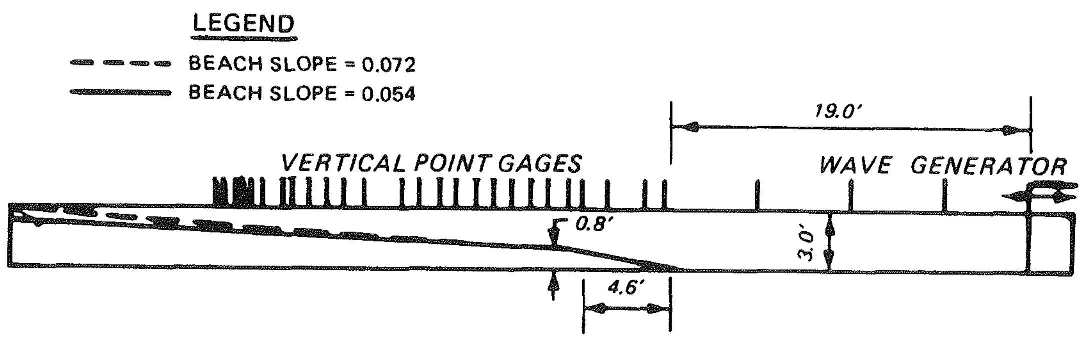

Figure 6.24. Channel configuration for shoaling experiments (after Iversen 1951)

For comparison with the Stokes wave model, three wave conditions were selected from Iversen's flume tests (Table 6.3). These wave conditions were selected because they were actually generated as deepwater waves. The remaining experimental tests were not generated as deepwater

Table 6.3

Wave Conditions for Wave Shoaling Comparison Tests

Case	H_o (ft)	T (sec)	D_o* (ft)	Beach Slope
1	0.351	0.865	2.55	0.072
2	0.333	0.860	2.44	0.054
3	0.320	0.965	2.44	0.054

* D_o is the depth in the constant depth region of the flume

waves due to the depth limitation of the flume. The laboratory data were also limited to plane beach tests because of the narrow flume width. The length of the flume restricted the experiments to beach slopes of 1:50 or steeper. Also, energy dissipation due to internal or bottom friction was not estimated in the experiments.

The numerical model is based on Stokes wave theory; therefore, it is correct to apply the model over the deeper regions of the laboratory flume. The model is applied until the limiting value of the Ursell number is reached ($U = 25$).

As shown in Figures 6.25 through 6.27, a comparison of the calculated and measured wave heights shows a good correlation between the general trends of the data (i.e., a decrease, then increase in wave height as the water depth decreases), but the magnitude of the wave heights differ by approximately 10 percent. The difference may be attributed, in part, to the frictional effect of the bottom and sides of the long, narrow experimental facility. Energy dissipation due to bottom friction causes a decrease in wave height, which is expected to be more prominent as the depth decreases. In addition, the sides of the

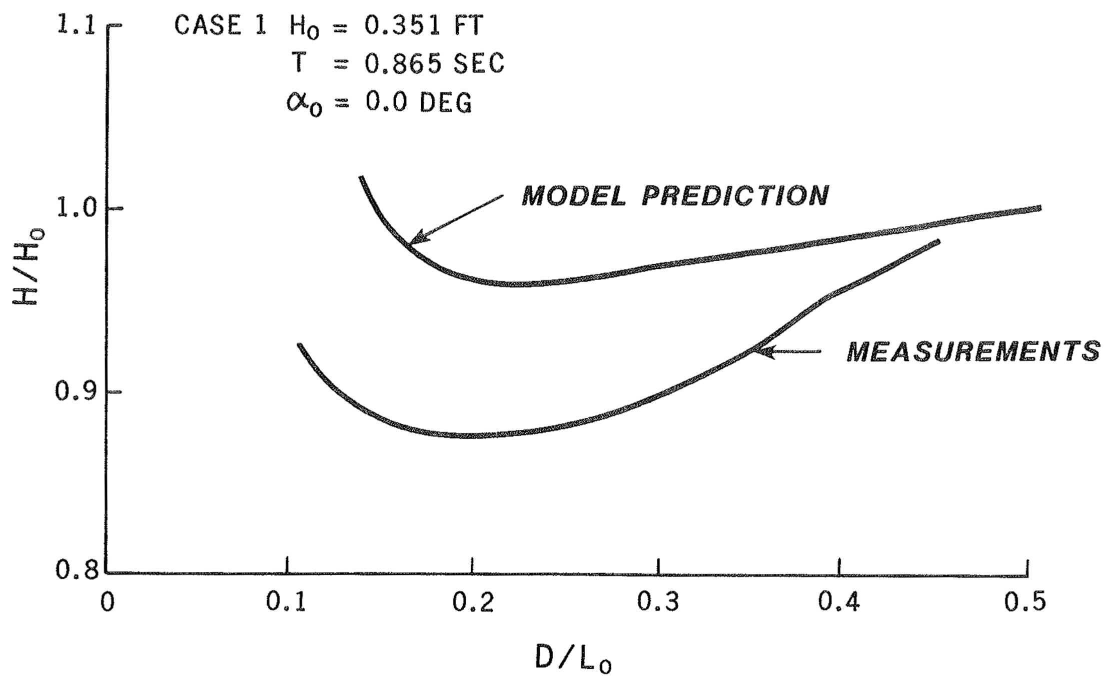

Figure 6.25. Comparison of predicted and measured shoaling curves

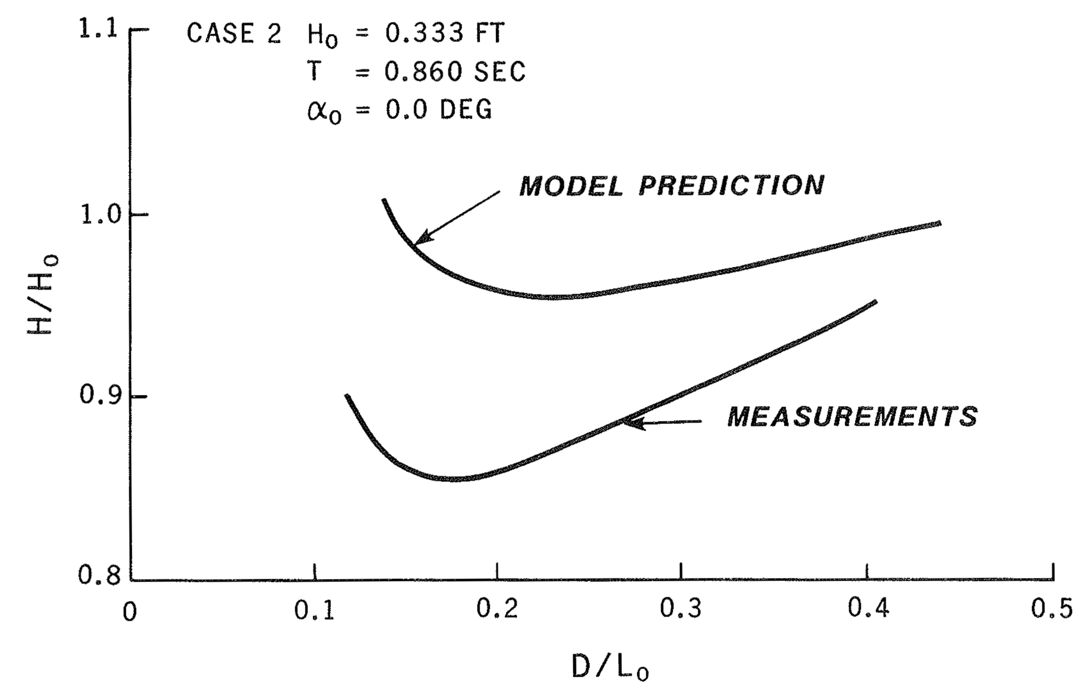

Figure 6.26. Comparison of predicted and measured shoaling curves

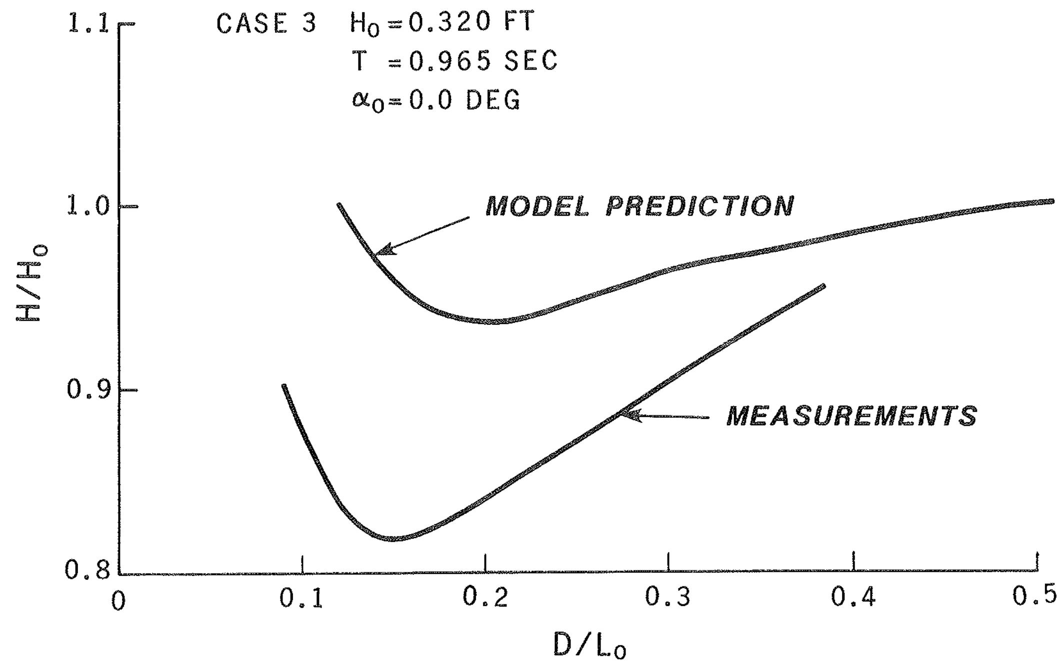

Figure 6.27. Comparison of predicted and measured shoaling curves

narrow flume will dissipate wave energy, thereby reducing the wave height further.

It is observed that the shoaling rate of finite amplitude waves is more rapid (a steeper curve) than small amplitude waves in shallow water (Figure 6.28). As in finite amplitude wave shoaling, the experimental results display a more rapid shoaling rate (a steeper curve) in shallow water than the small amplitude curve, but the entire curve is shifted down, below the finite amplitude and small amplitude curves. (The small amplitude wave transformation curve lies between Iversen's results and the finite amplitude model results.) All of Iversen's wave transformation tests fall below the small amplitude shoaling curve and all finite amplitude wave transformation results fall above the small amplitude shoaling curve (Figure 6.28). This observation supports the claim of

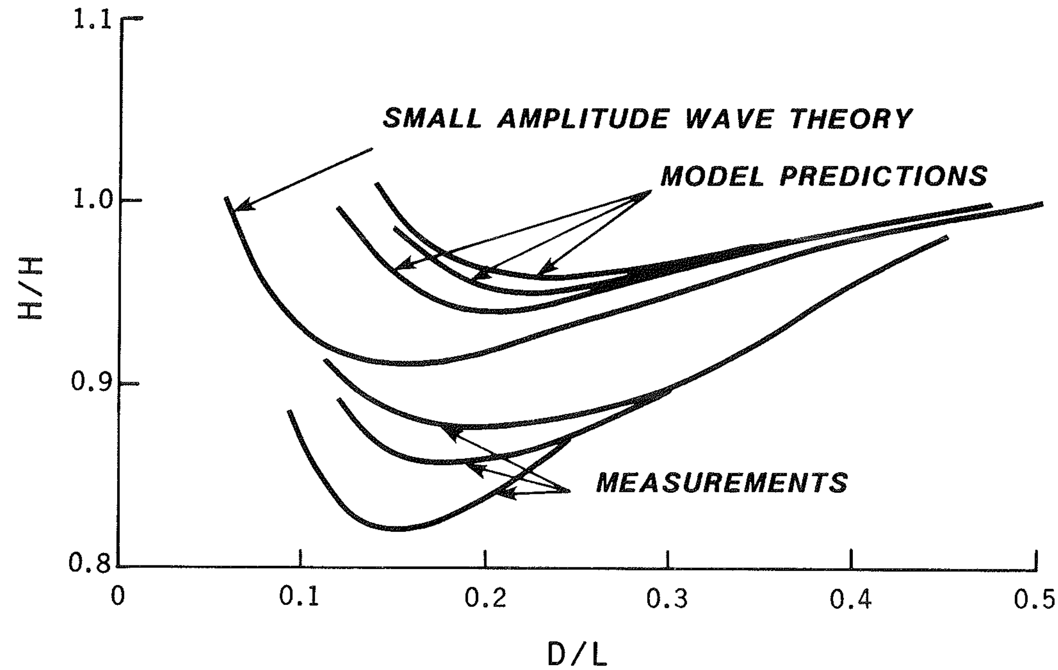

Figure 6.28. Small amplitude, finite amplitude, and measured shoaling curves

frictional effects reducing the wave height in the flume experiments. That is, the measured wave heights are consistently less than both the small amplitude and finite amplitude predicted wave heights. Therefore, it is believed that frictional dissipation reduced the measured wave heights and causes a downshift in the flume test shoaling curves.

C. Model Limitation

The model developed in this report has certain limitations which have been briefly discussed in previous sections and will be summarized in this section.

1. The Wave System

The finite amplitude wave model developed herein is based on the derivation of a third-order Stokes wave theory by Isobe and Kraus (1983a). In the derivation, it is assumed that waves of permanent form and finite height progress over a horizontal bottom. The fluid is assumed to be inviscid and incompressible and the motion is assumed to be irrotational. The solution is in two dimensions and therefore assumes long-crested waves. From the conservation of wave energy equation used in the derivation, $\nabla \cdot F = 0$, it is apparent that surface stresses (i.e., wind) and bottom stresses (i.e., friction) are neglected. The assumption of a horizontal bottom means modeling over a sloping bottom is not absolutely theoretically correct.

The model computes wave conditions resulting from the transformation of a monochromatic wave over an irregular bottom. It is a steady-state model, i.e., time dependent processes are not included. The inclusion of diffraction and steady, longshore currents was beyond the scope of this investigation.

2. Range of Validity

The finite amplitude wave model developed for this report is applicable from deep water to the depth at which the Ursell number reaches 25. This is the range of validity of Stokes waves. (Therefore, this model, or any other Stokes wave model, cannot be used to directly calculate breaking waves, because such waves generally have Ursell numbers larger than 25.) The range of validity is a function of the deepwater wave height and the wave period. The limiting values calculated by the model can be used as input to other wave transformation models applicable to shallow water and for sediment transport models in deeper water. The limitations imposed by the range of validity are mitigated by the model's ablility to aid in the solution process of other models.

3. Caustics

Any pure calculation of wave refraction, as presented here, will lead to caustics for certain bathymetric features. The inclusion or extension to combined refraction and diffraction is expected to alleviate the problem in most instances.

4. Lateral Boundary Conditions

The solution at the lateral boundaries is found by setting the boundary values equal to the values at adjacent grid points. This boundary condition implies that the change in any given variable in the y direction is zero and is therefore most valid if the contours are nearly straight and parallel to the y-axis.

VII. CONCLUDING DISCUSSION AND RECOMMENDATIONS FOR FUTURE WORK

A finite amplitude wave refraction and shoaling model has been developed from the third-order derivation of a Stokes wave theory presented by Isobe and Kraus (1983a).

Energy flux is the fundamental quantity required to calculate wave shoaling, and its determination is a central part of this project. An expression for the energy flux is derived using a unique simplification based on the second definition of wave celerity. Since the recent theory of Isobe and Kraus' was used as a basis for the calculations of wave energy, energy flux, and group velocity herein, the results provide an independent evaluation of the flux and serve to verify the limited previous work. The present work is also substantiated by the fact that the energy flux given by Le Méhauté and Webb (1964) is identical to the energy flux derived in this report at the deepwater limit. This condition does not necessarily mean that the fluxes are identical throughout the solution domain, however.

The model solves the dispersion relation for the wave number, the irrotationality condition on the wave number vector for the wave angle, and the conservation of wave energy equation for the wave height. The solution is accomplished on a grid using finite difference techniques. The interdependency of the variables requires an iterative scheme in the solution process.

The finite amplitude wave model has certain limitations imposed upon it by assumptions in the theoretical development, the derivation, and by the modeling process itself.

Since the model is based on Stokes wave theory, it is valid from relatively deep water to the depth where the Ursell number reaches 25. (The Ursell parameter, which incorporates the three wave characteristics needed to describe waves of permanent form, is evaluated at each grid point to determine if the Stokes wave model is applicable.) The wave steepness criterion ($H/L < 0.14$) must also be closely monitored in the model (Michell 1893). Application of the model outside the range of validity of third-order Stokes waves will produce erroneous results, and the model has an automatic "shut-off" if the validity is violated.

Model tests were run to compare the results of the finite amplitude wave model with small amplitude wave theory model results. It was found that small amplitude wave theory consistently underpredicts wave shoaling as compared to the third-order Stokes theory. The magnitude of the difference between small amplitude and finite amplitude wave theory predictions depends on the characteristics of the wave: the deepwater wave height, the wave period, and the water depth at which the wave is examined. High, short period waves in shallow water will have a large perturbation parameter and will therefore refract and shoal differently from small amplitude waves. The form of the finite amplitude wave profile is also quite different from the purely sinusoidal small amplitude wave profile.

Refraction of finite amplitude waves is found to be greater than small amplitude wave refraction in deep water and less than small amplitude wave refraction in shallower water.

In conclusion, the most significant differences between small amplitude and finite amplitude waves occur in shallow water. Small amplitude wave theory: (1) underpredicts wave shoaling and (2) overpredicts wave refraction in this region. The underprediction of wave shoaling by small amplitude wave theory is of a significantly larger magnitude than the overprediction of wave refraction.

The laboratory shoaling curves of Iversen were compared to the shoaling curves predicted by the finite amplitude wave model. Both the predicted wave model results and the measured flume data display the general trend of shoaling curves. That is, a gradual decrease in wave height as the water depth decreases, then a more rapid increase in wave height as the depth decreases further. The laboratory shoaling curves are consistently below the model shoaling curves (and are also below the small amplitude wave shoaling curve). Frictional effects are most probably the major cause of the lower wave heights in the laboratory data.

The derivation process for the energy flux, energy, and group velocity along with the numerical model development and applications were extensively examined in this report. Refinements and extensions of the model in possible future work include the following: (1) merging of the third-order Stokes wave model with a shallow water (cnoidal) model, (2) inclusion of diffraction in the wave model, (3) collection of field data and laboratory data to complete the model verification, and (4) derivation of the fifth-order Stokes energy flux, energy, and group velocity for use in a fifth-order Stokes wave model.

REFERENCES

Abernathy, C. L., and Gilbert, G. 1975. "Refraction of Wave Spectra," Hydraulics Research Station, Report No. 117.

Berkhoff, J. C. W. 1972. "Computation of Combined Refraction-Diffraction," Proceedings of the 13th Coastal Engineering Conference, American Society of Civil Engineers, Vol 1, pp 471-490.

Bretschneider, C. L. 1960. "A Theory for Waves of Finite Height," Proceedings of the 7th Coastal Engineering Conference, American Society of Civil Engineers, Vol 1, Chapter 9, pp 146-183.

Chappelear, J. E. 1961. "Direct Numerical Calculation of Wave Properties," Journal of Geophysical Research, Vol 66, pp 501-508.

Chu, H. L. 1975. "Numerical Model for Wave Refraction of Finite Amplitude Wave Theories," American Society of Civil Engineers Symposium on Modeling Techniques, Vol 2, Chapter 14, pp 1082-1100.

Dailey, J. E. 1978. "Stokes V Wave Computations in Deep Water," Journal of the Waterway, Port, Coastal and Ocean Division, American Society of Civil Engineers, Vol 104, No. WW4, pp 447-453.

De, S. C. 1955. "Contributions to the Theory of Stokes Waves," Proceedings of the Cambridge Philosophical Society, Vol 51, pp 713-736.

Dean, R. G. 1965. "Stream Function Representation of Nonlinear Ocean Waves," Journal of Geophysical Research, Vol 70, No. 18, pp 4561-4572.

__________. 1970. "Relative Validity of Water Wave Theories," Journal of the Waterways and Harbors Division, American Society of Civil Engineers, Vol 96, No. WW1, pp 105-119.

Dean, R. G., and Dalrymple, R. A. 1984. Water Wave Mechanics for Engineers and Scientists, Prentice-Hall, Inc., Englewood Cliffs, N. J.

Dobson, R. S. 1967. "Some Applications of Digital Computers to Hydraulic Engineering Problems," TR-80, Chapter 2, Department of Civil Engineering, Stanford University, Pasadena, Calif.

Dombs, C. and Sykes, M. F. 1957. "On the Susceptibility of a Ferromagnetic Above the Curie Point," Proceedings of the Royal Society of London, Series A, Vol 240, pp 214-228.

Ebersole, B. A. 1985. "Refraction-Diffraction Model for Linear Water Waves," Journal of Waterway, Port Coastal, and Ocean Engineering, American Society of Civil Engineers, Vol 111, No. 6, pp 939-953.

Fenton, J. D. 1985. "A Fifth-Order Stokes Wave Theory for Steady Waves," Journal of the Waterway, Port, Coastal and Ocean Engineering, American Society of Civil Engineers, Vol 111, No. 2, pp 216-234.

Goda, Y. 1983. "A Unified Nonlinear Parameter of Water Waves," Report of the Port and Harbour Research Institute, Vol 22, No. 3, pp 1-30.

Hardy, T. A., and Kraus, N. D. 1987. "The Numerical Model for the Shoaling and Refraction of Second-Order Cnoidal Waves over an Irregular Bottom," Miscellaneous Paper CERC-87-9, US Army Engineer Waterways Experiment Station, Vicksburg, Miss.

Havelock, T. H. 1919. "Periodic Irrotational Waves of Finite Height," Proceedings of the Royal Society, Vol A95, pp 38-45.

Headland, J. R., and Chu, H. L. 1984. "A Numerical Model for the Refraction of Linear and Cnoidal Waves," Proceedings of the 19th Coastal Engineering Conference, American Society of Civil Engineers, Vol 2, Chapter 76, pp 1118-1131.

Horiguchi, T. 1982. "Study of Water Particle Velocities of Shoaling and Breaking Waves," Coastal Engineering in Japan, Vol 25, pp 109-123.

Horikawa, K. 1978. Coastal Engineering: An Introduction to Ocean Engineering, Halsted Press, New York, N. Y.

Isobe, M., and Kraus, N. C. 1983a. "Derivation of a Third-Order Stokes Wave Theory," Hydraulics Laboratory Technical Report No. 83-1, Yokohama National University, Yokohama, Japan.

__________. 1983b. "Derivation of a Second-Order Cnoidal Wave Theory," Hydraulics Laboratory Technical Report No 83-2, Yokohama National University, Yokohama, Japan.

Isobe, M., Nishimura, H., and Horikawa, K. 1982. "Theoretical Considerations on Perturbation Solutions for Waves of Permanent Type," Bulletin of the Faculty of Engineering, Yokohama National University, Yokohama, Japan, pp 29-57.

Iversen, H. W. 1951. "Laboratory Studies on Breakers," Proceedings of the National Bureau of Standards Symposium on Gravity Waves, Chapter 3, pp 9-32.

Iwagaki, Y., and Yamaguchi, M. 1968. "Studies on Cnoidal Waves (Sixth Report)--Limiting Condition for Application of Cnoidal Theory," Annuals of the Disaster Prevention Research Institute, Kyoto University, No. 11 B, pp 477-502, (in Japanese).

Keulegan, G. H., and Patterson, G. W. 1940. "Mathematical Theory of Irrotational Translation Waves," Journal of Research of the National Bureau of Standards, Vol 24, pp 47-101.

Koh, R. C., and Le Méhauté, B. 1966a. "Wave Shoaling," Technical Report SN 134-9, National Engineering Science Company, for the Office of Naval Research, Washington, DC.

_________. 1966b. "Wave Shoaling," Journal of Geophysical Research, Vol 71, No 8, pp 2005-2012.

Korteweg, D.J., and DeVries, G. 1895. "On the Change of Form of Long Waves Advancing in a Rectangular Channel, and on a New Type of Long Stationary Waves," Philosophical Magazine, Series 5, Vol 39, pp 422-443.

Kraus, N. C., Cialone, M. A., and Hardy, T. A. 1987. Discussion on: "Numerical Study of Finite Amplitude Wave Refraction," Journal of Waterway, Port, Coastal, and Ocean Engineering, American Society of Civil Engineers, Vol 113, No. 2, pp 199-201.

Laitone, E. V. 1962. "Limiting Conditions for Cnoidal and Stokes Waves," Journal of Geophysical Research, Vol 67, No. 4, pp 1555-1564.

Le Méhauté, B. 1976. An Introduction to Hydrodynamics and Water Waves, Springer-Verlag, New York, N. Y.

Le Méhauté, B., Divoky, D., and Lin, A. 1968. "Shallow Water Waves: A Comparison of Theories and Experiments," Proceedings of the 11th Coastal Engineering Conference, American Society of Civil Engineers, Vol 1, Chapter 7, pp 86-107.

Le Méhauté, B., and Webb, L.M. 1964. "Periodic Gravity Waves Over a Gentle Slope at a Third Order of Approximation," Proceedings of the 9th Coastal Engineering Conference, American Society of Civil Engineers, Chapter 2, pp 23-40.

Liu, P. L.-F., and Tsay, T. K. 1984. "Refraction-Diffraction Model for Weakly Nonlinear Water Waves," Journal of Fluid Mechanics, Vol 131, pp 59-71.

Michell, J. H. 1893. "The Highest Waves in Water," Philosophical Magazine, Vol 36, pp 430-437.

Munk, W. H., and Arthur, R. S. 1951. "Wave Intensity Along a Refracted Ray," Proceedings of the National Bureau of Standards Symposium on Gravity Waves, Chapter 13, pp 95-108.

Nishimura, H., Isobe, M., and Horikawa, K. 1977. "Higher Order Solutions of the Stokes and Cnoidal Waves," Journal of the Faculty of Engineering, The University of Tokyo, Vol 34, No. 2, pp 267-293.

Noda, E. K., Sonu, C. J., Rupert, V. C., and Collins, J. I. 1974. "Nearshore Circulation Under Sea Breeze Conditions and Wave-Current Interactions in the Surf Zone," Report No. TC-149-4, Tetra Tech, Incorporated, Pasadena, California.

Oh, I. S., and Grosch, C. E. 1985. "Numerical Study of Finite Amplitude Wave Refraction," Journal of Waterway, Port, Coastal, and Ocean Engineering, American Society of Civil Engineers, Vol 111, No. 1, pp 78-95.

Phillips, O. M. 1977. The Dynamics of the Upper Ocean, Cambridge University Press, New York, N. Y.

Radder, A. C. 1979. "On the Parabolic Equation Method for Water Wave Propagation," Journal of Fluid Mechanics, Vol 95, pp 159-176.

Rouse, H., Editor. 1950. "Wave Motion," Engineering Hydraulics, John Wiley and Sons, New York, N. Y.

Sarpkaya, T., and Isaacson, M. 1981. Mechanics of Wave Forces on Structures, Van Nostrand Reinhold Co., New York, N. Y.

Schwartz, L. W. 1974. "Computer Extension and Analytical Continuation of Stokes Expansion for Gravity Waves," Journal of Fluid Mechanics, Vol 62, Part 3, pp 553-578.

Skjelbreia, L. 1958. "Gravity Waves Stokes Third Order Approximation Tables of Functions," Council on Wave Research, The Engineering Foundation.

Skjelbreia, L., and Hendrickson, J. 1960. "Fifth-Order Gravity Wave Theory," Proceedings of the 7th Coastal Engineering Conference, American Society of Civil Engineers, Vol 1, Chapter 10, pp 184-196.

Skovgaard, O. and Petersen, M. H. 1977. "Refraction of Cnoidal Waves," Coastal Engineering, Vol 1, pp 43-61.

Shore Protection Manual. 1984. 2 vols., 4th ed., US Army Engineer Waterways Experiment Station, Coastal Engineering Research Center, US Government Printing Office, Washington, D. C.

Stokes, G. G. 1847. "On the Theory of Oscillatory Waves," Transactions of the Cambridge Philosophical Society, Vol 8, pp 441-455.

Tsuchiya, Y., and Yamaguchi, M. 1972. "Some Considerations on Water Particle Velocities of Finite Amplitude Wave Theories," Coastal Engineering in Japan, Vol 15, pp 43-57.

Tsuchiya, Y., and Yasuda, T. 1981. "A New Approach to Stokes Wave Theory," Bulletin of the Disaster Prevention Research Institute, Vol 31, Part 1, No. 276, pp 17-34.

Wiegel, R. 1964. Oceanographical Engineering, Prentice-Hall, Inc., Englewood Cliffs, N J.

Wilson, W. S. 1966. "A Method for Calculating and Plotting Surface Wave Rays," TM-17, US Army, Corps of Engineers, Coastal Engineering Research Center, Washington, D. C.

APPENDIX A: DERIVATION OF THE MEAN ENERGY FLUX

The process of evaluating the mean energy flux, $\bar{F}$, will be shown. As derived in Section III D, $\bar{F}$ can be written

$$\bar{F} = \rho C \overline{\int_{-D}^{N} u^2 dz} \tag{A1}$$

by use of the second definition of wave celerity, where:

ρ = the fluid density

C = wave celerity

u = horizontal water particle velocity

dz = incremental depth

-D = elevation of the bottom boundary

N = free surface elevation

The following quantities are available from Isobe and Kraus (1983a):

$$C = C_{IK}\left[1 + \varepsilon^2\left(\frac{9c^4 - 10c^2 + 9}{16} - \frac{c}{2kD}\right)\right]$$

$$u = u_0 + u_1 \cosh k(z + D) \cos \theta + u_2 \cosh 2k(z + D) \cos 2\theta$$
$$+ u_3 \cosh 3k(z + D) \cos 3\theta$$

$$N = \frac{1}{k}\left(N_1 \cos \theta + N_2 \cos 2\theta + N_3 \cos 3\theta\right)$$

$$C_{IK} = \sqrt{\frac{g}{k} \tanh kD}$$

$$u_0 = C_{IK} B_0$$

$$u_1 = \frac{C_{IK} B_1}{\sinh kD}$$

$$u_2 = \frac{2\ C_{IK} B_2}{\sinh 2kD}$$

$$u_3 = \frac{3\ C_{IK}\ B_3}{\sinh 3kD}$$

$$B_0 = \varepsilon^2 \left(\frac{-c}{2kD}\right)$$

$$B_1 = \varepsilon + \frac{\varepsilon^3}{64} (-27c^6 - 3c^4 - 41c^2 + 39)$$

$$B_2 = \frac{\varepsilon^2}{4} \left(3c(c^2 - 1)\right)$$

$$B_3 = \frac{\varepsilon^3}{64} (27c^6 - 57c^4 + 17c^2 + 13)$$

$$N_1 = \varepsilon + \frac{3\varepsilon^3}{64} (-9c^6 + 3c^4 - 3c^2 + 1)$$

$$N_2 = \varepsilon^2 c \frac{(3c^2 - 1)}{4}$$

$$N_3 = \frac{3\varepsilon^3}{64} (9c^6 - 3c^4 + 3c^2 - 1)$$

$\theta = (kx - \sigma t)$

$\varepsilon = \frac{kH}{2}$

$c = \coth kD$

x = horizontal coordinate

z = vertical coordinate

g = gravitational acceleration

k = wave number = $\frac{2\pi}{L}$

H = wave height

σ = angular frequency = $\frac{2\pi}{T}$

t = time

The first step is to calculate the square of the horizontal water particle velocity.

$$
\begin{aligned}
u^2 = u_0^2 &+ 2u_0u_1 \cos\theta \cosh k(z+D) + 2u_0u_2 \cos 2\theta \cosh 2k(z+D) \\
&+ 2u_0u_3 \cos 3\theta \cosh 3k(z+D) + u_1^2 \cos^2\theta \cosh^2 k(z+D) \\
&+ 2u_1u_2 \cos\theta \cos 2\theta \cosh k(z+D) \cosh 2k(z+D) \\
&+ 2u_1u_3 \cos\theta \cos 3\theta \cosh k(z+D) \cosh 3k(z+D) \\
&\qquad + u_2^2 \cos^2 2\theta \cosh^2 2k(z+D) + \text{H.O.T.}
\end{aligned}
$$

where

H.O.T. = Higher Order Terms

= terms of order ε^4 (or $\frac{\varepsilon^5}{k}$) and higher.

Defining the symbol

$$\int_{-D}^{N} dz = \left\langle \quad \right\rangle ,$$

the next step is to integrate u^2 over the depth.

$$\langle u^2 \rangle = u_0^2(N + D) + \frac{2u_0u_1 \cos\theta}{k} \sinh k(N + D)$$

$$+ \frac{u_0u_2 \cos 2\theta}{k} \sinh 2k(N + D) + \frac{2u_0u_3 \cos 3\theta}{3k} \sinh 3k(N + D)$$

$$+ u_1^2 \cos^2\theta\left(\frac{\sinh 2k(N + D)}{4k} + \frac{N}{2} + \frac{D}{2}\right)$$

$$+ u_1u_2 \cos\theta \cos 2\theta\left(\frac{\sinh 3k(N + D)}{3k} + \frac{\sinh k(N + D)}{k}\right)$$

$$+ u_1u_3 \cos\theta \cos 3\theta\left(\frac{\sinh 4k(N + D)}{4k} + \frac{\sinh 2k(N + D)}{2k}\right)$$

$$+ u_2^2 \cos^2 2\theta\left(\frac{\sinh 4k(N + D)}{8k} + \frac{N}{2} + \frac{D}{2}\right) \tag{A2}$$

It is convenient to define the terms in Equation A2 as follows:

$$I_0 = u_0^2(N + D)$$

$$I_1 = \frac{2u_0u_1 \cos\theta}{k} \sinh k(N + D)$$

$$I_2 = \frac{u_0u_2 \cos 2\theta}{k} \sinh 2k(N + D)$$

$$I_3 = \frac{2u_0u_3 \cos 3\theta}{3k} \sinh 3k(N + D)$$

$$I_4 = \frac{u_1^2 \cos^2\theta}{4k} \sinh 2k(N + D)$$

$$I_5 = \frac{u_1^2 \cos^2\theta}{2} N$$

$$I_6 = \frac{u_1^2 \cos^2 \theta}{2} D$$

$$I_7 = \frac{u_1 u_2 \cos \theta \cos 2\theta}{3k} \sinh 3k(N + D)$$

$$I_8 = \frac{u_1 u_2 \cos \theta \cos 2\theta}{k} \sinh k(N + D)$$

$$I_9 = \frac{u_1 u_3 \cos \theta \cos 3\theta}{4k} \sinh 4k(N + D)$$

$$I_{10} = \frac{u_1 u_3 \cos \theta \cos 3\theta}{2k} \sinh 2k(N + D)$$

$$I_{11} = \frac{u_2^2 \cos^2 2\theta}{8k} \sinh 4k(N + D)$$

$$I_{12} = \frac{u_2^2 \cos^2 2\theta}{2} N$$

$$I_{13} = \frac{u_2^2 \cos^2 2\theta}{2} D$$

The time average of each I_i term must be calculated. For convenience, the following definition (symbol) is introduced:

$$\frac{1}{T} \int_t^{t+T} I_i \, dt = \overline{I}_i ,$$

and without any loss of generality, for waves of permanent form:

$$\frac{1}{T} \int_0^T I_i \, dt = \overline{I}_i .$$

The explicit integration of I_0 , I_1 , I_4 , and I_{11} will be shown and the results of the remaining integrals will only be listed. Identities used in the solution process are given in Appendix D.

$$\bar{I}_0 = \frac{1}{T}\left(\overline{u_0^2\ (N + D)}\right) \tag{A3}$$

$$\bar{I}_0 = \frac{\overline{u_0^2 N}}{T} + \frac{\overline{u_0^2 D}}{T} \tag{A4}$$

$$\bar{I}_0 = \frac{u_0^2 D}{T}\ (T - 0)$$

$$\boxed{I_0 = u_0^2 D}$$

The first term in Equation A4 is zero because the average value of the free surface elevation over one wave period (or wavelength) is equal to the mean water level, by definition.

$$\bar{I}_1 = \frac{2u_0 u_1}{kT}\left(\overline{\cos\theta \sinh k(N + D)}\right) \tag{A5}$$

Assuming N is small but finite, $\sinh k(N + D)$ can be expanded in a power series around D .

$$\sinh k(N + D) = \sinh kD + kN \cosh kD + \frac{(kN)^2}{2} \sinh kD + \frac{(kN)^3}{6} \cosh kD$$

$$\sinh k(N + D) = \sinh kD\left(1 + \frac{(kN)^2}{2}\right) + \cosh kD\left(kN + \frac{(kN)^3}{6}\right) \tag{A6}$$

Substitution of (A6) into (A5) yields:

$$\overline{I}_1 = \frac{2u_0u_1}{kT}\left[\overline{\left(\cos\theta \quad \sinh kD\left(1 + \frac{(kN)^2}{2}\right) + \cosh kD\left(kN + \frac{(kN)^3}{6}\right)\right)}\right] \qquad (A7)$$

Equation A7 is separated into the four terms defined below:

$$\overline{I}_{1_1} = \frac{2u_0u_1 \sinh kD}{kT} \left(\overline{\cos\theta}\right)$$

$$\overline{I}_{1_2} = \frac{u_0u_1 \sinh kD}{kT} \left(\overline{\cos\theta(kN)^2}\right)$$

$$\overline{I}_{1_3} = \frac{2u_0u_1 \cosh kD}{kT} \left(\overline{\cos\theta\ (kN)}\right)$$

$$\overline{I}_{1_4} = \frac{u_0u_1 \cosh kD}{3kT} \left(\overline{\cos\theta(kN)^3}\right)$$

Neglecting higher order terms,

$$(kN)^2 = N_1^2 \cos^2\theta + 2N_1N_2 \cos\theta \cos 2\theta$$

$$(kN)^3 = N_1^3 \cos^3\theta$$

These equations are to third-order in ε, as can be seen from Equations A46 through A48. In reality they need only be kept to first-order because they are multiplied by $\frac{u_0u_1}{k}$ which is to second-order, as can be seen from Equations A42 through A45. Since the lowest order of $(kN)^2$ and $(kN)^3$ is second-order, and they are multiplied by the second-order constant $\frac{u_0u_1}{k}$, these terms will not contribute to the mean energy flux to a third-order of approximation. To verify this, the four terms defined above will be evaluated.

$$\bar{I}_{1_1} = \frac{2u_0u_1 \sinh kD}{kT} \left(\overline{\cos \theta}\right)$$

$$\bar{I}_{1_1} = 0 \tag{A8}$$

$$\bar{I}_{1_2} = \frac{u_0u_1 \sinh kD}{kT} \overline{\left(\cos \theta\left(N_1{}^2\cos{}^2\theta + 2N_1N_2 \cos \theta \cos 2\theta\right)\right)}$$

$$\bar{I}_{1_2} = \frac{u_0u_1 \sinh kD}{kT} \left(\overline{N_1^2 \cos^3 \theta} + \overline{2N_1N_2 \cos^2 \theta \cos 2\theta}\right)$$

$$\bar{I}_{1_2} = \frac{u_0u_1 \sinh kD}{2k} N_1N_2 \tag{A9}$$

$$\bar{I}_{1_3} = \frac{2u_0u_1 \cosh kD}{kT} \overline{\left(\cos \theta\left(N_1 \cos \theta + N_2 \cos 2\theta + N_3 \cos 3\theta\right)\right)}$$

$$\bar{I}_{1_3} = \frac{2u_0u_1 \cosh kD}{kT} \left(\overline{N_1 \cos^2 \theta} + \overline{N_2 \cos \theta \cos 2\theta} + \overline{N_3 \cos \theta \cos 3\theta}\right)$$

$$\bar{I}_{1_3} = \frac{u_0u_1 \cosh kD}{k} N_1 \tag{A10}$$

$$\bar{I}_{1_4} = \frac{u_0u_1 \cosh kD}{3kT} \overline{\left(\cos \theta\left(N_1^3 \cos^3 \theta\right)\right)}$$

$$\bar{I}_{1_4} = \frac{u_0u_1 \cosh kD}{3kT} \overline{\left(N_1^3 \cos^4 \theta\right)}$$

$$\bar{I}_{1_4} = \frac{u_0u_1 \cosh kD}{8k} N_1^3 \tag{A11}$$

Adding Equations A8 through A11 yields:

$$\boxed{\bar{I}_1 = \frac{u_0 u_1}{2k} \sinh kD\, N_1 N_2 + \frac{u_0 u_1}{k} \cosh kD\, N_1 + \frac{u_0 u_1}{8k} \cosh kD\, N_1^3}$$

$$\bar{I}_4 = \frac{u_1^2}{4kT} \left(\overline{\cos^2 \theta \sinh 2k(N + D)}\right) \tag{A12}$$

Assuming N is small but finite, $\sinh 2k(N + D)$ can be expanded in a power series around D .

$$\sinh 2k(N + D) = \sinh 2kD + 2kN \cosh 2kD + \frac{(2kN)^2}{2} \sinh 2kD + \frac{(2kN)^3}{6} \cosh 2kD$$

$$\sinh 2k(N + D) = \sinh 2kD\left(1 + 2(kN)^2\right) + \cosh 2kD\left(2kN + \frac{4}{3} (kN)^3\right) \tag{A13}$$

Substitution of Equation A13 into Equation A12 yields:

$$\bar{I}_4 = \frac{u_1^2}{4kT}\left[\cos^2\left(\theta \sinh 2kD\left(1 + 2(kN)^2\right) + \cosh 2kD\left(2kN + \frac{4}{3} (kN)^3\right)\right)\right] \tag{A14}$$

Equation A14 is separated into the four terms defined below:

$$\bar{I}_{4_1} = \frac{u_1^2 \sinh 2kD}{4kT} \left(\overline{\cos^2 \theta}\right)$$

$$\bar{I}_{4_2} = \frac{u_1^2 \sinh 2kD}{2kT} \left(\overline{\cos^2 \theta (kN)^2}\right)$$

$$\bar{I}_{4_3} = \frac{u_1^2 \cosh 2kD}{2kT} \left(\overline{\cos^2 \theta (kN)}\right)$$

$$\bar{I}_{4_4} = \frac{u_1^2 \cosh 2kD}{3kT} \overline{\left(\cos^2 \theta (kN)^3\right)}$$

The four terms defined above are evaluated as follows:

$$\bar{I}_{4_1} = \frac{u_1^2 \sinh 2kD}{4kT} \overline{\left(\cos^2 \theta\right)}$$

$$\bar{I}_{4_1} = \frac{u_1^2 \sinh 2kD}{8k} \tag{A15}$$

$$\bar{I}_{4_2} = \frac{u_1^2 \sinh 2kD}{2kT} \overline{\left(\cos^2 \theta (kN)^2\right)}$$

$$\bar{I}_{4_2} = \frac{u_1^2 \sinh 2kD}{2kT} \overline{\left(\cos^2 \theta \left(N_1^2 \cos^2 \theta + 2N_1N_2 \cos \theta \cos 2\theta\right)\right)}$$

$$\bar{I}_{4_2} = \frac{u_1^2 \sinh 2kD}{2kT} \overline{\left(N_1^2 \cos^4 \theta + 2N_1N_2 \cos^3 \theta \cos 2\theta\right)}$$

$$\bar{I}_{4_2} = \frac{3u_1^2 \sinh 2kD}{16k} N_1^2 \tag{A16}$$

$$\bar{I}_{4_3} = \frac{u_1^2 \cosh 2kD}{2kT} \overline{\left(\cos^2 \theta \; (kN)\right)}$$

$$\bar{I}_{4_3} = \frac{u_1^2 \cosh 2kD}{2kT} \overline{\left(\cos^2 \theta \left(N_1 \cos \theta + N_2 \cos 2\theta + N_3 \cos 3\theta\right)\right)}$$

$$\bar{I}_{4_3} = \frac{u_1^2 \cosh 2kD}{2kT} \left(\overline{N_1 \cos^3 \theta} + \overline{N_2 \cos^2 \theta \cos 2\theta} + \overline{N_3 \cos^2 \theta \cos 3\theta}\right)$$

$$\bar{I}_{4_3} = \frac{u_1^2 \cosh 2kD}{8k} N_2 \tag{A17}$$

$$\bar{I}_{4_4} = \frac{u_1^2 \cosh 2kD}{3kT} \left(\overline{\cos^2 \theta (kN)^3}\right)$$

$$\bar{I}_{4_4} = \frac{u_1^2 \cosh 2kD}{3kT} \left(\overline{\cos^2 \theta \left(N_1^3 \cos^3 \theta\right)}\right)$$

$$\bar{I}_{4_4} = \frac{u_1^2 \cosh 2kD}{3kT} \left(\overline{N_1^3 \cos^5 \theta}\right)$$

$$\bar{I}_{4_4} = 0 \tag{A18}$$

Adding Equations A15 through A18 yields:

$$\boxed{\bar{I}_4 = \frac{u_1^2}{8k} \sinh 2kD + \frac{3u_1^2}{16k} \sinh 2kD\, N_1^2 + \frac{u_1^2}{8k} \cosh 2kD\, N_2}$$

$$\bar{I}_{11} = \frac{u_2^2}{8kT} \left(\overline{\cos^2 2\theta \sinh 4k(N + D)}\right) \tag{A19}$$

Assuming N is small but finite, $\sinh 4k(N + D)$ is expanded in a power series about D .

$$\sinh 4k(N + D) = \sinh 4kD + 4kN \cosh 4kD + \frac{(4kN)^2}{2} \sinh 4kD + \frac{(4kN)^3}{6} \cosh 4kD$$

$$\sinh 4k(N + D) = \sinh 4kD\left(1 + 8(kN)^2\right) + \cosh 4kD\left(4kN + \frac{32}{3}(kN)^3\right) \quad \text{(A20)}$$

Substitution of Equation A20 into A19 yields:

$$\bar{I}_{11} = \frac{u_2^2}{8kT}\left[\cos^2 2\theta\left(\sinh 4kD\left(1 + 8(kN)^2\right) + \cosh 4kD\left(4kN + \frac{32}{3}(kN)^3\right)\right)\right] \quad \text{(A21)}$$

Equation A21 is separated into the four terms defined below:

$$\bar{I}_{11_1} = \frac{u_2^2 \sinh 4kD}{8kT}\overline{\left(\cos^2 2\theta\right)}$$

$$\bar{I}_{11_2} = \frac{u_2^2 \sinh 4kD}{kT}\overline{\left(\cos^2 2\theta(kN)^2\right)}$$

$$\bar{I}_{11_3} = \frac{u_2^2 \cosh 4kD}{2kT}\overline{\left(\cos^2 2\theta(kN)\right)}$$

$$\bar{I}_{11_4} = \frac{4u_2^2 \cosh 4kD}{3kT}\overline{\left(\cos^2 2\theta(kN)^3\right)}$$

The four terms defined above are evaluated as follows:

$$\bar{I}_{11_1} = \frac{u_2^2 \sinh 4kD}{8kT} \left(\overline{\cos^2 2\theta}\right)$$

$$\bar{I}_{11_1} = \frac{u_2^2 \sinh 4kD}{16k} \tag{A22}$$

$$\bar{I}_{11_2} = \frac{u_2^2 \sinh 4kD}{kT} \left(\overline{\cos^2 2\theta (kN)^2}\right)$$

$$\bar{I}_{11_2} = \frac{u_2^2 \sinh 4kD}{kT} \left(\overline{\cos^2 2\theta \left(N_1{}^2 \cos^2 \theta + 2N_1N_2 \cos\theta \cos 2\theta\right)}\right)$$

$$\bar{I}_{11_2} = \frac{u_2^2 \sinh 4kD}{kT} \left(\overline{N_1^2 \cos^2 \theta \cos^2 2\theta} + \overline{2N_1N_2 \cos\theta \cos^3 2\theta}\right)$$

$$\bar{I}_{11_2} = \frac{u_2^2 \sinh 4kD}{4k} N_1^2 \tag{A23}$$

$$\bar{I}_{11_3} = \frac{u_2^2 \cosh 4kD}{2kT} \left(\overline{\cos^2 2\theta \left(N_1 \cos\theta + N_2 \cos 2\theta + N_3 \cos 3\theta\right)}\right)$$

$$\bar{I}_{11_3} = \frac{u_2^2 \cosh 4kD}{2kT} \left(\overline{N_1 \cos\theta \cos^2 2\theta} + \overline{N_2 \cos^3 2\theta} + \overline{N_3 \cos^2 2\theta \cos 3\theta}\right)$$

$$\bar{I}_{11_3} = 0 \tag{A24}$$

$$\bar{I}_{11_4} = \frac{4u_2^2 \cosh 4kD}{3kT} \left(\overline{\cos^2 2\theta (kN)^3}\right)$$

$$\bar{I}_{11_4} = \frac{4u_2^2 \cosh 4kD}{3kT} \left(\overline{\cos^2 2\theta \left(N_1^3 \cos^3 \theta\right)}\right)$$

$$\overline{I}_{11_4} = \frac{4u_2^2 \cosh 4kD}{3kT} \left(\overline{N_1^3 \cos^3 \theta \cos^2 2\theta} \right)$$

$$\overline{I}_{11_4} = 0 \qquad \text{(A25)}$$

Adding Equations A22 through A25 yields:

$$\boxed{\overline{I}_{11} = \frac{u_2^2 \sinh 4kD}{16k} + \frac{u_2^2 \sinh 4kD}{4k} N_1^2}$$

The final results for the integrals $\overline{I}_0$ through $\overline{I}_{13}$ are as follows:

$$\overline{I}_0 = u_0^2 D$$

$$\overline{I}_1 = \frac{u_0 u_1}{k} \left[\frac{\sinh kD}{2} N_1 N_2 + \cosh kD \; N_1 + \frac{\cosh kD}{8} N_1^3 \right]$$

$$\overline{I}_2 = \frac{u_0 u_2}{k} \left[\frac{\sinh 2kD}{2} N_1^2 + \cosh 2kD \; N_2 \right]$$

$$\overline{I}_3 = \frac{u_0 u_3}{k} \left[\frac{3 \sinh 3kD}{2} N_1 N_2 + \cosh 3kD \; N_3 + \frac{3 \cosh 3kD}{8} N_1^3 \right]$$

$$\overline{I}_4 = \frac{u_1^2}{8k} \left[\sinh 2kD + \frac{3 \sinh 2kD}{2} N_1^2 + \cosh 2kD \; N_2 \right]$$

$$\overline{I}_5 = \frac{u_1^2 N_2}{8k}$$

$$\bar{I}_6 = \frac{u_1^2 D}{4}$$

$$\bar{I}_7 = \frac{u_1 u_2}{4k}\left[3 \sinh 3kD\ N_1 N_2 + \cosh 3kD(N_1 + N_3) + \frac{3}{2} \cosh 3kD\ N_1^3\right]$$

$$\bar{I}_8 = \frac{u_1 u_2}{4k}\left[\sinh kD\ N_1 N_2 + \cosh kD(N_1 + N_3) + \frac{\cosh kD}{6} N_1^3\right]$$

$$\bar{I}_9 = \frac{u_1 u_3}{4k}\left[\sinh 4kD\ N_1^2 + \cosh 4kD\ N_2\right]$$

$$\bar{I}_{10} = \frac{u_1 u_3}{k}\left[\frac{\sinh 2kD}{8} N_1^2 + \frac{\cosh 2kD}{4} N_2\right]$$

$$\bar{I}_{11} = \frac{u_2^2}{k}\left[\frac{\sinh 4kD}{16} + \frac{\sinh 4kD}{4} N_1^2\right]$$

$$\bar{I}_{12} = 0$$

$$\bar{I}_{13} = \frac{u_2^2 D}{4}$$

Keeping only terms of $O\left(\frac{\varepsilon^4}{k}\right) = O(\varepsilon^3)$ yields

$$\bar{I}_0 = u_0^2 D \tag{A26}$$

$$\bar{I}_1 = \frac{u_0 u_1}{k} \cosh kD\ N_1 \tag{A27}$$

$$\bar{I}_2 = 0 \tag{A28}$$

$$\bar{I}_3 = 0 \tag{A29}$$

$$\bar{I}_4 = \frac{u_1^2}{8k}\left[\sinh 2kD + \frac{3 \sinh 2kD}{2} N_1^2 + \cosh 2kD\ N_2\right] \tag{A30}$$

$$\bar{I}_5 = \frac{u_1^2 N_2}{8k} \tag{A31}$$

$$\bar{I}_6 = \frac{u_1^2 D}{4} \tag{A32}$$

$$\bar{I}_7 = \frac{u_1 u_2}{4k} \cosh 3kD\ N_1 \tag{A33}$$

$$\bar{I}_8 = \frac{u_1 u_2}{4k} \cosh kD\ N_1 \tag{A34}$$

$$\bar{I}_9 = 0 \tag{A35}$$

$$\bar{I}_{10} = 0 \tag{A36}$$

$$\bar{I}_{11} = \frac{u_2^2 \sinh 4kD}{16k} \tag{A37}$$

$$\bar{I}_{12} = 0 \tag{A38}$$

$$\bar{I}_{13} = \frac{u_2^2 D}{4} \tag{A39}$$

Combining (A30) with (A31) yields:

$$\bar{I}_4 + \bar{I}_5 = \frac{u_1^2}{8k}\left[\sinh 2kD + \frac{3 \sinh 2kD}{2} N_1^2 + 2 \cosh^2 kD\ N_2\right] \tag{A40}$$

Combining (A33) with (A34) yields:

$$\bar{I}_7 + \bar{I}_8 = \frac{u_1 u_2}{2k} (\cosh kD \cosh 2kD) N_1 \qquad \text{A41)}$$

The evaluation of u_0 , u_1 , u_2 , u_3 , N_1 , N_2 , and N_3 yields the following:

$$u_0 = \frac{-1}{2kD}\sqrt{\frac{gc}{k}}\,\varepsilon^2 \qquad \text{(A42)}$$

$$u_1 = \sqrt{\frac{g}{k \sinh kD \cosh kD}}\left(\varepsilon + \frac{\varepsilon^3}{64}(-27c^6 - 3c^4 - 41c^2 + 39)\right) \qquad \text{(A43)}$$

$$u_2 = \frac{3}{4}\sqrt{\frac{g}{k \sinh^3 kD \cosh kD}}\,(c^2 - 1)\varepsilon^2 \qquad \text{(A44)}$$

$$u_3 = \frac{3\varepsilon^3}{64}\sqrt{\frac{g \tanh kD}{k \sinh^2 3kD}}\,(27c^6 - 57c^4 + 17c^2 + 13) \qquad \text{(A45)}$$

$$N_1 = \varepsilon + \frac{3\varepsilon^3}{64}(-9c^6 + 3c^4 - 3c^2 + 1) \qquad \text{(A46)}$$

$$N_2 = \frac{\varepsilon^2 c(3c^2 - 1)}{4} \qquad \text{(A47)}$$

$$N_3 = \frac{3\varepsilon^3}{64}(9c^6 - 3c^4 + 3c^2 - 1) \qquad \text{(A48)}$$

Substituting Equations A42 through A48 into Equations A26 through A41 yields:

$$\bar{I}_0 = \frac{gc\varepsilon^4}{4k^3 D}$$

$$\bar{I}_1 = -\frac{gc\varepsilon^4}{2k^3 D}$$

$$\overline{I}_2 = \overline{I}_3 = \overline{I}_9 = \overline{I}_{10} = \overline{I}_{12} = 0$$

$$\overline{I}_4 + \overline{I}_5 = \frac{g}{4k^2} \quad \varepsilon^2 + \frac{\varepsilon^4}{32}(-27c^6 - 3c^4 - 41c^2 + 39)$$

$$+ \frac{3g\varepsilon^4}{8k^2} + \frac{gc^2(3c^2 - 1)\varepsilon^4}{16k^2}$$

$$\overline{I}_6 = \frac{gD}{2k \sinh 2kD} \quad \varepsilon^2 + \frac{\varepsilon^4}{32}(-27c^6 - 3c^4 - 41c^2 + 39)$$

$$\overline{I}_7 + \overline{I}_8 = \frac{3g\varepsilon^4 \cosh 2kD(c^2 - 1)}{4k^2(\cosh 2kD - 1)}$$

$$\overline{I}_{11} = \frac{9g\varepsilon^4(c^6 - c^4 - c^2 + 1)}{64k^2}$$

$$\overline{I}_{13} = \frac{9gD\varepsilon^4(c^4 - 2c^2 + 1)}{64kc \sinh^4 kD}$$

Recall,

$$\overline{F} = \rho C \overline{\int_{-D}^{N} u^2 dz}$$

This equation can now be written as:

$$\boxed{\overline{F} = \rho C \sum_{i=0}^{i=13} \overline{I}_i} \qquad \text{(A49)}$$

Substituting $\overline{I}_0$ through $\overline{I}_{13}$ into Equation A49 results in the following:

$$\overline{F} = \rho C \left[\frac{gc\varepsilon^4}{4k^3D} - \frac{gc\varepsilon^4}{2k^3D} + \left(\frac{g}{4k^2} + \frac{gD}{2k \sinh 2kD} \right) \left(\varepsilon^2 + \frac{\varepsilon^4}{32} (-27c^6 - 3c^4 \right.\right.$$

$$\left. -41c^2 + 39) \right) + \frac{3g\varepsilon^4}{8k^2} + \frac{gc^2(3c^2 - 1)\varepsilon^4}{16k^2} + \frac{3g\varepsilon^4 \cosh 2kD(c^2 - 1)}{4k^2(\cosh 2kD - 1)}$$

$$\left. + \frac{9g\varepsilon^4(c^6 - c^4 - c^2 + 1)}{64k^2} + \frac{9gD\varepsilon^4(c^4 - 2c^2 + 1)}{64kc \sinh^4 kD} \right]$$

Combining terms,

$$\overline{F} = \frac{\gamma C}{k^2} \left[\frac{\varepsilon^2 n}{2} + \varepsilon^4 \left(\frac{-c}{4kD} + \frac{n}{64} (-27c^6 - 3c^4 - 41c^2 + 39) + \frac{1}{64} (9c^6 + 3c^4 \right.\right.$$

$$\left.\left. - 13c^2 + 33) + \frac{3 \cosh 2kD(c^2 - 1)}{4(\cosh 2kD - 1)} + \frac{9kD(c^4 - 2c^2 + 1)}{64c \sinh^4 kD} \right) \right]$$

where

$$n = \frac{1}{2} \left(1 + \frac{2kD}{\sinh 2kD} \right)$$

$$\gamma = \rho g$$

Inserting Equation 141 from Isobe and Kraus (1983a)

$$C = C_{IK} \left(1 + \varepsilon^2 \left(\frac{9c^4 - 10c^2 + 9}{16} - \frac{c}{2kD} \right) \right)$$

into $\overline{F}$ and rearranging,

$$\overline{F} = \frac{\gamma C_{IK}}{k^2}\left[\frac{\varepsilon^2 n}{2} + \varepsilon^4\left(\frac{-c(1 + n)}{4kD} + \frac{n}{64}(-27c^6 + 15c^4 - 61c^2 + 57)\right.\right.$$

$$+ \frac{1}{64}(9c^6 + 3c^4 - 13c^2 + 33) + \frac{3 \cosh 2kD(c^2 - 1)}{4(\cosh 2kD - 1)}$$

$$\left.\left. + \frac{9kD(c^4 - 2c^2 + 1)}{64c \sinh^4 kD}\right)\right]$$

Substituting in

$$\varepsilon = \frac{kH}{2}$$

yields

$$\overline{F} = \frac{\gamma H^2 n C_{IK}}{8} + \frac{\gamma k^2 H^4 C_{IK}}{16}\left[\frac{-c(1 + n)}{4kD} + \frac{n}{64}(-27c^6 + 15c^4 - 61c^2 + 57)\right.$$

$$+ \frac{1}{64}(9c^6 + 3c^4 - 13c^2 + 33) + \frac{3 \cosh 2kD(c^2 - 1)}{4(\cosh 2kD - 1)}$$

$$\left. + \frac{9kD(c^4 - 2c^2 + 1)}{64c \sinh^4 kD}\right]$$

APPENDIX B: DERIVATION OF THE AVERAGE ENERGY

The process of evaluating the integrals for the average energy per unit surface area will be shown. The average energy of a wave system is the sum of its kinetic and potential energies.

$$\bar{E} = \overline{KE} + \overline{PE}$$

where:

$\bar{E}$ = average energy per unit surface area,

$\overline{KE}$ = average kinetic energy per unit surface area

$$= \frac{\rho}{2} \overline{\int_{-D}^{N} (u^2 + w^2)\, dz} \ ,$$

and

$\overline{PE}$ = average potential energy per unit surface area

$$= \gamma \overline{\int_{-D}^{N} z\, dz} \ .$$

Therefore,

$$\bar{E} = \frac{\rho}{2} \overline{\int_{-D}^{N} (u^2 + w^2)\, dz} + \gamma \overline{\int_{-D}^{N} z\, dz}$$

where

ρ = the fluid density

u = horizontal water particle velocity

w = vertical water particle velocity

dz = incremental depth

$-D$ = elevation of the bottom

N = free surface elevation

γ = specific gravity of the fluid

z = vertical coordinate

The following quantities are available from Isobe and Kraus (1983a):

$$u = u_0 + u_1 \cosh k(z + D) \cos \theta + u_2 \cosh 2k(z + D) \cos 2\theta + u_3 \cosh 3k(z + D) \cos 3\theta$$

$$w = w_1 \sinh k(z + D) \sin \theta + w_2 \sinh 2k(z + D) \sin 2\theta + w_3 \sinh 3k(z + D) \sin 3\theta$$

$$N = \frac{1}{k}\left(N_1 \cos \theta + N_2 \cos 2\theta + N_3 \cos 3\theta\right)$$

$$u_0 = C_{IK}B_0$$

$$u_1 = w_1 = \frac{C_{IK}B_1}{\sinh kD}$$

$$u_2 = w_2 = \frac{2C_{IK}B_2}{\sinh 2kD}$$

$$u_3 = w_3 = \frac{3C_{IK}B_3}{\sinh 3kD}$$

$$N_1 = \varepsilon + \frac{3\varepsilon^3}{64}(-9c^6 + 3c^4 - 3c^2 + 1)$$

$$N_2 = \frac{\varepsilon^2 c(3c^2 - 1)}{4}$$

$$N_3 = \frac{3\varepsilon^3}{64}(9c^6 - 3c^4 + 3c^2 - 1)$$

$\theta = (kx - \sigma t)$

$\varepsilon = \frac{kH}{2}$

$c = \coth kD$

x = horizontal coordinate

k = wave number = $\frac{2\pi}{L}$

H = wave height

σ = angular frequency = $\frac{2\pi}{T}$

t = time

T = wave period

For the average kinetic energy, the first step is to calculate the square of the horizontal and vertical water particle velocities.

$$u^2 = u_0^2 + 2u_0u_1 \cos\theta \cosh k(z + D) + 2u_0u_2 \cos 2\theta \cosh 2k\,(z + D)$$

$$+ 2u_0u_3 \cos 3\theta \cosh 3k(z + D) + u_1^2 \cos^2\theta \cosh^2 k\,(z + D)$$

$$+ 2u_1u_2 \cos\theta \cos 2\theta \cosh k(z + D) \cosh 2k(z + D)$$

$$+ 2u_1u_3 \cos\theta \cos 3\theta \cosh k(z + D) \cosh 3k(z + D)$$

$$+ u_2^2 \cos^2 2\theta \cosh^2 2k(z + D) + \underline{\text{H}}\text{igher } \underline{\text{O}}\text{rder } \underline{\text{T}}\text{erms}$$

$$w^2 = w_1^2 \sin^2\theta \sinh^2 k(z + D)$$

$$+ 2w_1w_2 \sin\theta \sin 2\theta \sinh k(z + D) \sinh 2k(z + D)$$

$$+ 2w_1w_3 \sin\theta \sin 3\theta \sinh k(z + D) \sinh 3k(z + D)$$

$$+ w_2^2 \sin^2 2\theta \sinh^2 2k(z + D) + \text{H.O.T.}$$

where:

H.O.T. = Higher Order Terms

= terms of order $\varepsilon^4 \left(\text{or } \frac{\varepsilon^5}{k}\right)$ and higher.

Defining the symbol

$$\int_{-D}^{N} dz = \left\langle \quad \right\rangle ,$$

the next step is to integrate u^2 and w^2 over the depth.

$$\langle u^2 \rangle = u_0^2(N + D) + \frac{2u_0u_1 \cos\theta}{k} \sinh k(N + D) +$$

$$\frac{u_0u_2 \cos 2\theta}{k} \sinh 2k(N + D) + \frac{2u_0u_3 \cos 3\theta}{3k} \sinh 3k(N + D)$$

$$+ u_1^2 \cos^2\theta\left(\frac{\sinh 2k(N + D)}{4k} + \frac{N}{2} + \frac{D}{2}\right)$$

$$+ u_1u_2 \cos\theta \cos 2\theta\left(\frac{\sinh 3k(N + D)}{3k} + \frac{\sinh k(N + D)}{k}\right)$$

$$+ u_1u_3 \cos\theta \cos 3\theta\left(\frac{\sinh 4k(N + D)}{4k} + \frac{\sinh 2k(N + D)}{2k}\right)$$

$$+ u_2^2 \cos^2 2\theta\left(\frac{\sinh 4k(N + D)}{8k} + \frac{N}{2} + \frac{D}{2}\right) \qquad \text{(B1)}$$

$$\langle w^2 \rangle = w_1^2 \sin^2\theta\left(\frac{\sinh 2k(N + D)}{4k} - \frac{N}{2} - \frac{D}{2}\right)$$

$$+ w_1w_2 \sin\theta \sin 2\theta\left(\frac{\sinh 3k(N + D)}{3k} - \frac{\sinh k(N + D)}{k}\right)$$

$$+ w_1w_3 \sin\theta \sin 3\theta\left(\frac{\sinh 4k(N + D)}{4k} - \frac{\sinh 2k(N + D)}{2k}\right)$$

$$+ w_2^2 \sin^2 2\theta\left(\frac{\sinh 4k(N + D)}{8k} - \frac{N}{2} - \frac{D}{2}\right) \qquad \text{(B2)}$$

It is convenient to define the terms in Equations B1 and B2 as follows:

$$I_0 = u_0^2(N + D)$$

$$I_1 = \frac{2u_0u_1 \cos\theta}{k} \sinh k(N + D)$$

$$I_2 = \frac{u_0u_2 \cos 2\theta}{k} \sinh 2k(N + D)$$

$$I_3 = \frac{2u_0u_3 \cos 3\theta}{3k} \sinh 3k(N + D)$$

$$I_4 = \frac{u_1^2 \cos^2\theta}{4k} \sinh 2k(N + D)$$

$$I_5 = \frac{u_1^2 \cos^2\theta}{2} N$$

$$I_6 = \frac{u_1^2 \cos^2\theta}{2} D$$

$$I_7 = \frac{u_1u_2 \cos\theta \cos 2\theta}{3k} \sinh 3k(N + D)$$

$$I_8 = \frac{u_1u_2 \cos\theta \cos 2\theta}{k} \sinh k(N + D)$$

$$I_9 = \frac{u_1u_3 \cos\theta \cos 3\theta}{4k} \sinh 4k(N + D)$$

$$I_{10} = \frac{u_1u_3 \cos\theta \cos 3\theta}{2k} \sinh 2k(N + D)$$

$$I_{11} = \frac{u_2^2 \cos^2 2\theta}{8k} \sinh 4k(N + D)$$

$$I_{12} = \frac{u_2^2 \cos^2 2\theta}{2} N$$

$$I_{13} = \frac{u_2^2 \cos^2 2\theta}{2} D$$

$$I_{14} = \frac{w_1^2 \sin^2 \theta}{4k} \sinh 2k(N + D)$$

$$I_{15} = - \frac{w_1^2 \sin^2 \theta}{2} N$$

$$I_{16} = - \frac{w_1^2 \sin^2 \theta}{2} D$$

$$I_{17} = \frac{w_1 w_2 \sin \theta \sin 2\theta}{3k} \sinh 3k(N + D)$$

$$I_{18} = - \frac{w_1 w_2 \sin \theta \sin 2\theta}{k} \sinh k(N + D)$$

$$I_{19} = \frac{w_1 w_3 \sin \theta \sin 3\theta}{4k} \sinh 4k(N + D)$$

$$I_{20} = - \frac{w_1 w_3 \sin \theta \sin 3\theta}{2k} \sinh 2k(N + D)$$

$$\overline{I}_{21} = \frac{w_2^2 \sin^2 2\theta}{8k} \sinh 4k(N + D)$$

$$\overline{I}_{22} = - \frac{w_2^2 \sin^2 2\theta}{2} N$$

$$\overline{I}_{23} = - \frac{w_2^2 \sin^2 2\theta}{2} D$$

The time average of each I_i term must be calculated. For convenience, the following definition (symbol) is introduced:

$$\frac{1}{T} \int_{t}^{t + T} I_i \, dt = \overline{I}_i$$

and without any loss of generality, for waves of permanent form,

$$\frac{1}{T}\int_0^T I_i \, dt = \overline{I}_i \ .$$

From the evaluation of $\overline{F}$ in Appendix A, $\overline{I}_0$ through $\overline{I}_{13}$ are determined to order $\left(\frac{\varepsilon^4}{k}\right)$ as follows:

$$\overline{I}_0 = u_0^2 \, D \tag{B3}$$

$$\overline{I}_1 = \frac{u_0 u_1}{k} \cosh kD \; N_1 \tag{B4}$$

$$\overline{I}_2 = 0 \tag{B5}$$

$$\overline{I}_3 = 0 \tag{B6}$$

$$\overline{I}_4 + \overline{I}_5 = \frac{u_1^2}{8k}\left[\sinh 2kD + \frac{3 \sinh 2kD}{2} N_1^2 + 2 \cosh^2 kD \; N_2\right] \tag{B7}$$

$$\overline{I}_6 = \frac{u_1^2 D}{4} \tag{B8}$$

$$\overline{I}_7 + \overline{I}_8 = \frac{u_1 u_2}{2k} (\cosh kD \cosh 2kD) \; N_1 \tag{B9}$$

$$\overline{I}_9 = 0 \tag{B10}$$

$$\overline{I}_{10} = 0 \tag{B11}$$

$$\overline{I}_{11} = \frac{u_2^2}{16k} \sinh 4kD \tag{B12}$$

$$\overline{I}_{12} = 0 \tag{B13}$$

$$\overline{I}_{13} = \frac{u_2^2 D}{4} \tag{B14}$$

The explicit integration of I_{14} , I_{15} , and I_{16} will be shown and the results of the remaining integrals will only be listed. Identities used in the solution process are given in Appendix D.

$$\overline{I}_{14} = \frac{w_1^2}{4kT} \left(\overline{\sin^2 \theta \sinh 2k(N + D)}\right) \tag{B15}$$

Assuming N is small but finite, $\sinh 2k(N + D)$ can be expanded in a power series around D .

$$\sinh 2k(N + D) = \sinh 2kD + 2kN \cosh 2kD + \frac{(2kN)^2}{2} \sinh 2kD + \frac{(2kN)^3}{6} \cosh 2kD$$

$$\sinh 2k(N + D) = \sinh 2kD\left(1 + 2(kN)^2\right) + \cosh 2kD\left(2kN + \frac{4}{3}(kN)^3\right) \tag{B16}$$

Substitution of (B16) into (B15) yields:

$$\bar{I}_{14} = \frac{w_1^2}{4kT}\left[\sin^2\theta\left(\sinh 2kD\left(1 + 2(kN)^2\right) + \cosh 2kD\left(2kN + \frac{4}{3}(kN)^3\right)\right)\right] \quad \text{(B17)}$$

Equation (B17) is separated into the four terms defined below:

$$\bar{I}_{14_1} = \frac{w_1^2 \sinh 2kD}{4kT}\,\overline{(\sin^2\theta)}$$

$$\bar{I}_{14_2} = \frac{w_1^2 \sinh 2kD}{2kT}\,\overline{(\sin^2\theta\,(kN)^2)}$$

$$\bar{I}_{14_3} = \frac{w_1^2 \cosh 2kD}{2kT}\,\overline{(\sin^2\theta\,(kN))}$$

$$\bar{I}_{14_4} = \frac{w_1^2 \cosh 2kD}{3kT}\,\overline{(\sin^2\theta(kN)^3)}$$

Evaluating $\bar{I}_{14_1}$ through $\bar{I}_{14_4}$:

$$\bar{I}_{14_1} = \frac{w_1^2 \sinh 2kD}{8kT}\,(\overline{1 - \cos 2\theta})$$

$$\bar{I}_{14_1} = \frac{w_1^2 \sinh 2kD}{8kT}\,(T - 0)$$

$$\bar{I}_{14_1} = \frac{w_1^2 \sinh 2kD}{8k} \quad \text{(B18)}$$

$$\bar{I}_{14_2} = \frac{w_1^2 \sinh 2kD}{2kT} \left(\overline{\sin^2\left(\theta \quad N_1^2 \cos^2 \theta + 2N_1N_2 \cos \theta \cos 2\theta\right)}\right)$$

$$\bar{I}_{14_2} = \frac{w_1^2 \sinh 2kD}{2kT} \left(\overline{N_1^2 \cos^2 \theta \sin^2 \theta} + \overline{2N_1N_2 \cos \theta \cos 2\theta \sin^2 \theta}\right)$$

$$\bar{I}_{14_2} = \frac{w_1^2 \sinh 2kD}{2kT} \left(\frac{N_1^2 T}{8}\right)$$

$$\bar{I}_{14_2} = \frac{w_1^2 \sinh 2kD}{16k} N_1^2 \qquad \text{(B19)}$$

$$\bar{I}_{14_3} = \frac{w_1^2 \cosh 2kD}{2kT} \left(\overline{\sin^2 \theta \left(N_1 \cos \theta + N_2 \cos 2\theta + N_3 \cos 3\theta\right)}\right)$$

$$\bar{I}_{14_3} = \frac{w_1^2 \cosh 2kD}{2kT} \left(\overline{N_1 \cos \theta \sin^2 \theta} + \overline{N_2 \cos 2\theta \sin^2 \theta}\right.$$

$$\left. + \overline{N_3 \cos 3\theta \sin^2 \theta}\right)$$

$$\bar{I}_{14_3} = \frac{w_1^2 \cosh 2kD}{2kT} \left(- \frac{N_2 T}{4}\right)$$

$$\bar{I}_{14_3} = - \frac{w_1^2 \cosh 2kD}{8k} N_2 \qquad \text{(B20)}$$

$$\bar{I}_{14_4} = \frac{w_1^2 \cosh 2kD}{3kT} \left(\overline{\sin^2 \theta \left(N_1^3 \cos^3 \theta\right)}\right)$$

$$\bar{I}_{14_4} = \frac{w_1^2 \cosh 2kD}{3kT} \left(\overline{N_1^3 \sin^2 \theta \cos^3 \theta}\right)$$

$$\bar{I}_{14_4} = 0 \qquad \text{(B21)}$$

Adding (B18) through (B21) yields:

$$\boxed{\bar{I}_{14} = \frac{w_1^2 \sinh 2kD}{8k} + \frac{w_1^2 \sinh 2kD}{16k} N_1^2 - \frac{w_1^2 \cosh 2kD}{8k} N_2}$$

$$\bar{I}_{15} = -\frac{w_1^2}{2kT}\left[\overline{\sin^2 \theta \left(N_1 \cos \theta + N_2 \cos 2\theta + N_3 \cos 3\theta\right)}\right]$$

$$\bar{I}_{15} = -\frac{w_1^2}{2kT}\left[\overline{N_1 \cos \theta \sin^2 \theta} + \overline{N_2 \cos 2\theta \sin^2 \theta} + \overline{N_3 \cos 3\theta \sin^2 \theta}\right]$$

$$\bar{I}_{15} = -\frac{w_1^2}{2kT}\left[-\frac{N_2 T}{4}\right]$$

$$\boxed{\bar{I}_{15} = \frac{w_1^2}{8k} N_2}$$

$$\bar{I}_{16} = -\frac{w_1^2 D}{2T}\left(\overline{\sin^2 \theta}\right)$$

$$\bar{I}_{16} = -\frac{w_1^2 D}{4T}\left(\overline{1 - \cos 2\theta}\right)$$

$$\bar{I}_{16} = -\frac{w_1^2 D}{4T}(T - 0)$$

$$\boxed{\bar{I}_{16} = -\frac{w_1^2 D}{4}}$$

The final results for the integrals $\bar{I}_{17}$ through $\bar{I}_{23}$ are as follows:

$$\bar{I}_{17} = \frac{w_1 w_2 \cosh 3kD}{4k}\left[N_1 - N_3 + \frac{3}{4} N_1^3\right]$$

$$\bar{I}_{18} = -\frac{w_1 w_2 \cosh kD}{4k}\left[N_1 - N_3 + \frac{N_1^3}{12}\right]$$

$$\bar{I}_{19} = \frac{w_1 w_3}{4k}\left[\sinh 4kD\, N_1^2 + \cosh 4kD\, N_2\right]$$

$$\bar{I}_{20} = -\frac{w_1 w_3}{4k}\left[\frac{\sinh 2kD}{2} N_1^2 + \cosh 2kD\, N_2\right]$$

$$\bar{I}_{21} = \frac{w_2^2 \sinh 4kD}{4k}\left[\frac{1}{4} + N_1^2\right]$$

$$\bar{I}_{22} = 0$$

$$\bar{I}_{23} = -\frac{w_2^2 D}{4}$$

Keeping only terms of $0\left(\frac{\varepsilon^4}{k}\right) = 0(\varepsilon^3)$, terms $\bar{I}_{14}$ through $\bar{I}_{17}$ are as follows:

$$\bar{I}_{14} = \frac{w_1^2}{8k}\left[\sinh 2kD + \frac{\sinh 2kD}{2} N_1^2 - \cosh 2kD\, N_2\right] \qquad \text{(B22)}$$

$$\bar{I}_{15} = \frac{w_1^2 N_2}{8k} \tag{B23}$$

$$\bar{I}_{16} = -\frac{w_1^2 D}{4} \tag{B24}$$

$$\bar{I}_{17} = \frac{w_1 w_2 \cosh 3kD}{4k} N_1 \tag{B25}$$

$$\bar{I}_{18} = -\frac{w_1 w_2 \cosh kD}{4k} N_1 \tag{B26}$$

$$\bar{I}_{19} = 0 \tag{B27}$$

$$\bar{I}_{20} = 0 \tag{B28}$$

$$\bar{I}_{21} = \frac{w_2^2 \sinh 4kD}{16k} \tag{B29}$$

$$\bar{I}_{22} = 0 \tag{B30}$$

$$\bar{I}_{23} = -\frac{w_2^2 D}{4} \tag{B31}$$

Combining (B22) with (B23) yields:

$$\bar{I}_{14} + \bar{I}_{15} = \frac{w_1^2}{8k}\left[\sinh 2kD + \frac{\sinh 2kD}{2} N_1^2 - 2 \sinh^2 kD \; N_2\right] \tag{B32}$$

Combining (B25) with (B26) yields:

$$\bar{I}_{17} + \bar{I}_{18} = \frac{w_1 w_2}{2k} N_1 \text{ (sinh kD sinh 2kD)} \tag{B33}$$

The evaluation of u_0 , u_1 , u_2 , u_3 , w_1 , w_2 , w_3 , N_1 , N_2 , and N_3 yields the following:

$$u_0 = -\frac{1}{2kD}\sqrt{\frac{gc}{k}}\ \varepsilon^2 \tag{B34}$$

$$u_1 = w_1 = \sqrt{\frac{g}{k \sinh kD \cosh kD}}\left(\varepsilon + \frac{\varepsilon^3}{64}(-27c^6 - 3c^4 - 41c^2 + 39)\right) \tag{B35}$$

$$u_2 = w_2 = \frac{3}{4}\sqrt{\frac{g}{k \sinh^3 kD \cosh kD}}\ (c^2 - 1)\ \varepsilon^2 \tag{B36}$$

$$u_3 = w_3 = \frac{3\varepsilon^3}{64}\sqrt{\frac{g \tanh kD}{k \sinh^2 3kD}}\ (27c^6 - 57c^4 + 17c^2 + 13) \tag{B37}$$

$$N_1 = \varepsilon + \frac{3\varepsilon^3}{64}(-9c^6 + 3c^4 - 3c^2 + 1) \tag{B38}$$

$$N_2 = \frac{\varepsilon^2 c(3c^2 - 1)}{4} \tag{B39}$$

$$N_3 = \frac{3\varepsilon^3}{64}(9c^6 - 3c^4 + 3c^2 - 1) \tag{B40}$$

Substituting equations (B22) through (B28) into (B3) through (B14) and (B24) through (B33) yields

$$\bar{I}_0 = \frac{gc\varepsilon^4}{4k^3D}$$

$$\bar{I}_1 = -\frac{gc\varepsilon^4}{2k^3 D}$$

$$\bar{I}_2 = \bar{I}_3 = \bar{I}_9 = \bar{I}_{10} = \bar{I}_{12} = \bar{I}_{19} = \bar{I}_{20} = \bar{I}_{22} = 0$$

$$\bar{I}_4 + \bar{I}_5 = \frac{g}{4k^2}\left(\varepsilon^2 + \frac{\varepsilon^4}{32}(-27c^6 - 3c^4 - 41c^2 + 39)\right) + \frac{3g\varepsilon^4}{8k^2}$$

$$+ \frac{gc^2\,(3c^2 - 1)\varepsilon^4}{16k^2}$$

$$\bar{I}_6 = \frac{gD}{2k\ \sinh\ 2kD}\left(\varepsilon^2 + \frac{\varepsilon^4}{32}(-27c^6 - 3c^4 - 41c^2 + 39)\right)$$

$$\bar{I}_7 + \bar{I}_8 = \frac{3g\varepsilon^4\ \cosh\ 2kD(c^2 - 1)}{4k^2(\cosh\ 2kD - 1)}$$

$$\bar{I}_{11} = \frac{9g\varepsilon^4(c^6 - c^4 - c^2 + 1)}{64k^2}$$

$$\bar{I}_{13} = \frac{9gD\varepsilon^4(c^4 - 2c^2 + 1)}{64kc\ \sinh^4\ kD}$$

$$\bar{I}_{14} + \bar{I}_{15} = \frac{g}{4k^2}\left(\varepsilon^2 + \frac{\varepsilon^4}{32}(-27c^6 - 3c^4 - 41c^2 + 39)\right) + \frac{g\varepsilon^4}{8k^2}$$

$$- \frac{g\varepsilon^4(3c^2 - 1)}{16k^2}$$

$$\bar{I}_{16} = -\frac{gD}{2k\ \sinh\ 2kD}\left(\varepsilon^2 + \frac{\varepsilon^4}{32}(-27c^6 - 3c^4 - 41c^2 + 39)\right)$$

$$\bar{I}_{17} + \bar{I}_{18} = \frac{3g\varepsilon^4(c^2 - 1)}{4k^2}$$

$$\bar{I}_{21} = \frac{9g\varepsilon^4}{64k^2}(c^6 - c^4 - c^2 + 1)$$

$$\bar{I}_{23} = -\frac{9gD\varepsilon^4(c^4 - 2c^2 + 1)}{64kc \sinh^4 kD}$$

Recall,

$$\overline{KE} = \frac{\rho}{2}\overline{\int_{-D}^{N}(u^2 + w^2)dz}$$

This equation can now be written as:

$$\boxed{\overline{KE} = \frac{\rho}{2}\sum_{i=0}^{i=23}\bar{I}_i} \qquad \text{(B41)}$$

Substituting $\bar{I}_0$ through $\bar{I}_{23}$ into Equation B41 results in the following:

$$\overline{KE} = \frac{\rho}{2}\left[\frac{gc\varepsilon^4}{4k^3D} - \frac{gc\varepsilon^4}{2k^3D} + \left(\frac{g}{4k^2} + \frac{gD}{2k \sinh 2kD} + \frac{g}{4k^2} - \frac{gD}{2k \sinh 2kD}\right)\right.$$

$$\times \left(\varepsilon^2 + \frac{\varepsilon^4}{32}(-27c^6 - 3c^4 - 41c^2 + 39)\right) + \frac{9g\varepsilon^4}{64k^2}\left((c^6 - c^4 - c^2 + 1)\right.$$

$$\left. + \frac{kD(c^4 - 2c^2 + 1)}{c \sinh^4 kD} + (c^6 - c^4 - c^2 + 1) - \frac{kD(c^4 - 2c^2 + 1)}{c \sinh^4 kD}\right)$$

$$+ \frac{3g\varepsilon^4 \cosh 2kD(c^2 - 1)}{4k^2(\cosh 2kD - 1)} + \frac{g\varepsilon^4 c^2(3c^2 - 1)}{16k^2} - \frac{g\varepsilon^4(3c^2 - 1)}{16k^2} + \frac{3g\varepsilon^4}{8k^2}$$

$$\left. + \frac{g\varepsilon^4}{8k^2} + \frac{3g\varepsilon^4(c^2 - 1)}{4k^2}\right]$$

Combining terms,

$$\overline{KE} = \frac{\gamma\varepsilon^2}{4k^2}\left[1 + \varepsilon^2\left(-\frac{c}{2kD} - \frac{9}{32}(c^6 + c^4 + 3c^2 - 5) + \frac{3(c^2 - 1)\cosh 2kD}{2(\cosh 2kD - 1)}\right)\right]$$

where

$$\gamma = \rho g \ .$$

Substituting in

$$\varepsilon = \frac{kH}{2}$$

yields:

$$\overline{KE} = \frac{\gamma H^2}{16} + \frac{\gamma k^2 H^4}{64}\left(- \frac{c}{2kD} - \frac{9}{32}(c^6 + c^4 + 3c^2 - 5) + \frac{3(c^2 - 1)\cosh 2kD}{2(\cosh 2kD - 1)}\right) \tag{B42}$$

This completes the evaluation of the average kinetic energy per unit surface area. The next step is to evaluate the average potential energy per unit surface area. Recall,

$$\overline{PE} = \gamma \overline{\int_{-D}^{N} z \, dz} \; .$$

Integrating in the z direction yields

$$\overline{PE} = \frac{\gamma}{2}\left(\overline{N^2 + D^2}\right)$$

where the overbar denotes the time average.

Define

$$\bar{J}_1 = \frac{\gamma}{2}\left(\overline{N^2}\right)$$

$$\bar{J}_2 = \frac{\gamma}{2}\left(\overline{D^2}\right)$$

Evaluating $\overline{J_1}$ and $\overline{J_2}$:

$$\overline{J_1} = \frac{\gamma}{2T}\left[\frac{1}{k^2}\left(\overline{N_1 \cos\theta} + \overline{N_2 \cos 2\theta} + \overline{N_3 \cos 3\theta}\right)^2\right]$$

$$\overline{J_1} = \frac{\gamma}{2T}\left[\frac{1}{k^2}\left(\overline{N_1^2 \cos^2\theta} + \overline{2N_1N_2 \cos\theta \cos 2\theta} + \overline{2N_1N_3 \cos\theta \cos 3\theta}\right.\right.$$

$$\left.\left. + \overline{N_2^2 \cos^2 2\theta} + \text{H.O.T.}\right)\right]$$

$$\overline{J_1} = \frac{\gamma}{4k^2}\left(N_1^2 + N_2^2\right)$$

Inserting N_1 and N_2 into $\overline{J_1}$ yields

$$\overline{J_1} = \frac{\gamma}{4k^2}\left[\varepsilon^2 + \frac{3\varepsilon^4}{32}(-9c^6 + 3c^4 - 3c^2 + 1) + \frac{\varepsilon^4 c^2 (3c^2 - 1)^2}{16}\right]$$

The evaluation of $\overline{J_2}$ is simply:

$$\bar{J}_2 = \frac{\gamma D^2}{2},$$

but this is the potential energy of the fluid when no waves are present. The potential energy per unit surface area due to the wave is:

$$\overline{PE} = \frac{\gamma}{4k^2}\left[\varepsilon^2 + \frac{3\varepsilon^4}{32}(-9c^6 + 3c^4 - 3c^2 + 1) + \frac{\varepsilon^4 c^2 (3c^2 - 1)^2}{16}\right]$$

Inserting

$$\varepsilon = \frac{kH}{2}$$

and combining terms yields

$$\overline{PE} = \frac{\gamma H^2}{16} + \frac{\gamma k^2 H^4}{2048} (-9c^6 - 3c^4 - 7c^2 + 3) \tag{B43}$$

This completes the evaluation of the average potential energy per unit surface area. Combining (B42) and (B43) results in the average energy per unit surface area.

$$\overline{E} = \frac{\gamma H^2}{8} + \frac{\gamma k^2 H^4}{128} \left[- \frac{c}{kD} + \frac{(-9c^6 - 6c^4 - 17c^2 + 24)}{8} + \frac{3(c^2 - 1) \cosh 2kD}{(\cosh 2kD - 1)} \right]$$

This completes the evaluation of the average energy per unit surface area.

APPENDIX C: DERIVATION OF THE GROUP VELOCITY

The group velocity is defined as the velocity at which the wave energy is propagated. Mathematically,

$$\overline{F} = \overline{E}Cg$$

or

$$Cg = \frac{\overline{F}}{\overline{E}} \tag{C1}$$

From Appendices A and B we have:

$$\overline{F} = \frac{\gamma H^2}{8} n\, C_{IK} + \frac{\gamma k^2 H^4}{16} C_{IK} \left[- \frac{c}{4kD}(1 + n) + \frac{n}{64}(-27c^6 + 15c^4 - 61c^2 + 57) + \frac{(9c^6 + 3c^4 - 13c^2 + 33)}{64} + \frac{3 \cosh 2kD(c^2 - 1)}{4(\cosh 2kD - 1)} + \frac{9kD(c^4 - 2c^2 + 1)}{64c \sinh^4 kD} \right] \tag{C2}$$

$$\overline{E} = \frac{\gamma H^2}{8} + \frac{\gamma k^2 H^4}{128} \left[- \frac{c}{kD} + \frac{(-9c^6 - 6c^4 - 17c^2 + 24)}{8} + \frac{3(c^2 - 1) \cosh 2kD}{(\cosh 2kD - 1)} \right] \tag{C3}$$

Defining

$$B = -\frac{c(1+n)}{4kD} + \frac{n}{64}(-27c^6 + 15c^4 - 61c^2 + 57) + \frac{(9c^6 + 3c^4 - 13c^2 + 33)}{64}$$

$$+ \frac{3 \cosh 2kD(c^2 - 1)}{4(\cosh 2kD - 1)} + \frac{9kD(c^4 - 2c^2 + 1)}{64c \sinh^4 kD}$$

and

$$A = -\frac{c}{kD} + \frac{(-9c^6 - 6c^4 - 17c^2 + 24)}{8} + \frac{3(c^2 - 1)\cosh 2kD}{(\cosh 2kD - 1)}$$

and inserting into (C2) and (C3) yields

$$\overline{F} = \frac{\gamma H^2 n C_{IK}}{8}\left[1 + \frac{k^2H^2}{2n} B\right] \tag{C4}$$

$$\overline{E} = \frac{\gamma H^2}{8}\left[1 + \frac{k^2H^2}{16} A\right] \tag{C5}$$

Inserting (C4) and (C5) into (C1) yields:

$$C_g = \frac{n\, C_{IK}\left[1 + \frac{k^2H^2}{2n} B\right]}{\left[1 + \frac{k^2H^2}{16} A\right]}$$

Using the series,

$$(1 + x)^{-1} = 1 - x + x^2 - x^3 + x^4 - \ldots$$

$$Cg = n\, C_{IK}\left[1 + \frac{k^2H^2}{2n} B - \frac{k^2H^2}{16} A + \text{H.O.T.}\right]$$

Inserting

$$\varepsilon = \frac{kH}{2}$$

yields

$$Cg = n \, C_{IK} \left[1 + \varepsilon^2 \left(\frac{2B}{n} - \frac{A}{4} \right) \right]$$

This completes the derivation of the group velocity.

APPENDIX D: IDENTITIES USED IN APPENDICES A AND B

The identities used in Appendices A and B are given here. Integrals are reduced until there is only integrals of constants, single trigonometric functions, or orthogonal functions for example:

$$\frac{1}{8} \int_0^T (1)\, dt = \frac{T}{8} \qquad \text{(D1)}$$

$$\frac{1}{2} \int_0^T \cos\,(kx - \sigma t)\, dt = 0 \qquad \text{(D2)}$$

$$\frac{3}{4} \int_0^T \cos\,(kx - \sigma t) \cos 2(kx - \sigma t)\, dt = 0 \qquad \text{(D3)}$$

Equations D1 and D2 are self-explanatory, but the orthogonality condition will be restated for the reader.

$$\int_a^b \cos mx \cos nx\, dx = \begin{pmatrix} 0 & n \neq m \\ \delta_{nm} & n = m \end{pmatrix}$$

The limits of integration will henceforth be omitted for brevity. For convenience, let $\theta = kx - \sigma t$, then:

$$\boxed{\int \cos^2 \theta\, d\theta}$$

$$\frac{1}{2} \int (1 + \cos 2\theta)\, d\theta$$

$$\frac{1}{2} \int (1)\, d\theta + \frac{1}{2} \int \cos 2\theta\, d\theta$$

$$\boxed{\int \cos^3 \theta \, d\theta}$$

$$\frac{1}{2} \int (1 + \cos 2\theta) \cos \theta \, d\theta$$

$$\frac{1}{2} \int \cos \theta \, d\theta + \frac{1}{2} \int \cos \theta \cos 2\theta \, d\theta$$

$$\boxed{\int \cos^4 \theta \, d\theta}$$

$$\frac{1}{4} \int (1 + \cos 2\theta)^2 \, d\theta$$

$$\frac{1}{4} \int (1 + 2 \cos 2\theta + \cos^2 2\theta) \, d\theta$$

$$\frac{1}{4} \quad (1) \, d\theta + \frac{1}{2} \quad \cos 2\theta \, d\theta + \frac{1}{8} \quad (1 + \cos 4\theta) \, d\theta$$

$$\frac{3}{8} \quad (1) \, d\theta + \frac{1}{2} \quad \cos 2\theta \, d\theta + \frac{1}{8} \quad \cos 4\theta \, d\theta$$

$$\boxed{\int \cos^5 \theta \, d\theta}$$

$$\frac{1}{4} \int (1 + \cos 2\theta)^2 \cos \theta \, d\theta$$

$$\frac{1}{4} \int (\cos \theta + 2 \cos \theta \cos 2\theta + \cos \theta \cos^2 2\theta) \, d\theta$$

$$\frac{1}{4} \int \cos \theta \, d\theta + \frac{1}{2} \int \cos \theta \cos 2\theta \, d\theta + \frac{1}{8} \int \cos \theta (1 + \cos 4\theta) \, d\theta$$

$$\frac{3}{8} \int \cos \theta \, d\theta + \frac{1}{2} \int \cos \theta \cos 2\theta \, d\theta + \frac{1}{8} \int \cos \theta \cos 4\theta \, d\theta$$

$$\boxed{\int \cos^2 2\theta \, d\theta}$$

$$\frac{1}{2}\int (1 + \cos 4\theta) \, d\theta$$

$$\frac{1}{2}\int (1) \, d\theta + \frac{1}{2}\int \cos 4\theta \, d\theta$$

$$\boxed{\int \cos^3 2\theta \, d\theta}$$

$$\frac{1}{2}\int (1 + \cos 4\theta) \cos 2\theta \, d\theta$$

$$\frac{1}{2}\int \cos 2\theta \, d\theta + \frac{1}{2}\int \cos 2\theta \cos 4\theta \, d\theta$$

$$\boxed{\int \cos^2 3\theta \, d\theta}$$

$$\frac{1}{2}\int (1 + \cos 6\theta) \, d\theta$$

$$\frac{1}{2}\int (1) \, d\theta + \frac{1}{2}\int \cos 6\theta \, d\theta$$

$$\int \cos \theta \cos^2 2\theta \, d\theta$$

$$\frac{1}{2}\int \cos \theta \, (1 + \cos 4\theta) \, d\theta$$

$$\frac{1}{2}\int \cos \theta \, d\theta + \frac{1}{2}\int \cos \theta \cos 4\theta \, d\theta$$

$$\boxed{\int \cos\theta \cos 2\theta \cos 3\theta \, d\theta}$$

$$\frac{1}{2}\int (\cos\theta + \cos 3\theta) \cos 3\theta \, d\theta$$

$$\frac{1}{2}\int \cos\theta \cos 3\theta \, d\theta + \frac{1}{2}\int \cos^2 3\theta \, d\theta$$

$$\frac{1}{2}\int \cos\theta \cos 3\theta \, d\theta + \frac{1}{4}\int (1 + \cos 6\theta) \, d\theta$$

$$\frac{1}{2}\int \cos\theta \cos 3\theta \, d\theta + \frac{1}{4}\int (1) \, d\theta + \frac{1}{4}\int \cos 6\theta \, d\theta$$

$$\boxed{\int \cos\theta \cos^2 3\theta \, d\theta}$$

$$\frac{1}{2}\int \cos\theta \, (1 + \cos 6\theta) \, d\theta$$

$$\frac{1}{2}\int \cos\theta \, d\theta + \frac{1}{2}\int \cos\theta \cos 6\theta \, d\theta$$

$$\boxed{\int \cos\theta \cos^3 2\theta \, d\theta}$$

$$\frac{1}{2}\int \cos\theta \cos 2\theta \, (1 + \cos 4\theta) \, d\theta$$

$$\frac{1}{2}\int \cos\theta \cos 2\theta \, d\theta + \frac{1}{2}\int \cos\theta \cos 2\theta \cos 4\theta \, d\theta$$

$$\frac{1}{2}\int \cos\theta \cos 2\theta \, d\theta + \frac{1}{4}\int (\cos\theta + \cos 3\theta) \cos 4\theta \, d\theta$$

$$\frac{1}{2}\int \cos\theta \cos 2\theta \, d\theta + \frac{1}{4}\int \cos\theta \cos 4\theta \, d\theta + \frac{1}{4}\int \cos 3\theta \cos 4\theta \, d\theta$$

$$\boxed{\int \cos^2 \theta \cos 2\theta \, d\theta}$$

$$\frac{1}{2} \int (1 + \cos 2\theta) \cos 2\theta \, d\theta$$

$$\frac{1}{2} \int \cos 2\theta \, d\theta + \frac{1}{2} \int \cos^2 2\theta \, d\theta$$

$$\frac{1}{2} \int \cos 2\theta \, d\theta + \frac{1}{4} \int (1 + \cos 4\theta) \, d\theta$$

$$\frac{1}{2} \int \cos 2\theta \, d\theta + \frac{1}{4} \int (1) \, d\theta + \frac{1}{4} \int \cos 4\theta \, d\theta$$

$$\boxed{\int \cos^2 \theta \cos 2\theta \cos 3\theta \, d\theta}$$

$$\frac{1}{4} \int (1 + \cos 2\theta)(\cos \theta + \cos 5\theta) \, d\theta$$

$$\frac{1}{4} \int \cos \theta \, d\theta + \frac{1}{4} \int \cos \theta \cos 2\theta \, d\theta + \frac{1}{4} \int \cos 5\theta \, d\theta + \frac{1}{4} \int \cos 2\theta \cos 5\theta \, d\theta$$

$$\boxed{\int \cos^2 \theta \cos 3\theta \, d\theta}$$

$$\frac{1}{2} \int (1 + \cos 2\theta) \cos 3\theta \, d\theta$$

$$\frac{1}{2} \int \cos 3\theta \, d\theta + \frac{1}{2} \int \cos 2\theta \cos 3\theta \, d\theta$$

$$\boxed{\int \cos^2 \theta \cos^2 2\theta \, d\theta}$$

$$\frac{1}{4} \int (1 + \cos 2\theta)(1 + \cos 4\theta) \, d\theta$$

$$\frac{1}{4}\int (1 + \cos 2\theta + \cos 4\theta + \cos 2\theta \cos 4\theta)\ d\theta$$

$$\frac{1}{4}\int (1)\ d\theta + \frac{1}{4}\int \cos 2\theta\ d\theta + \frac{1}{4}\int \cos 4\theta\ d\theta + \frac{1}{4}\int \cos 2\theta \cos 4\theta\ d\theta$$

$$\boxed{\int \cos^3 \theta \cos 2\theta\ d\theta}$$

$$\frac{1}{4}\int (1 + \cos 2\theta)(\cos \theta + \cos 3\theta)\ d\theta$$

$$\frac{1}{4}\int \cos \theta\ d\theta + \frac{1}{4}\int \cos 3\theta\ d\theta + \frac{1}{4}\int \cos \theta \cos 2\theta\ d\theta + \frac{1}{4}\int \cos 2\theta \cos 3\theta\ d\theta$$

$$\boxed{\int \cos^3 \theta \cos 3\theta\ d\theta}$$

$$\frac{1}{4}\int (1 + \cos 2\theta)(\cos 2\theta + \cos 4\theta)\ d\theta$$

$$\frac{1}{4}\int \cos 2\theta\ d\theta + \frac{1}{4}\int \cos 4\theta\ d\theta + \frac{1}{4}\int \cos^2 2\theta\ d\theta + \frac{1}{4}\int \cos 2\theta \cos 4\theta\ d\theta$$

$$\frac{1}{4}\int \cos 2\theta\ d\theta + \frac{1}{4}\int \cos 4\theta\ d\theta + \frac{1}{8}\int (1 + \cos 4\theta)\ d\theta + \frac{1}{4}\int \cos 2\theta \cos 4\theta\ d\theta$$

$$\frac{1}{4}\int \cos 2\theta\ d\theta + \frac{3}{8}\int \cos 4\theta\ d\theta + \frac{1}{8}\int (1)\ d\theta + \frac{1}{4}\int \cos 2\theta \cos 4\theta\ d\theta$$

$$\boxed{\int \cos^3 \theta \cos^2 2\theta\ d\theta}$$

$$\frac{1}{4}\int (1 + \cos 2\theta)(1 + \cos 4\theta) \cos \theta\ d\theta$$

$$\frac{1}{4}\int (\cos \theta + \cos \theta \cos 2\theta + \cos \theta \cos 4\theta + \cos \theta \cos 2\theta \cos 4\theta)\ d\theta$$

$$\frac{1}{4}\int \cos\theta\, d\theta + \frac{1}{4}\int \cos\theta \cos 2\theta\, d\theta + \frac{1}{4}\int \cos\theta \cos 4\theta\, d\theta$$

$$+ \frac{1}{8}\int (\cos\theta + \cos 3\theta) \cos 4\theta\, d\theta$$

$$\frac{1}{4}\int \cos\theta\, d\theta + \frac{1}{4}\int \cos\theta \cos 2\theta\, d\theta + \frac{3}{8}\int \cos\theta \cos 4\theta\, d\theta$$

$$+ \frac{1}{8}\int \cos 3\theta \cos 4\theta\, d\theta$$

$$\boxed{\int \cos^4\theta \cos 2\theta\, d\theta}$$

$$\frac{1}{4}\int (1 + \cos 2\theta)^2 \cos 2\theta\, d\theta$$

$$\frac{1}{4}\int (\cos 2\theta + 2\cos^2 2\theta + \cos^3 2\theta)\, d\theta$$

$$\frac{1}{4}\int \cos 2\theta\, d\theta + \frac{1}{4}\int (1 + \cos 4\theta)\, d\theta + \frac{1}{8}\int (1 + \cos 4\theta) \cos 2\theta\, d\theta$$

$$\frac{3}{8}\int \cos 2\theta\, d\theta + \frac{1}{4}\int (1)\, d\theta + \frac{1}{4}\int \cos 4\theta\, d\theta + \frac{1}{8}\int \cos 2\theta \cos 4\theta\, d\theta$$

$$\boxed{\int \cos^4\theta \cos 3\theta\, d\theta}$$

$$\frac{1}{4}\int (1 + \cos 2\theta)^2 \cos 3\theta\, d\theta$$

$$\frac{1}{4}\int (\cos 3\theta + 2\cos 2\theta \cos 3\theta + \cos^2 2\theta \cos 3\theta)\, d\theta$$

$$\frac{1}{4}\int \cos 3\theta\, d\theta + \frac{1}{2}\int \cos 2\theta \cos 3\theta\, d\theta + \frac{1}{8}\int (1 + \cos 4\theta) \cos 3\theta\, d\theta$$

$$\frac{3}{8}\int \cos 3\theta \, d\theta + \frac{1}{2}\int \cos 2\theta \cos 3\theta \, d\theta + \frac{1}{8}\int \cos 3\theta \cos 4\theta \, d\theta$$

$$\boxed{\int \sin^2 \theta \, d\theta}$$

$$\frac{1}{2}\int (1 - \cos 2\theta) \, d\theta$$

$$\frac{1}{2}\int (1) \, d\theta - \frac{1}{2}\int \cos 2\theta \, d\theta$$

$$\boxed{\int \sin^2 \theta \cos \theta \, d\theta}$$

$$\frac{1}{2}\int (1 - \cos 2\theta) \cos \theta \, d\theta$$

$$\frac{1}{2}\int \cos \theta \, d\theta - \frac{1}{2}\int \cos \theta \cos 2\theta \, d\theta$$

$$\boxed{\int \sin^2 \theta \cos \theta \cos 2\theta \, d\theta}$$

$$\frac{1}{4}\int (1 - \cos 2\theta)(\cos \theta + \cos 3\theta) \, d\theta$$

$$\frac{1}{4}\int \cos \theta \, d\theta - \frac{1}{4}\int \cos \theta \cos 2\theta \, d\theta + \int \cos 3\theta \, d\theta - \int \cos 2\theta \cos 3\theta \, d\theta$$

$$\boxed{\int \sin^2 \theta \cos^2 \theta \, d\theta}$$

$$\frac{1}{4}\int (1 - \cos 2\theta)(1 + \cos 2\theta) \, d\theta$$

$$\frac{1}{4}\int (1) \, d\theta - \frac{1}{4}\int \cos^2 2\theta \, d\theta$$

$$\frac{1}{4}\int(1)\,d\theta - \frac{1}{8}\int(1 + \cos 4\theta)\,d\theta$$

$$\frac{1}{8}\int(1)\,d\theta - \frac{1}{8}\int\cos 4\theta\,d\theta$$

$$\boxed{\int\sin^2\theta\cos^3\theta\,d\theta}$$

$$\frac{1}{4}\int(1 - \cos 2\theta)(1 + \cos 2\theta)\cos\theta\,d\theta$$

$$\frac{1}{4}\int\cos\theta\,d\theta - \frac{1}{4}\int\cos^2 2\theta\cos\theta\,d\theta$$

$$\frac{1}{4}\int\cos\theta\,d\theta - \frac{1}{8}\int(1 + \cos 4\theta)\cos\theta\,d\theta$$

$$\frac{1}{8}\int\cos\theta\,d\theta - \frac{1}{8}\int\cos\theta\cos 4\theta\,d\theta$$

$$\boxed{\int\sin^2\theta\cos 2\theta\,d\theta}$$

$$\frac{1}{2}\int(1 - \cos 2\theta)\cos 2\theta\,d\theta$$

$$\frac{1}{2}\int\cos 2\theta\,d\theta - \frac{1}{4}\int(1 + \cos 4\theta)\,d\theta$$

$$\frac{1}{2}\int\cos 2\theta\,d\theta - \frac{1}{4}\int(1)\,d\theta - \frac{1}{4}\int\cos 4\theta\,d\theta$$

$$\boxed{\int\sin^2\theta\cos 3\theta\,d\theta}$$

$$\frac{1}{2}\int(1 - \cos 2\theta)\cos 3\theta\,d\theta$$

$$\frac{1}{2}\int \cos 3\theta \; d\theta - \frac{1}{2}\int \cos 2\theta \cos 3\theta \; d\theta$$

$$\boxed{\int \sin \theta \sin 2\theta \cos \theta \; d\theta}$$

$$\frac{1}{2}\int (\cos \theta - \cos 3\theta) \cos \theta \; d\theta$$

$$\frac{1}{2}\int \cos^2 \theta \; d\theta - \frac{1}{2}\int \cos \theta \cos 3\theta \; d\theta$$

$$\frac{1}{4}\int (1 + \cos 2\theta) \; d\theta - \frac{1}{2}\int \cos \theta \cos 3\theta \; d\theta$$

$$\frac{1}{4}\int (1) \; d\theta + \frac{1}{4}\int \cos 2\theta \; d\theta - \frac{1}{2}\int \cos \theta \cos 3\theta \; d\theta$$

$$\boxed{\int \sin \theta \sin 2\theta \cos \theta \cos 2\theta \; d\theta}$$

$$\frac{1}{4}\int (\cos \theta - \cos 3\theta)(\cos \theta + \cos 3\theta) \; d\theta$$

$$\frac{1}{4}\int (\cos^2 \theta - \cos^2 3\theta) \; d\theta$$

$$\frac{1}{8}\int \Big((1 + \cos 2\theta) - (1 + \cos 6\theta)\Big) d\theta$$

$$\frac{1}{8}\int \cos 2\theta \; d\theta - \frac{1}{8}\int \cos 6\theta \; d\theta$$

$$\boxed{\int \sin \theta \sin 2\theta \cos^2 \theta \; d\theta}$$

$$\frac{1}{4}\int (\cos \theta - \cos 3\theta)(1 + \cos 2\theta) \; d\theta$$

$$\frac{1}{4}\int \cos\theta\, d\theta - \frac{1}{4}\int \cos 3\theta\, d\theta + \frac{1}{4}\int \cos\theta \cos 2\theta\, d\theta - \frac{1}{4}\int \cos 2\theta \cos 3\theta\, d\theta$$

$$\boxed{\int \sin\theta \sin 2\theta \cos^3\theta\, d\theta}$$

$$\frac{1}{4}\int (\cos\theta - \cos 3\theta)(1 + \cos 2\theta) \cos\theta\, d\theta$$

$$\frac{1}{4}\int \cos^2\theta\, d\theta - \frac{1}{4}\int \cos\theta \cos 3\theta\, d\theta + \frac{1}{4}\int \cos^2\theta \cos 2\theta\, d\theta$$

$$- \frac{1}{4}\int \cos\theta \cos 2\theta \cos 3\theta\, d\theta$$

$$\frac{1}{8}\int (1 + \cos 2\theta)\, d\theta - \frac{1}{4}\int \cos\theta \cos 3\theta\, d\theta + \frac{1}{8}\int (1 + \cos 2\theta) \cos 2\theta\, d\theta$$

$$- \frac{1}{8}\int (\cos\theta + \cos 3\theta) \cos 3\theta\, d\theta$$

$$\frac{1}{8}\int (1)\, d\theta + \frac{1}{4}\int \cos 2\theta\, d\theta - \frac{1}{4}\int \cos\theta \cos 3\theta\, d\theta + \frac{1}{16}\int (1 + \cos 4\theta)\, d\theta$$

$$- \frac{1}{8}\int \cos\theta \cos 3\theta\, d\theta - \frac{1}{16}\int (1 + \cos 6\theta)\, d\theta$$

$$\frac{1}{8}\int (1)\, d\theta + \frac{1}{4}\int \cos 2\theta\, d\theta$$

$$- \frac{3}{8}\int \cos\theta \cos 3\theta\, d\theta + \frac{1}{16}\int \cos 4\theta\, d\theta - \frac{1}{16}\int \cos 6\theta\, d\theta$$

$$\boxed{\int \sin\theta \sin 2\theta \cos 2\theta\, d\theta}$$

$$\frac{1}{2}\int (\cos\theta - \cos 3\theta) \cos 2\theta\, d\theta$$

$$\frac{1}{2}\int \cos\theta \cos 2\theta \, d\theta - \frac{1}{2}\int \cos 2\theta \cos 3\theta \, d\theta$$

$$\boxed{\int \sin\theta \sin 2\theta \cos 3\theta \, d\theta}$$

$$\frac{1}{2}\int (\cos\theta - \cos 3\theta) \cos 3\theta \, d\theta$$

$$\frac{1}{2}\int \cos\theta \cos 3\theta \, d\theta - \frac{1}{4}\int (1 + \cos 6\theta) \, d\theta$$

$$\frac{1}{2}\int \cos\theta \cos 3\theta \, d\theta - \frac{1}{4}\int (1) \, d\theta - \frac{1}{4}\int \cos 6\theta \, d\theta$$

$$\boxed{\int \sin\theta \sin 3\theta \cos\theta \, d\theta}$$

$$\frac{1}{2} \quad (\cos 2\theta - \cos 4\theta) \cos\theta \, d\theta$$

$$\frac{1}{2}\int \cos\theta \cos 2\theta \, d\theta - \frac{1}{2}\int \cos\theta \cos 4\theta \, d\theta$$

$$\boxed{\int \sin\theta \sin 3\theta \cos\theta \cos 2\theta \, d\theta}$$

$$\frac{1}{4}\int (\cos 2\theta - \cos 4\theta)(\cos\theta + \cos 3\theta) \, d\theta$$

$$\frac{1}{4}\int \cos\theta \cos 2\theta \, d\theta - \frac{1}{4}\int \cos\theta \cos 4\theta \, d\theta + \frac{1}{4}\int \cos 2\theta \cos 3\theta \, d\theta$$

$$- \frac{1}{4}\int \cos 3\theta \cos 4\theta \, d\theta$$

$$\boxed{\int \sin\theta \sin 3\theta \cos^2\theta \, d\theta}$$

$$\frac{1}{4}\int (\cos 2\theta - \cos 4\theta)(1 + \cos 2\theta)\, d\theta$$

$$\frac{1}{4}\int \cos 2\theta\, d\theta - \frac{1}{4}\int \cos 4\theta\, d\theta + \frac{1}{8}\int (1 + \cos 4\theta)\, d\theta - \frac{1}{4}\int \cos 2\theta \cos 4\theta\, d\theta$$

$$\frac{1}{4}\int \cos 2\theta\, d\theta - \frac{1}{8}\int \cos 4\theta\, d\theta + \frac{1}{8}\int (1)\, d\theta - \frac{1}{4}\int \cos 2\theta \cos 4\theta\, d\theta$$

$$\boxed{\int \sin\theta \sin 3\theta \cos^3\theta \, d\theta}$$

$$\frac{1}{4}\int (\cos 2\theta - \cos 4\theta)(1 + \cos 2\theta) \cos\theta\, d\theta$$

$$\frac{1}{4}\int \cos\theta \cos 2\theta\, d\theta - \frac{1}{4}\int \cos\theta \cos 4\theta\, d\theta + \frac{1}{4}\int \cos\theta \cos^2 2\theta\, d\theta$$

$$- \frac{1}{4}\int \cos\theta \cos 2\theta \cos 4\theta\, d\theta$$

$$\frac{1}{4}\int \cos\theta \cos 2\theta\, d\theta - \frac{1}{4}\int \cos\theta \cos 4\theta\, d\theta + \frac{1}{8}\int \cos\theta\, (1 + \cos 4\theta)\, d\theta$$

$$- \frac{1}{8}\int (\cos\theta + \cos 3\theta) \cos 4\theta\, d\theta$$

$$\frac{1}{4}\int \cos\theta \cos 2\theta\, d\theta - \frac{1}{4}\int \cos\theta \cos 4\theta\, d\theta + \frac{1}{8}\int \cos\theta\, d\theta$$

$$- \frac{1}{8}\int \cos 3\theta \cos 4\theta\, d\theta$$

$$\boxed{\int \sin\theta \sin 3\theta \cos 2\theta \, d\theta}$$

$$\frac{1}{2}\int (\cos 2\theta - \cos 4\theta) \cos 2\theta \, d\theta$$

$$\frac{1}{2}\int \cos^2 2\theta \, d\theta - \frac{1}{2}\int \cos 2\theta \cos 4\theta \, d\theta$$

$$\frac{1}{4}\int (1 + \cos 4\theta) \, d\theta - \frac{1}{2}\int \cos 2\theta \cos 4\theta \, d\theta$$

$$\frac{1}{4}\int (1) \, d\theta + \frac{1}{4}\int \cos 4\theta \, d\theta - \frac{1}{2}\int \cos 2\theta \cos 4\theta \, d\theta$$

$$\boxed{\int \sin\theta \sin 3\theta \cos 3\theta \, d\theta}$$

$$\frac{1}{2}\int (\cos 2\theta - \cos 4\theta) \cos 3\theta \, d\theta$$

$$\frac{1}{2}\int \cos 2\theta \cos 3\theta \, d\theta - \frac{1}{2}\int \cos 3\theta \cos 4\theta \, d\theta$$

$$\boxed{\int \sin^2 2\theta \, d\theta}$$

$$\frac{1}{2}\int (1 - \cos 4\theta) \, d\theta$$

$$\frac{1}{2}\int (1) \, d\theta - \frac{1}{2} \quad \cos 4\theta \, d\theta$$

$$\boxed{\int \sin^2 2\theta \cos\theta \, d\theta}$$

$$\frac{1}{2}\int (1 - \cos 4\theta) \cos\theta \, d\theta$$

$$\frac{1}{2}\int \cos\theta\, d\theta - \frac{1}{2}\int \cos\theta \cos 4\theta\, d\theta$$

$$\boxed{\int \sin^2 2\theta \cos\theta \cos 2\theta\, d\theta}$$

$$\frac{1}{4}\int (1 - \cos 4\theta)(\cos\theta + \cos 3\theta)\, d\theta$$

$$\frac{1}{4}\int \cos\theta\, d\theta + \frac{1}{4}\int \cos 3\theta\, d\theta - \frac{1}{4}\int \cos\theta \cos 4\theta\, d\theta - \frac{1}{4}\int \cos 3\theta \cos 4\theta\, d\theta$$

$$\boxed{\int \sin^2 2\theta \cos^2\theta\, d\theta}$$

$$\frac{1}{4}\int (1 - \cos 4\theta)(1 + \cos 2\theta)\, d\theta$$

$$\frac{1}{4}\int (1)\, d\theta - \frac{1}{4}\int \cos 4\theta\, d\theta + \frac{1}{4}\int \cos 2\theta\, d\theta - \frac{1}{4}\int \cos 2\theta \cos 4\theta\, d\theta$$

$$\boxed{\int \sin^2 2\theta \cos^3\theta\, d\theta}$$

$$\frac{1}{4}\int (1 - \cos 4\theta)(1 + \cos 2\theta)\cos\theta\, d\theta$$

$$\frac{1}{4}\int (\cos\theta - \cos\theta\cos 4\theta + \cos\theta\cos 2\theta - \cos\theta\cos 2\theta\cos 4\theta)\, d\theta$$

$$\frac{1}{4}\int \cos\theta\, d\theta - \frac{1}{4}\int \cos\theta\cos 4\theta\, d\theta + \frac{1}{4}\int \cos\theta\cos 2\theta\, d\theta$$

$$- \frac{1}{8}\int (\cos\theta + \cos 3\theta)\cos 4\theta\, d\theta$$

$$\frac{1}{4}\int \cos\theta\, d\theta - \frac{3}{8}\int \cos\theta \cos 4\theta\, d\theta + \frac{1}{4}\int \cos\theta \cos 2\theta\, d\theta$$

$$- \frac{1}{8}\int \cos 3\theta \cos 4\theta\, d\theta$$

$$\boxed{\int \sin^2 2\theta \cos 2\theta\, d\theta}$$

$$\frac{1}{2}\int (1 - \cos 4\theta) \cos 2\theta\, d\theta$$

$$\frac{1}{2}\int \cos 2\theta\, d\theta - \frac{1}{2}\int \cos 2\theta \cos 4\theta\, d\theta$$

$$\boxed{\int \sin^2 2\theta \cos 3\theta\, d\theta}$$

$$\frac{1}{2}\int (1 - \cos 4\theta) \cos 3\theta\, d\theta$$

$$\frac{1}{2}\int \cos 3\theta\, d\theta - \frac{1}{2}\int \cos 3\theta \cos 4\theta\, d\theta$$

APPENDIX E: PROGRAM LISTING

```
      PROGRAM STK3REF
C*******
C
C     THIS FINITE AMPLITUDE WAVE MODEL USES A
C     THIRD ORDER SOLUTUION TO STOKES WAVE THEORY
C
C*******
      PARAMETER(IQ=500,JQ=50)
      COMMON/CONST/M,N,DX,DY,H0,T,THETA0,CNTR,IORDER,G
      COMMON/CONST2/PI,PI2,RAD,C0,L0,K0,SIGMA,S2G,GAM
      COMMON/CONST3/I,J,ICOUNT,IC,NM1
      COMMON/ARRAY/D(JQ,IQ),K(JQ,IQ),TH(JQ,IQ),H(JQ,IQ),B(JQ,IQ)
      COMMON/ARR2/C(JQ,IQ),F(JQ,IQ),NEWH(JQ),L(JQ,IQ),CG(JQ,IQ)
      COMMON/ARR3/E(JQ,IQ),C1(JQ,IQ),UU(JQ,IQ)
      REAL K0,L0,K,L,NEWH
C
C**** SUBROUTINE DATAIN READS IN INPUT DATA
C
      CALL DATAIN
C
C**** CHECK THE ORDER OF THE SOLUTION
C
      IF(IORDER.NE.1.AND.IORDER.NE.3) THEN
       WRITE(6,98) IORDER
   98  FORMAT(1X,'THE SOLUTION TO ORDER',I5,' CANNOT BE CALCULATED
     1  BY THIS PROGRAM.  CHOOSE ORDER 1 OR 3 AND RERUN')
       STOP
      END IF
C
C****  SUBROUTINE DEPTH READS IN OR CALCULATES
C****  THE DEPTH IN EACH GRID CELL
C
       CALL DEPTH
C
C****  SUBROUTINE INITIAL DEFINES AND CALCULATES
C****  CONSTANTS USED THROUGHOUT THE PROGRAM
C
       CALL INITIAL
C
C****  SUBROUTINE BNDRY CALCULATES H,K,TH ON THE OFFSHORE BOUNDARY
C
       CALL BNDRY
C
       I=M+1
       CALL URSELL(U,BR)
       IF(U.GE.25.) STOP
       IF(BR.GE..78) STOP
```

```
C
C****  BEGIN CALCULATION LOOP
C
      DO 30 I=M,3,-1
      ICOUNT=0
      IU=I
   10 CALL DISPERS
      IF(ICOUNT.EQ.20) GO TO 94
      IF(IC.EQ.20) GO TO 94
      CALL DELK
      IF(IC.EQ.20) GO TO 94
      CALL DELF
      IF(IC.EQ.20) GO TO 94
      DO 20 J=1,N
      TOL=ABS(NEWH(J)-H(J,I-1))
      IF(TOL.GT..0001) GO TO 10
      H(J,I-1)=NEWH(J)
   20 CONTINUE
C****  FINALIZE ROW I-1
      CALL DISPERS
      CALL DELK
      CALL DELF
C****  CHECK URSELL NUMBER
      CALL URSELL(U,BR)
      IF(IORDER.EQ.3.AND.U.GE.25.) GO TO 94
      IF(IORDER.EQ.1.AND.BR.GT..78) GO TO 94
   30 CONTINUE
C**** END CALCULATION LOOP
   94 CONTINUE
C**** OUTPUT TABLE OF RESULTS
      DO 40 I=1,M
      DO 40 J=1,N
      TH(J,I)=(TH(J,I)-PI)/RAD
   40 CONTINUE
       CALL TABLE(IU,M,2,1,N,' DEPTH          ',D,10.0)
       CALL TABLE(IU,M,2,1,N,' WAVE    HEIGHT ',H,1000.0)
       CALL TABLE(IU,M,2,1,N,' WAVE    ANGLE  ',TH,10.)
       CALL TABLE(IU,M,2,1,N,' WAVE NUMBER    ',K,1000000.)
      STOP
      END
C*********************
C
C
      SUBROUTINE DATAIN
C
C
```

```
C*********************
C
C     SUBROUTINE DATAIN READS IN INPUT DATA
C
C****
C
C     DEFINITION OF INPUT VARIABLES
C     ---------- -- ----- ---------
C
C     M = NUMBER OF GRID CELLS IN THE X DIRECTION
C
C     N = NUMBER OF GRID CELLS IN THE Y DIRECTION
C
C     DX = GRID CELL SIZE IN THE X DIRECTION
C
C     DY = GRID CELL SIZE IN THE Y DIRECTION
C
C     THETAO = DEEP WATER WAVE DIRECTION
C     (+) COUNTER-CLOCKWISE FROM THE X-AXIS
C     (-) CLOCK-WISE FROM THE X-AXIS
C
C     CNTR = APPROXIMATE ANGLE THE OFFSHORE CONTOURS
C     MAKE WITH THE Y-AXIS
C     (+) COUNTER-CLOCKWISE FROM THE Y-AXIS
C     (-) CLOCKWISE FROM THE Y-AXIS
C
C     HO = DEEP WATER WAVE HEIGHT
C
C     T = WAVE PERIOD
C
C     IORDER = DEGREE OF SOLUTION (1 OR 3)
C
C     G = ACCELERATION OF GRAVITY
C
C********************************
C
      PARAMETER(IQ=500,JQ=50)
      COMMON/CONST/M,N,DX,DY,HO,T,THETAO,CNTR,IORDER,G
      COMMON/CONST2/PI,PI2,RAD,CO,LO,KO,SIGMA,S2G,GAM
      COMMON/CONST3/I,J,ICOUNT,IC,NM1
      COMMON/ARRAY/D(JQ,IQ),K(JQ,IQ),TH(JQ,IQ),H(JQ,IQ),B(JQ,IQ)
      COMMON/ARR2/C(JQ,IQ),F(JQ,IQ),NEWH(JQ),L(JQ,IQ),CG(JQ,IQ)
      COMMON/ARR3/E(JQ,IQ),C1(JQ,IQ),UU(JQ,IQ)
      REAL KO,LO,K,L,NEWH
C**** READ IN GRID CHARACTERISTICS
      READ(1,10) M,N,DX,DY
      READ(1,11) HO,T,THETAO,CNTR
```

```
      READ(1,12) IORDER,G
      WRITE(6,13)
      WRITE(6,14) M
      WRITE(6,15) N
      WRITE(6,16) DX
      WRITE(6,17) DY
      WRITE(6,18) HO
      WRITE(6,19) T
      WRITE(6,20) THETAO
      WRITE(6,21) CNTR
      WRITE(6,22) IORDER
      WRITE(6,23) G
   10 FORMAT(2I5,2F10.5)
   11 FORMAT(4F10.5)
   12 FORMAT(I5,F10.5)
   13 FORMAT(15X,'*********** INPUT DATA ************',//)
   14 FORMAT(1X,'THE NUMBER OF GRID CELLS IN THE X DIRECTION IS '
     1,I5,/)
   15 FORMAT(1X,'THE NUMBER OF GRID CELLS IN THE Y DIRECTION IS '
     1,I5,/)
   16 FORMAT(1X,'THE GRID CELL SIZE IN THE X DIRECTION IS',F10.5,/
     1)
   17 FORMAT(1X,'THE GRID CELL SIZE IN THE Y DIRECTION IS ',F10.5,/
     1)
   18 FORMAT(1X,'THE DEEPWATER WAVE HEIGHT ',F10.5,/)
   19 FORMAT(1X,'THE WAVE PERIOD IS ',F10.5,/)
   20 FORMAT(1X,'THE DEEPWATER WAVE ANGLE ',F10.5,/)
   21 FORMAT(1X,'ANGLE WHICH THE OFFSHORE CONTOURS MAKE WITH THE
     1 GRID Y AXIS ',F10.5,/)
   22 FORMAT(1X,'THE ORDER OF THE SOLUTION IS ',I5,/)
   23 FORMAT(1X,'THE ACCELERATION OF GRAVITY IS ',F10.5,/)
      RETURN
      END
C************************************
C
C
      SUBROUTINE DEPTH
C
C
C************************************
C
C     THIS SUBROUTINE READS IN OR CALCULATES
C     THE DEPTHS AT EACH GRID CELL
C
C     D(J,I) = THE DEPTH IN GRID CELL (J,I)
C
      PARAMETER(IQ=500,JQ=50)
```

```
      COMMON/CONST/M,N,DX,DY,H0,T,THETA0,CNTR,IORDER,G
      COMMON/ARRAY/D(JQ,IQ),K(JQ,IQ),TH(JQ,IQ),H(JQ,IQ),B(JQ,IQ)
      REAL K0,L0,K,L,NEWH
      DO 100 I=1,M
      READ(3,200) (D(J,I),J=1,N)
  100 CONTINUE
  200 FORMAT(10F8.2)
      RETURN
      END
C**************************
C
C
      SUBROUTINE INITIAL
C
C
C**************************
C
C**** SUBROUTINE INITIAL DEFINES AND CALCULATES
C**** CONSTANTS USED THROUGHOUT THE PROGRAM
C
      PARAMETER(IQ=500,JQ=50)
      COMMON/CONST/M,N,DX,DY,H0,T,THETA0,CNTR,IORDER,G
      COMMON/CONST2/PI,PI2,RAD,C0,L0,K0,SIGMA,S2G,GAM
      COMMON/CONST3/I,J,ICOUNT,IC,NM1
      COMMON/ARRAY/D(JQ,IQ),K(JQ,IQ),TH(JQ,IQ),H(JQ,IQ),B(JQ,IQ)
      COMMON/ARR2/C(JQ,IQ),F(JQ,IQ),NEWH(JQ),L(JQ,IQ),CG(JQ,IQ)
      COMMON/ARR3/E(JQ,IQ),C1(JQ,IQ),UU(JQ,IQ)
      REAL K0,L0,K,L,NEWH
      NM1=N-1
      PI=3.14159
      PI2=2.*PI
      RAD=PI/180.
      THETA0=(THETA0+180.)*RAD
      CNTR=CNTR*RAD
      C0=(G*T)/PI2
      L0=C0*T
      K0=PI2/L0
      IF(IORDER.EQ.3) THEN
      C0=C0*(1.+((K0*H0/2.)**2))
      L0=C0*T
      K0=PI2/L0
      END IF
      SIGMA=PI2/T
      S2G=(SIGMA**2)/G
      IF(G.GE.32.0.AND.G.LE.32.3) THEN
        G=32.2
        GAM=64.0
```

```
      ELSE IF(G.GE.9.8.AND.G.LE.9.81) THEN
        G=9.806
        GAM=10051.
      END IF
      IF(G.NE.32.2.AND.G.NE.9.806) THEN
        WRITE(6,10) G
   10   FORMAT(1X,'THE VALUE OF G = ',F10.5,' THIS MODEL REQUIRES
     1 G=32.2 OR G=9.806.  PLEASE CORRECT AND RERUN')
        STOP
      END IF
      RETURN
      END
C************************
C
C
      SUBROUTINE BNDRY
C
C
C************************
C
C
C**** SUBROUTINE BNDRY CALCULATES H,K,TH ON THE BOUNDARY (I=M)
      PARAMETER(IQ=500,JQ=50)
      COMMON/CONST/M,N,DX,DY,H0,T,THETA0,CNTR,IORDER,G
      COMMON/CONST2/PI,PI2,RAD,C0,L0,K0,SIGMA,S2G,GAM
      COMMON/CONST3/I,J,ICOUNT,IC,NM1
      COMMON/ARRAY/D(JQ,IQ),K(JQ,IQ),TH(JQ,IQ),H(JQ,IQ),B(JQ,IQ)
      COMMON/ARR2/C(JQ,IQ),F(JQ,IQ),NEWH(JQ),L(JQ,IQ),CG(JQ,IQ)
      COMMON/ARR3/E(JQ,IQ),C1(JQ,IQ),UU(JQ,IQ)
      DIMENSION TEMPH(JQ)
      REAL K0,L0,K,L,NEWH,KK,KD,KDN,KD2,K1,K2,NN,NNM
      SN=SIN(THETA0-CNTR)
      CS=COS(THETA0-CNTR)
      SNK0=SN*K0
      F0=GAM*H0*H0*C0/16.
       IF(IORDER.EQ.3) THEN
        EPS2=(K0*H0/2.)**2
        F0=F0*(1.+2*EPS2)
       END IF
      FOC0=F0*CS
       DO 100 J=1,N
        K(J,M)=K0
        H(J,M)=H0
        TH(J,M)=THETA0
        NEWH(J)=H0
        F(J,M)=F0
  100  CONTINUE
```

```
      ICOUNT=0
10    ICOUNT=ICOUNT+1
       IF(ICOUNT.EQ.20) THEN
        WRITE(6,15)
15      FORMAT(1X,'CONVERGENCE NOT REACHED IN 20 ITERATIONS
     1  AT THE OFFSHORE BOUNDARY')
        STOP
       END IF
      DO 200 J=1,N
       H(J,M)=NEWH(J)
        DD=D(J,M)
         KD=K(J,M)*DD
          S2GD=S2G*DD
           IF(KD.LT.1.0) KD=SQRT(S2GD)
            IC=0
20           IC=IC+1
                IF(IC.EQ.20) THEN
                 WRITE(6,85) M,J
85               FORMAT(1X,'CONVERGENCE NOT REACHED IN
     1           20 ITERATIONS AT I=',I5,' J=',I5)
                 STOP
                END IF
                COT=COSH(KD)/SINH(KD)
                COT2=COT*COT
                IF(IORDER.EQ.1)THEN
                 FAC=1.0
                 GO TO 25
                END IF
                EPS2=((KD*H(J,M))/(2.*DD))**2
               DUM=((9.*(COT2**2))-(10.*COT2)+9.)/16.
              FAC=(1.+(EPS2*(DUM-(COT/(2.*KD)))))**2
25           KDN=KD-(KD*FAC-S2GD*COT)/(FAC+S2GD*(COT2-1.))
            TOL=ABS(KDN-KD)
           KD=KDN
          IF(TOL.GT..0001) GO TO 20
         K(J,M)=KD/DD
        L(J,M)=PI2/K(J,M)
       C1(J,M)=SQRT(G*TANH(KD)/K(J,M))
      TH(J,M)=PI-ASIN(SNKO/K(J,M))+CNTR
200   CONTINUE
      DO 350 J=1,N
       HH=NEWH(J)
        KK=K(J,M)
         KD=KK*D(J,M)
          KD2=2.*KD
           SI2=SINH(KD2)
            NN=0.5*(1.+KD2/SI2)
```

```
                C(J,M)=C1(J,M)
                 F(J,M)=.125*GAM*HH*HH*NN*C1(J,M)
                  IF(IORDER.EQ.3) THEN
                   CO=COSH(KD)
                   SI=SINH(KD)
                   COT=CO/SI
                   COT2=COT*COT
                   EPS2=(KK*HH/2.)**2
                   T1=(9.*COT2**2-10.*COT2+9.)/16.
                  T2=COT/KD2
                 C(J,M)=C1(J,M)*(1.+EPS2*(T1-T2))
                S1=(-.25*COT/KD)*(1.+NN)
               S2=(NN/64.)*(-27.*COT2**3+15.*COT2**2-61.*COT2+57.)
              CSH2=COSH(KD2)
             S4KD=(SINH(KD))**4
            S3=(9.*COT2**3+3.*COT2**2-13.*COT2+33.)/64.
           S4=9.*KD*(COT2**2-2.*COT2+1.)/(64.*COT*S4KD)
          S5=0.75*CSH2*(COT2-1.)/(CSH2-1.)
          B(J,M)=S1+S2+S3+S4+S5
          F(J,M)=F(J,M)*(1.+(0.5*KK*KK*HH*HH*B(J,M)/NN))
         END IF
  350   CONTINUE
        DO 400 J=2,NM1
            IC=0
             KD2=2.*K(J,M)*D(J,M)
              CON1=FOCO/COS(TH(J,M))
   40          IC=IC+1
               IF(IC.EQ.20) THEN
                WRITE(6,41) J,IC
   41           FORMAT(1X,'ON BOUNDARY ELEMENT',I3,' THE SOLUTION DID NOT
     1          CONVERGE IN ',I3,' ITERATIONS')
                STOP
               END IF
               CON2=GAM*(K(J,M)**2)*(NEWH(J)**4)*C1(J,M)*B(J,M)/16.
              NNM=0.5*(1.+KD2/SINH(KD2))
             CON3=8./(GAM*NNM*C1(J,M))
            TEMPH(J)=SQRT(CON3*(CON1-CON2))
           TOL=ABS(TEMPH(J)-NEWH(J))
          NEWH(J)=TEMPH(J)
         IF(TOL.GT..0001) GO TO 40
  400   CONTINUE
        NEWH(1)=NEWH(2)
        NEWH(N)=NEWH(NM1)
        DO 450 J=1,N
        TOL=ABS(NEWH(J)-H(J,M))
        IF(TOL.GT..0001) GO TO 10
        H(J,M)=NEWH(J)
```

```
  450 CONTINUE
  90  RETURN
      END
C******************************
C
C
      SUBROUTINE URSELL(U,BR)
C
C
C******************************
C
C
C**** CALCULATE THE URSELL NUMBER ALONG THE ENTIRE ROW
      PARAMETER(IQ=500,JQ=50)
      COMMON/CONST/M,N,DX,DY,H0,T,THETA0,CNTR,IORDER,G
      COMMON/CONST2/PI,PI2,RAD,C0,L0,K0,SIGMA,S2G,GAM
      COMMON/CONST3/I,J,ICOUNT,IC,NM1
      COMMON/ARRAY/D(JQ,IQ),K(JQ,IQ),TH(JQ,IQ),H(JQ,IQ),B(JQ,IQ)
      COMMON/ARR2/C(JQ,IQ),F(JQ,IQ),NEWH(JQ),L(JQ,IQ),CG(JQ,IQ)
      COMMON/ARR3/E(JQ,IQ),C1(JQ,IQ),UU(JQ,IQ)
      REAL K0,L0,K,L,NEWH
      DO 10 J=1,N
      U=(H(J,I-1)*(L(J,I-1)**2))/(D(J,I-1)**3)
      UU(J,I-1)=U
      IF(IORDER.EQ.3.AND.U.GE.25.) THEN
      WRITE(6,30) I-1
      RETURN
      END IF
      IF(IORDER.EQ.1) THEN
      BR=H(J,I-1)/D(J,I-1)
      IF(BR.GT..78) RETURN
      ENDIF
   10 CONTINUE
   30 FORMAT(//,' STOP HERE!! YOU ARE OUT OF THE RANGE OF VALIDITY.'
     1,/,' FIRST INVALID ROW IS ',I5)
      RETURN
      END
C******************************
C
C
      SUBROUTINE DISPERS
C
C
C******************************
      PARAMETER(IQ=500,JQ=50)
      COMMON/CONST/M,N,DX,DY,H0,T,THETA0,CNTR,IORDER,G
      COMMON/CONST2/PI,PI2,RAD,C0,L0,K0,SIGMA,S2G,GAM
```

```
      COMMON/CONST3/I,J,ICOUNT,IC,NM1
      COMMON/ARRAY/D(JQ,IQ),K(JQ,IQ),TH(JQ,IQ),H(JQ,IQ),B(JQ,IQ)
      COMMON/ARR2/C(JQ,IQ),F(JQ,IQ),NEWH(JQ),L(JQ,IQ),CG(JQ,IQ)
      COMMON/ARR3/E(JQ,IQ),C1(JQ,IQ),UU(JQ,IQ)
      REAL K0,L0,K,L,NEWH,KD,KD2,KDN
      ICOUNT=ICOUNT+1
      IF(ICOUNT.EQ.20) THEN
      WRITE(6,65) I-1,J
   65 FORMAT(1X,'CONVERGENCE NOT REACHED IN 20 ITERATIONS AT I='
     1,I5,' J=',I5,'SUB IS DISPERS')
      RETURN
      END IF
      IF(ICOUNT.EQ.1) THEN
      DO 10 J=1,N
       K(J,I-1)=K(J,I)
       H(J,I-1)=NEWH(J)
       F(J,I-1)=F(J,I)
   10 CONTINUE
      END IF
      DO 40 J=1,N
       H(J,I-1)=NEWH(J)
       DD=D(J,I-1)
       KD=K(J,I-1)*DD
       S2GD=S2G*DD
       IF(KD.LT.1.0) KD=SQRT(S2GD)
       IC=0
   45  IC=IC+1
       IF(IC.EQ.20) THEN
       WRITE(6,65) I-1,J
       RETURN
       END IF
       COT=COSH(KD)/SINH(KD)
       COT2=COT*COT
       IF(IORDER.EQ.1) THEN
       FAC=1.0
       GO TO 50
       END IF
        EPS2=((KD*H(J,I-1))/(2.*DD))**2
        DUM=((9.*(COT2**2))-(10.*COT2)+9.)/16.
        FAC=(1.+(EPS2*(DUM-(COT/(2.*KD)))))**2
   50 KDN=KD-(KD*FAC-S2GD*COT)/(FAC+S2GD*(COT2-1.))
      TOL=ABS(KDN-KD)
      KD=KDN
      IF(TOL.GT..0001) GO TO 45
      K(J,I-1)=KD/DD
      C1(J,I-1)=SQRT(G*TANH(KD)/K(J,I-1))
      L(J,I-1)=PI2/K(J,I-1)
```

```
   40 CONTINUE
      RETURN
      END
C******************************
C
C
      SUBROUTINE DELK
C
C
C******************************
      PARAMETER(IQ=500,JQ=50)
      COMMON/CONST/M,N,DX,DY,HO,T,THETAO,CNTR,IORDER,G
      COMMON/CONST2/PI,PI2,RAD,CO,LO,KO,SIGMA,S2G,GAM
      COMMON/CONST3/I,J,ICOUNT,IC,NM1
      COMMON/ARRAY/D(JQ,IQ),K(JQ,IQ),TH(JQ,IQ),H(JQ,IQ),B(JQ,IQ)
      COMMON/ARR2/C(JQ,IQ),F(JQ,IQ),NEWH(JQ),L(JQ,IQ),CG(JQ,IQ)
      COMMON/ARR3/E(JQ,IQ),C1(JQ,IQ),UU(JQ,IQ)
      DIMENSION TEMPTH(JQ)
      REAL KO,LO,K,L,NEWH
      IC=0
      IF(ICOUNT.EQ.1) THEN
      DO 10 J=1,N
       TH(J,I-1)=TH(J,I)
   10 CONTINUE
      END IF
   25 IC=IC+1
      IF(IC.EQ.20) THEN
       WRITE(6,50) I
   50  FORMAT(1X,'NON-CONVERGENCE IN DELK, ROW I=',I5)
       RETURN
      END IF
      DO 30 J=2,NM1
       AVGK=(K(J,I)+K(J,I-1))/2.
       DKY=(.25/DY)*(K(J+1,I)+K(J+1,I-1)-K(J-1,I)-K(J-1,I-1))
       DKX=(K(J,I)-K(J,I-1))/DX
       DAY=(.25/DY)*(TH(J+1,I)-TH(J-1,I)+TH(J+1,I-1)-TH(J-1,I-1))
       TT=TAN((TH(J,I)+TH(J,I-1))/2.)
       TEMPTH(J)=TH(J,I)-DX*(DKY/AVGK-TT*(DKX/AVGK+DAY))
   30 CONTINUE
      IOUT=0
      DO 35 J=2,NM1
      TOL=ABS(TH(J,I-1)-TEMPTH(J))
      TH(J,I-1)=TEMPTH(J)
      IF(TOL.GT..0001) IOUT=1
   35 CONTINUE
      TH(1,I-1)=TH(2,I-1)
      TH(N,I-1)=TH(N-1,I-1)
```

```
      IF(IOUT.EQ.1) GO TO 25
      RETURN
      END
C******************************
C
C
      SUBROUTINE DELF
C
C
C******************************
      PARAMETER(IQ=500,JQ=50)
      COMMON/CONST/M,N,DX,DY,HO,T,THETAO,CNTR,IORDER,G
      COMMON/CONST2/PI,PI2,RAD,CO,LO,KO,SIGMA,S2G,GAM
      COMMON/CONST3/I,J,ICOUNT,IC,NM1
      COMMON/ARRAY/D(JQ,IQ),K(JQ,IQ),TH(JQ,IQ),H(JQ,IQ),B(JQ,IQ)
      COMMON/ARR2/C(JQ,IQ),F(JQ,IQ),NEWH(JQ),L(JQ,IQ),CG(JQ,IQ)
      COMMON/ARR3/E(JQ,IQ),C1(JQ,IQ),UU(JQ,IQ)
      DIMENSION TEMPH(JQ)
      REAL KO,LO,K,L,NEWH,KK,KD,KD2,NN,NNM
      IC=0
    5 IC=IC+1
      IF(IC.EQ.20) THEN
       WRITE(6,50)
   50  FORMAT(1X,'CONVERGENCE NOT REACHED IN 20
     1 ITERATIONS IN SUB DELF')
       RETURN
      END IF
      DO 10 J=1,N
        HH=NEWH(J)
         KK=K(J,I-1)
          KD=KK*D(J,I-1)
           KD2=2.*KD
            SI2=SINH(KD2)
             NN=0.5*(1.+KD2/SI2)
              C(J,I-1)=C1(J,I-1)
               F(J,I-1)=.125*GAM*HH*HH*NN*C1(J,I-1)
                IF(IORDER.EQ.3) THEN
                EPS2=(KK*HH/2.)**2
                CO=COSH(KD)
                SI=SINH(KD)
                COT=CO/SI
                COT2=COT**2
                T1=(9.*COT2**2-10.*COT2+9.)/16.
                T2=COT/KD2
               C(J,I-1)=C1(J,I-1)*(1.+EPS2*(T1-T2))
              S1=(-.25*COT/KD)*(1.+NN)
             S2=(NN/64.)*(-27.*COT2**3+15.*COT2**2-61.*COT2+57.)
```

```
          CSH2=COSH(KD2)
          S4KD=(SINH(KD))**4
          S3=(9.*COT2**3+3.*COT2**2-13.*COT2+33.)/64.
          S4=(9.*KD*(COT2**2-2.*COT2+1.))/(64.*COT*S4KD)
          S5=0.75*CSH2*(COT2-1.)/(CSH2-1.)
          B(J,I-1)=S1+S2+S3+S4+S5
          F(J,I-1)=F(J,I-1)*(1.+2.*EPS2*B(J,I-1)/NN)
        END IF
   10 CONTINUE
      IOUT=0
      DO 20 J=2,N-1
      KD2=2.*K(J,I-1)*D(J,I-1)
      NNM=0.5*(1.+KD2/SINH(KD2))
      F1=F(J+1,I)*SIN(TH(J+1,I))
      F2=F(J-1,I)*SIN(TH(J-1,I))
      F3=F(J+1,I-1)*SIN(TH(J+1,I-1))
      F4=F(J-1,I-1)*SIN(TH(J-1,I-1))
      TERM2=(.25/DY)*(F1-F2+F3-F4)
      CON1=(F(J,I)*COS(TH(J,I))+DX*TERM2)/COS(TH(J,I-1))
      CON2=GAM*(K(J,I-1)**2)*(NEWH(J)**4)*C1(J,I-1)*B(J,I-1)/16.
      CON3=8./(GAM*NNM*C1(J,I-1))
      TEMPH(J)=SQRT(CON3*(CON1-CON2))
   20 CONTINUE
      NEWH(1)=TEMPH(2)
      NEWH(N)=TEMPH(NM1)
      DO 30 J=2,NM1
      TOL=ABS(TEMPH(J)-NEWH(J))
      NEWH(J)=TEMPH(J)
      IF(TOL.GT..0001) IOUT=1
   30 CONTINUE
      IF(IOUT.EQ.1) GO TO 5
      RETURN
      END
C******************************
C
C
      SUBROUTINE TABLE(I1,I2,IVAL,JSTART,JEND,ITITLE,DUM1,FACT)
C
C
C******************************
      PARAMETER(IQ=500,JQ=50)
      COMMON/CONST/M,N,DX,DY,HO,T,THETAO,CNTR,IORDER,G
      COMMON/CONST2/PI,PI2,RAD,CO,LO,KO,SIGMA,S2G,GAM
      COMMON/CONST3/I,J,ICOUNT,IC,NM1
      COMMON/ARRAY/D(JQ,IQ),K(JQ,IQ),TH(JQ,IQ),H(JQ,IQ),B(JQ,IQ)
      COMMON/ARR2/C(JQ,IQ),F(JQ,IQ),NEWH(JQ),L(JQ,IQ),CG(JQ,IQ)
      COMMON/ARR3/E(JQ,IQ),C1(JQ,IQ),UU(JQ,IQ)
```

```
      REAL K0,L0,K,L,NEWH
      INTEGER IX(JQ+20),ITITLE(4)
      DIMENSION DUM1(JQ,IQ)
      NC=20
      WRITE(6,10) ITITLE,FACT
      J1=JSTART
      J2=JSTART+NC-1
   20 IF(J2.GT.JEND) J2=JEND
      WRITE(6,30) (J,J=J1,J2)
      WRITE(6,40)
      DO 50 I=I1,I2,IVAL
      DO 45 J=J1,J2
      RND=0.5
      IF(DUM1(J,I).LT.0.0) RND=-0.5
   45 IX(J)=INT(FACT*DUM1(J,I)+RND)
  50  WRITE(6,55) I,(IX(J),J=J1,J2)
      J1=J1+NC
      J2=J2+NC
      IF(J1.LE.JEND) GO TO 20
      WRITE(6,60)
  10  FORMAT(///,4A4,5X,'(MULTIPLIED BY ',F10.5,')')
  30  FORMAT(/,3X,'I/J:',20I6)
  40  FORMAT(1X,'----------------------------------------',
     *          '----------------------------------------',
     *          '-------------------------------------------------')
  55  FORMAT(1X,I3,2X,':',20I6)
  60  FORMAT(//)
      RETURN
      END
```

APPENDIX F: LIST OF VARIABLES

B	Term use to condense the expression for the energy flux
C	Wave celerity
C_g	Group velocity
C_{IK}	Wave celerity from wave theory of Isobe and Kraus
C_o	Deepwater wave celerity
c	coth kD
D	Still water depth
d	Dimensionless still water depth
$\overline{E}$	Average energy per unit surface area
F	Energy flux
$\overline{F}$	Average energy flux per unit surface area
g	Gravitational acceleration
H	Wave height
H_o	Deepwater wave height
H.O.T.	Higher Order Terms
I	x-coordinate of a grid point in the model
$\overline{I}$	Terms used in the derivation of $\overline{F}$ and $\overline{E}$
J	y-coordinate of a grid point in the model
$\overline{J}$	Terms used in the derivation of $\overline{PE}$
$\overline{KE}$	Average kinetic energy per unit surface area
k	Wave number
L	Wavelength
L_o	Deepwater wavelength
M.W.L.	Mean Water Level

M	Number of grid points in the model x-direction
N	Number of grid points in the model y-direction
N	Water surface elevation
$\overline{PE}$	Average potential energy per unit surface area
P	Pressure
Q	Flow rate
q	Dimensionless flow rate
T	Wave period
t	Time
U	Ursell parameter
U_s	Shallow water Ursell parameter
u	Horizontal component of water particle velocity
u_i	Terms of u
w	Vertical component of water particle velocity
w_i	Terms of w
x	On-offshore direction in the model
x	Direction of wave propagation in the derivation
y	Lonshore direction in the model
z	Vertical direction in the derivation
α	Wave angle with respect to the model x-axis
δ	Auxiliary parameter
ε	Perturbation parameter
η	Dimensionless water surface elevation
P_β/ρ	Bernoulli constant
ρ	Fluid density
Φ	Velocity potential

ϕ	Dimensionless velocity potential
Ψ	Stream function
ψ	Dimensionless stream function
θ	Phase function
γ	Specific gravity of a fluid
σ	Angular frequency